

Czech Technical University in Prague

Faculty of Civil Engineering

Department of Architectural Engineering



DOCTORAL THESIS

**Behaviour of textile-reinforced concrete structures at elevated
temperatures**

*Chování stavebních konstrukcí z textilního betonu za zvýšené
teploty*

by

Ing. Richard Fürst

A dissertation submitted in partial fulfilment of the requirements
for the degree of *Doctor of Philosophy* (PhD)
in *Civil Engineering*

Doctoral Degree Program: Building Engineering

Supervisor: doc. Ing. Vladimír Mózer, PhD

Co-supervisor: Ing. Tomáš Vlach, PhD

Prague 2023

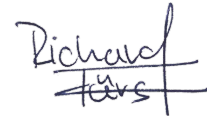
DECLARATION OF THE CANDIDATE

Author: Richard Fürst

Title of doctoral thesis: Behaviour of textile-reinforced concrete structures at elevated temperatures

I hereby affirm that the entire doctoral thesis has been written by myself under the supervision of doc. Ing. Vladimír Mózer, PhD and Ing. Tomáš Vlach, PhD at the Czech Technical University in Prague, Faculty of Civil Engineering, Department of Architectural Engineering. Several parts of this thesis have already been published in science journal papers, as mentioned in the appropriate parts of the thesis. All sources of information that have been used in the doctoral thesis are acknowledged in the text and listed in the Bibliography following the requirements given by the CTU Guideline¹.

In Prague on 31st January, 2023



.....
Ing. Richard Fürst

¹ Metodický pokyn č. 1/2009 O dodržování etických principů při přípravě vysokoškolských závěrečných prací (in Czech).

ACKNOWLEDGEMENTS

The research presented in this thesis would not have been possible without the invaluable support from a number of people. I am truly grateful for all the support, discussions, and cooperation I have had the chance to experience during this time. First of all, I would like to appreciate to the patience and support of my thesis supervisors doc. Ing. Vladimír Mózser, PhD, Ing. Tomáš Vlach, PhD, Ing. Marek Pokorný, PhD, and my colleague Ing. arch. Bc. Petr Hejtmánek PhD. I thank them for all discussions and motivation they provided to help me solving questions in the research part of this thesis. Subsequently, I would like to thank my friend Michal Topolovsky, who supported me with my choice to focus on fire engineering. Next, I would like to appreciate my wonderful wife, Eliška, for being a great help during my entire PhD studies and my internship in Germany, which was one of the most important steps in my research career. Finally, I thank my parents, who supported me during my whole studying journey.

I am also grateful for the financial support provided by the following organizations:

Grant Agency of the Czech Technical University in Prague

- Project No. SGS21/094/OHK1/2T/11, 2021-2022 (principal investigator)

Technology Agency of the Czech Republic

- Project No. TJ02000119, 2019-2021 (research team member)

<https://doi.org/10.14311/dis.fsv.2023.001>

ABSTRACT

Textile reinforced concrete (TRC) is a modern composite consisting of high-performance concrete (HPC), textile reinforcement, and its matrix, most often from synthetic resins. Since it is a new building material, its use is dominant in non-load-bearing constructions such as facade panels or design elements. Nevertheless, due to its excellent mechanical properties, TRC may be used as an alternative load-bearing material to traditional structures materials. But before that, a detailed assessment from a fire resistance point of view is necessary. The development of TRC described in the thesis responds to the lack of knowledge about the fire design of TRC structures and focuses on the determination of TRC behaviour at elevated temperatures. At the same time, it aims to increase passive fire resistance and minimize the use of additional fire protection systems. Based on the multi-scale testing, risk areas such as high risk of spalling of HPC layers, contribution to the development of fire or loss of interaction between materials due to the temperature degradation of synthetic resin matrix of textile reinforcement were defined. Based on the findings, material optimization is proposed to reduce or eliminate these risks. Furthermore, the work describes the influence of the polypropylene (PP) fibres in the HPC mixture and their influence on spalling risk and load-bearing capacity of TRC. At the same time, the substitution of a flammable synthetic matrix of textile reinforcement with non-flammable cement-based materials is described as well as its behaviour at ambient and elevated temperatures. All conclusions determined based on the multi-scale experimental investigation were finally verified by real-scale testing where the official fire resistance of TRC structural members was classified. All these conclusions expand the development of TRC at elevated temperatures and thus should serve as a basis for the theoretical design of TRC structural members considering their behaviour at fire exposure.

Keywords: Textile-reinforced concrete; high-performance concrete; carbon fibres; epoxy resin; load-bearing structures; fire resistance

ABSTRAKT (CZECH)

Textilní železobeton (TRC – z anglického textile-reinforced concrete) je moderní kompozitní materiál, skládající se z textilní výztuže, vysokohodnotného betonu (HPC – z anglického high-performance concrete) a matrice textilní výztuže, nejčastěji provedené ze syntetických pryskyřic. Vzhledem k tomu, že jde o relativně nový stavební materiál, je hojně využíván především u nenosných konstrukcí jako jsou fasádní panely nebo designové prvky. Nicméně díky výborným mechanickým vlastnostem má tento materiál vysoký potenciál pro použití u nosných konstrukcí. Než však dojde k jeho použití u nosných konstrukcí, je nezbytné posoudit chování TRC z hlediska požární odolnosti. Vývoj TRC popsáný v disertační práci se zaměřuje na prohloubení znalostí o chování textilního betonu za zvýšené teploty. Dílčím cílem práce je minimalizovat nutnost použití dodatečné požární ochrany a zvýšení pasivní požární odolnosti TRC. Na základě provedených experimentů byly definovány rizikové oblasti TRC jako je vysoké riziko odlupování betonových vrstev HPC, příspěvek k rozvoji požáru vlivem vzplanutí syntetických pryskyřic nebo ztráta interakce mezi materiály v důsledku teplotní degradace matrice textilní výztuže. V návaznosti na tato zjištění byla provedena optimalizace materiálů za účelem snížení nebo úplného odstranění těchto rizikových oblastí. V práci je též popsán zásadní vliv polypropylenových vláken ve směsi HPC, nebo použití alternativních materiálů matrice textilní výztuže na cementové bázi. Tyto materiálové optimalizace byly testovány jak za běžné, tak zvýšené teploty. Nakonec jsou všechny závěry stanovené na základě experimentální činnosti ověřeny za pomoci zkoušek v reálném měřítku, přičemž byla stanovena oficiální požární odolnost zkoušených prvků z TRC. Veškeré závěry uvedené v této práci by měly prohloubit znalosti o chování dílčích materiálů použitých při vývoji textilního betonu a tím zefektivnit budoucí návrh těchto prvků pro nosné konstrukce s přihlédnutím na účinky požáru.

Klíčová slova: Textilní beton; vysokohodnotný beton, uhlíkové vlákno; epoxidová pryskyřice; nosné konstrukce; požární odolnost

LIST OF SYMBOLS AND ABBREVIATIONS

Name	Units	Description
Symbols		
A	m^2	Cross-sectional area of the specimen
V	m^3	Volume
E	MPa	Modulus of elasticity
t	min	Time
T_g	$^{\circ}C$	Glass transition temperature
T_m	$^{\circ}C$	Melting point temperature
T_f	$^{\circ}C$	Flow point temperature
k_u	-	Uncertainty coefficient
f_c	MPa	Compressive strength
f_{cf}	MPa	Tensile bending strength
h	mm	Total height of real scale specimen
C	mm	Vertical compression deformation limit

Abbreviations

TRC	-	Textile-reinforced concrete
HPC	-	High-performance concrete
UHPC	-	Ultra-high-performance concrete
ER	-	Epoxy resin
PFS	-	Passive fire protection system
RFS	-	Reactive fire protection system
IC	-	Intumescent coating
LCC	-	Life cycle costs
TACR	-	Technical Agency of the Czech Republic
DSC	-	Differential scan calorimetry
CFRP	-	Carbon fibre reinforced polymer

Since the thesis contains the results that have been published in different publications, it was not possible to keep the uniform nomenclature throughout the entire thesis. Therefore, the list of symbols contains only general symbols and abbreviations used in the thesis. The rest is explained in the appropriate parts of the thesis or related papers.

TABLE OF CONTENTS

1. Introduction.....	1
Motivation.....	1
High-performance concrete	3
Textile reinforcement	4
Matrix of the textile reinforcement.....	6
Fire design of the load-bearing structures and fire protection systems	7
Passive and reactive fire-protection systems	8
Research gaps.....	10
2. Objectives of the Ph.D. thesis.....	11
Main goal of the thesis	11
Thesis subobjectives	11
Limitations of presented research	12
3. Overview of thesis publications	13
Thesis papers.....	13
Author’s contribution to the papers	13
Related research projects and publications included in the thesis	14
Related research projects	14
Related publications included in the thesis.....	15
Author’s other publications not included in the thesis.....	15
4. Methodology, results and discussion.....	17
Methodology	17
Introduction to the appended publications and its relation to the subobjectives	20
Results and discussion	23
Determination of mechanical properties of TRC at ambient temperature.....	23
Establishing risk areas of textile-reinforced concrete at elevated temperatures....	26

Substitution of the flammable epoxy resin matrix.....	29
Verification of the cement suspension at elevated temperatures.....	32
Validation of conclusion at the real-scale fire tests	36
5. Conclusions.....	43
6. Future work (outlook)	48
Determination of heat release rate of TRC	48
Use of geopolymers as alternative matrix.....	48
Use of intumescent coatings as an alternative fire protection.....	49
Real-scale fire test.....	49
References	50
List of tables.....	56
List of figures	57
Annex A – Appended Papers	59

1. INTRODUCTION

Motivation

Textile reinforced concrete (TRC) is a modern composite material consisting of high-performance concrete (HPC) or ultra-high-performance concrete (UHPC), textile reinforcement and a textile reinforcement matrix, most often made of synthetic resins. The development of TRC dates back to approximately the 1980s [1, 2], which means it is a relatively new material in civil engineering. TRC is most commonly used for non-load-bearing structures, i.e. shell constructions, design elements, facade panels, rarely as load-bearing members [3, 4]. For this reason, limited design regulations and standards are available for load-bearing structures. Consequently, it has not been necessary to assess the TRC elements in terms of fire resistance. Before using TRC in civil engineering for structural members, it is necessary to extend knowledge about its behaviour at elevated temperatures.

In general, TRCs can be manufactured from different materials. However, the most common combination of materials consists of HPC, which achieves compressive strength exceeding 100 MPa, and textile reinforcement from carbon, basalt or glass fibres. Textile reinforcement can be used in variants with or without impregnation, i.e. reinforcement matrix. The impregnation is most often performed from synthetic resins due to their homogeneity and therefore ability to saturate the whole textile yarn. The matrix combines the textile yarn together and enables its full tensile utilization because all the individual filaments interact in the yarn. Therefore, the impregnated variant of reinforcement reached higher mechanical properties [5, 6]. Due to the combination of materials with higher mechanical properties, i.e. the compressive strength of HPC and the tensile strength of textile reinforcement, TRC achieves excellent mechanical properties, visual quality and, thanks to the use of less amount of materials during production, also lower impact on the environment [7, 8].

These materials proved its excellent mechanical properties at ambient temperatures. However, before using TRC for load-bearing structures, it is necessary to define its behaviour at elevated temperatures. From the fire resistance point of view, insufficient behaviour of some materials can be expected during fire exposure. Based on the material and literature investigation, low-temperature resistance of synthetic resin matrix was

determined as the most critical part of TRC hot design together with behaviour of HPC at elevated temperatures [9, 10]. The behaviour of these materials is directly linked to the structural design of lightweight slender constructions. Due to the possibility of producing subtle structures, TRC structural members heat up faster than massive traditional reinforced concrete structures. Therefore, it is necessary to assess the individual components, determine the risk areas and extend the knowledge about designing slender load-bearing TRC members from the fire resistance point of view.

The experimental work presented in this thesis aims to describe the TRC risk areas after fire exposure and simultaneously improve the behaviour of TRC at elevated temperatures. The output of the experimental work should be a proposal for further material optimization, replacement of the flammable TRC components (i.e. epoxy resin matrix) or a recommendation for an adequate fire protection system to avoid temperature degradation of materials at fire exposure. The presented research is based on the previously performed research in this field [3, 4, 11, 12] and focuses primarily on fire testing. At the same time, all the performed research work follows the author's conclusions from the master thesis [13] with the support of research projects [14, 15] focused on the development of TRC for lightweight load-bearing structural members. For a schematic load-bearing structure with hollow section from TRC, see Figure 1.

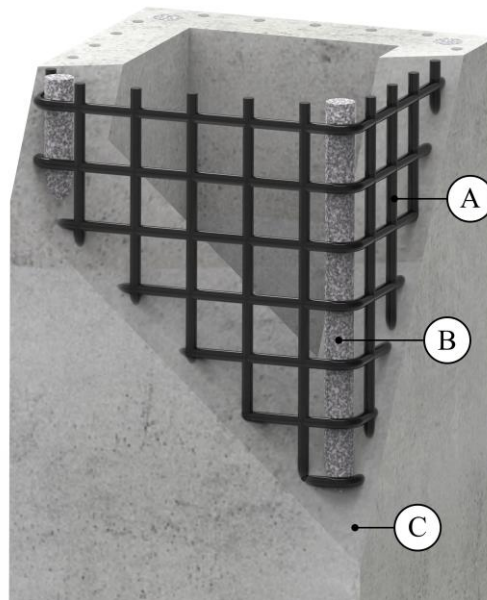


Figure 1: Schematic TRC load-bearing member with hollow section
Legend: A – carbon textile reinforcement; B – carbon fibre reinforced polymer (CFRP) bending rebars; C – high-performance concrete

Textile-reinforced concrete – review of materials

The review of materials given in this chapter focuses primarily on the behaviour of the materials, especially from the point of view of elevated temperatures [7, 8, 11, 16]. Since detailed description of materials is given in the introduction chapters of the attached publications, listed in Annex A – Appended papers, this chapter provide only a brief summary of the topic.

In general, TRC achieves excellent mechanical properties at ambient temperature compared to traditional construction materials such as dominantly used reinforced concrete. Moreover, the resulting environmental impact of TRC is significantly lower [17–19]. A better environmental rating of TRC can be achieved because less materials with better mechanical properties are used. Also, due to the higher strength of materials, it is possible to design structural members with hollow sections. At the same time, the material reduction is associated with better resistance of the textile reinforcement against atmospheric corrosion. Consequently, the covering layers can be designed only from the viewpoint of interaction between materials. However, using materials with higher strengths is also associated with a more complicated HPC production process or an emphasis on the precise definition of the cover layers distances. Therefore, this construction material is intended exclusively for prefabrication [20, 21]. The description of the individual mechanical properties and the basic description of the individual materials are summarized in the following subchapters.

High-performance concrete

For the manufacturing of TRC, HPC is used for its higher compressive strength, better workability and modulus of elasticity in comparison to concretes with standard mechanical parameters [22, 23]. The HPC mixture used for the preparation of experimental samples was developed for different applications under previous research projects at CTU in Prague [24]. The production of HPC was carried out according to the prescribed procedure, where the cured concrete has the following material properties: compressive strength 115.0 MPa, tensile strength 11.5 MPa and modulus of elasticity 49.5 GPa.

HPC can be produced with the use of plasticizers, which makes it possible to use a smaller water/cement ratio (W/C) during the HPC mixture preparation. Since less water is used in the manufacturing of the concrete mixture, the final hardened construction element has a significantly higher compressive strength associated with lower porosity, see Figure 2.

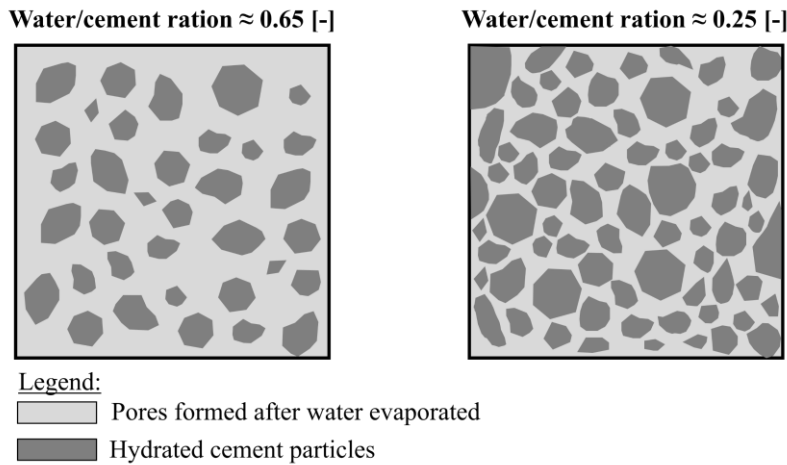


Figure 2: Comparison of the concretes with different water/cement ration [22]

From the fire resistance point of view, HPCs have worse fire resistance than standard concretes, which should be considered during the TRC structure design. It is mainly due to the higher risk of spalling and the related weakening of the structures [22]. This negative behaviour at elevated temperatures is primarily affected by the absence of pores caused by the small W/C ration. It implies that HPC cannot provide water vapour migration through the pores from the central part of the structure to the outside and thus, the vapour pressure in the construction can increase [25]. Therefore, the risk of spalling rapidly increases, as does the associated risk of structural weakening in the case of slender structures. The absence of pores of HPC can be substituted by adding polypropylene (PP) fibres to the concrete mixture. These fibres evaporate at a relatively low temperature (170 °C, according to [26]) and allow water vapor to migrate out of the concrete structure. However, the addition of these fibres fundamentally reduces the workability of the concrete mixture and can negatively affect the manufacturing process.

Textile reinforcement

In TRC, traditional steel reinforcement is replaced by technical textiles, most often in the form of glass, carbon, basalt, or aramid fibres. The advantage of textile reinforcements is their significantly better resistance to atmospheric corrosion and thus the possibility to design the covering layer while considering the interaction between the materials only.

Therefore, the final covering layer can reach from 5 mm to 10 mm, and it is possible to avoid the covering layers of traditional reinforced concrete structures reaching from 10 mm to 60 mm, which serves primarily as protection against atmospheric corrosion [27, 28]. Due to this, it is possible to design significantly more slender and lightweight structures and, in combination with the high compressive strength of HPC, also reduce the total amount of the materials used. Moreover, the use of less amount of materials with higher quality significantly reduces the environmental impact, as well as the structure assessment in terms of the life cycle cost (LCC) [29]. However, these solutions negatively affect the temperature resistance of the overall TRC structure because this thin cover layer does not provide sufficient temperature protection compared to traditional structures.

Based on the mechanical tests at ambient and elevated temperatures, textile reinforcement from carbon fibres appears to be the most advantageous material for use in TRC because the temperature resistance is significantly higher in comparison to the rest of materials. At the same time, carbon reinforcement reaches better mechanical properties and the lowest required energy for its production [30–32]. Comparison of the mechanical properties of textile reinforcements and the related temperature resistance is given in Table 1.

Table 1: Comparison of mechanical properties and melting points of selected textile reinforcement materials

Mechanical attribute	Type of textile reinforcement			Units
	Carbon fibres [30]	Glass fibres [31]	Basalt fibres [32]	
Density	~2.0	~2.5	~2.75	kg·m ⁻³
Tensile strength (average)	4.3	3.5	~2.48	GPa
Modulus of elasticity (average)	240	57	76	GPa
Diameter of yarn's filament	7–10	10–16	~12.8	µm
Melting temperature	3650	800	1100	°C

For the manufacturing of TRC construction elements, a distinction is made between impregnated and non-impregnated textile fibres, i.e. textile reinforcement with or without a matrix. Textile reinforcement is commonly used in yarns, called “rovings”, which can be further impregnated by a matrix in variable shapes, as shown in Figure 3a. Alternatively, it is possible to use already impregnated prefabricated grids, as shown in Figure 3b, which brings small restrictions regarding the shaping of the reinforcement.

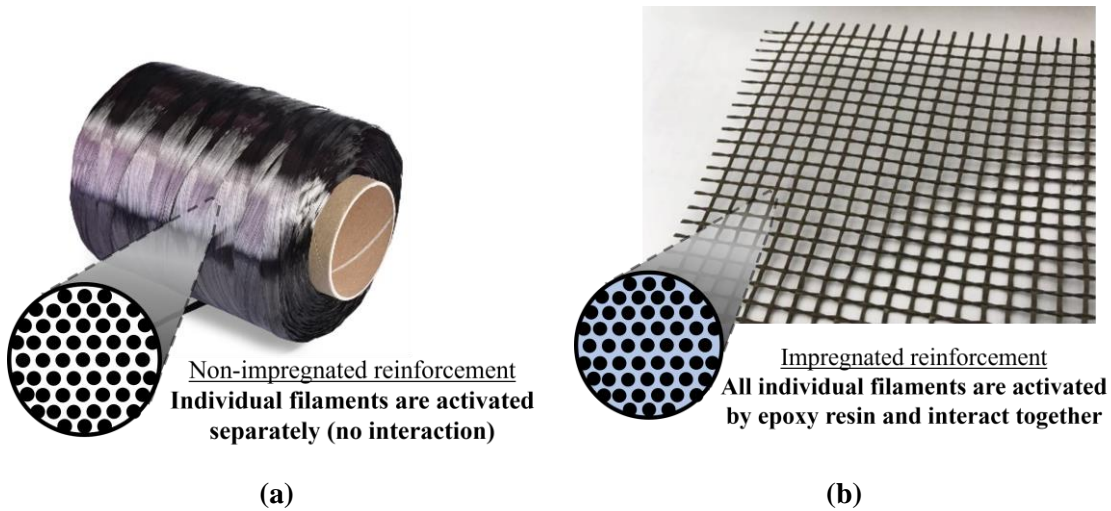


Figure 3: Variants of the carbon textile reinforcement with schematic yarn cross-section: (a) carbon roving bundle (unimpregnated); (b) prefabricated textile reinforcement grid impregnated with epoxy resin matrix

Matrix of the textile reinforcement

The textile reinforcement matrix is used primarily for homogenization of all the filaments in the yarn and thus allows the use of the entire tensile capacity of reinforcement. At the same time, the matrix also serves as additional protection against mechanical damage and extra protection against atmospheric corrosion. Due to the total number of the individual fibrils in the textile yarn with diameter from 5 μm to 16 μm (see Table 1), materials with homogeneous character, e.g. synthetics resins, are chosen as a suitable material for the matrix of textile reinforcement. Resins are chosen because they reach suitable mechanical properties, workability and homogenized structure, allowing full saturation of the yarn. However, from the fire resistance point of view, it is a flammable material which due to its general low temperature resistance loses its mechanical properties during exposure to higher temperatures around 50–100 $^{\circ}\text{C}$ [9].

The temperature interval where the mechanical properties of synthetic resin, i.e. the modulus of elasticity, are decreasing (loss of interaction between materials is expected), is what is known as the glass transition temperature (T_g) [33]. The glass transition temperature is a temperature interval where the modulus of elasticity of resin rapidly decreases, and the deformation significantly increases. A schematic description of the synthetic resin phase states change at increasing temperature is given in Figure 4.

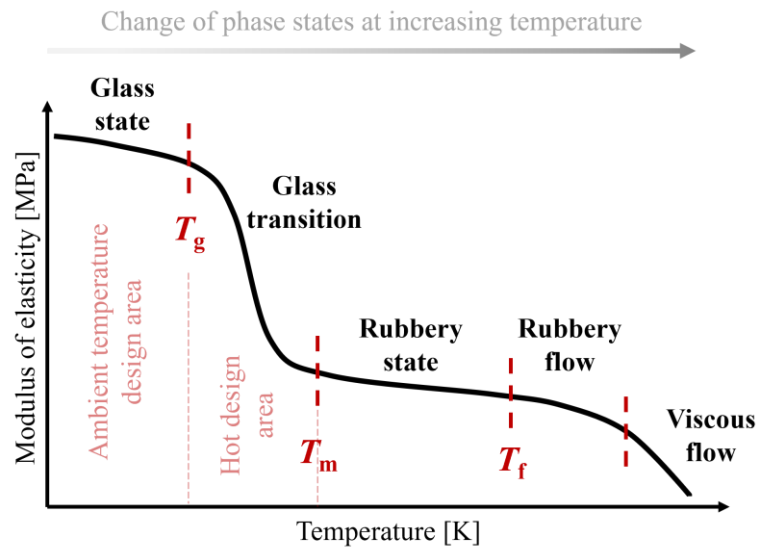


Figure 4: Change of the epoxy resin phase states [9]

Therefore, preventing the temperature increase over the ER glass-transition temperature value is necessary. One of the options for avoiding the degradation of the mechanical properties of ER due to increased temperature is the use of a resin with higher temperature resistance or the application of an additional fire protection layer that would prevent the glass transition temperature from being exceeded. Synthetic materials can be substituted by non-flammable materials based on the types of cement or geopolymers. These materials inherently have a higher temperature resistance. However, particles in these materials generally have a bigger diameter than the individual fibrils in the textile reinforcement yarn. And the saturation ability can be negatively affected [6, 34].

Fire design of the load-bearing structures and fire protection systems

Generally, the design of the load-bearing structures exposed to fire is focused on maintaining their mechanical properties for the required fire-resistance time. This means that the construction element should not be deformed over the load-bearing capacity limit of the structure or even collapse during the fire exposure. If the structural element has not only a load-bearing but also a fire-separating function, it must retain both its integrity and insulating ability [35]. Generally, structures bearing load only in compression do not exist due to the imperfection of the structure.

For bend elements, it is required to ensure the transfer of tensile tension giving rise to the bending moments by which the bend structures as columns and beams are dominantly bearing load [25]. Therefore, the effective hot design of structures preventing loss of mechanical properties due to the heating of members is necessary. One way to do this is

to use materials with sufficient temperature resistance or protect them against rising temperatures. In general, the fire resistance of various structures can be increased by applying additional fire-protection layers. These can be made of multiple materials where, depending on their thickness, adequate fire resistance is achieved. Generally, they are divided into two categories as passive and reactive fire-protection systems.

Passive and reactive fire-protection systems

Passive fire-protection systems (PFP) represent board materials in several variants, such as homogeneous structures (e.g. lime silicate), non-homogeneous (e.g. cement chips), and sandwich boards (e.g. plasterboard), or silica-fibres-based materials (e.g. mineral wool). The advantage of these materials is their diversity in use, as these boards can be used on a broad scale, such as for humid environments or as exterior or structural boards. The insulation principle of the board materials is to slow down the heating of the protected members through their passive fire resistance. The disadvantage of these protection systems is their effective thickness. The resulting thickness is designed based on the intended fire-resistance time, ranging from 15 mm to 50 mm [35]. Given that some systems allow protection without interfering with the protected structure, they enable the achievement of almost any fire resistance. However, due to the character of the protected material, it is mainly intended for structures with uncomplicated shapes, i.e. rectangular cross-sections, walls or ceilings (Figure 5).





Figure 5: Variants of applied fire protection systems on a TRC hollow section column: (a) functional sample of a TRC column with gypsum plaster [36]; (b) functional sample of a TRC column with calcium-silicate boards [37]

Reactive fire protection systems (RFP) are divided into four commonly used groups: solvent-based, water-based, epoxy-based and acrylic-based. Each RFP consists of three main parts: a primer, an intumescent layer, whose thickness is referred to as dry film thickness (DFT), and a top coat. Because of the profile-following application and the comparatively low coating thickness reaching approximately 3 millimetres, intumescent coatings are a suitable measure to improve the fire resistance of the protected structures and maintain the architectural character of the protected members [38]. In case of fire, the intumescent coating forms a thermal insulation layer around the coated steel member, activated by the high gas temperature. This foam body has a low thermal conductivity, significantly reducing the heating of the structures and delaying the temperature degradation of materials, and a longer fire-resistance time can thus be achieved. A general disadvantage is that these materials are intended for internal use. The principle of the intumescent coating reaction course and the foam formation is shown in Figure 6.

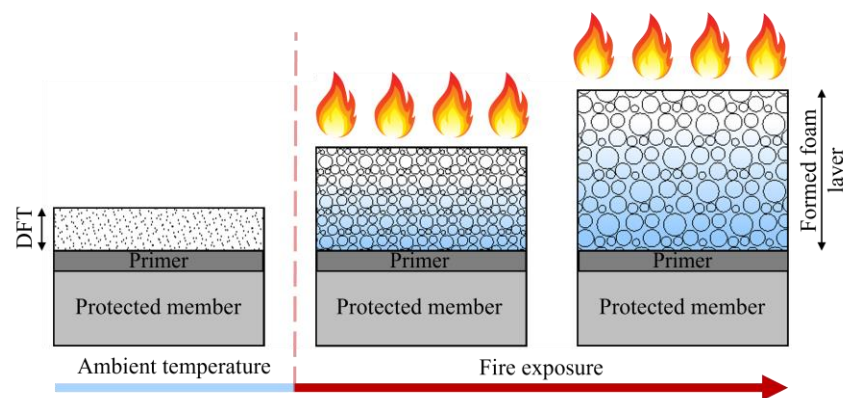


Figure 6: Reaction of the intumescent coating and foam forming

Research gaps

Constructions made of TRC achieve excellent mechanical and visual properties and due to the use of higher-quality materials, it is possible to save a considerable amount of the material used and reduce the total carbon footprint [18, 39]. These constructions are suitable especially for prefabrication because following the production procedure precisely is of essence. However, before the TRC will be widely used for load-bearing structures, it is necessary to assess this composite material in terms of fire resistance. Based on the literature and material research, also presented in the appended papers (see Annex A), certain research gaps were identified, serving as a background for the determination of the main goal of the thesis. The main research gaps were summarized in the following points:

- Faster heating of slender TRC structural members in comparison to traditional structures from reinforced concrete. Higher sensitivity to the weakening of the structure due to the smaller cross-section area.
- The behaviour of HPC and UHPC at elevated temperatures. Higher risk of the spalling of concrete layers during fire exposure and the associated weakening of the structural member.
- Temperature resistance of the technical textiles used and their temperature resistance, including the temperature point when mechanical degradation due to the elevated temperature starts.
- Low temperature resistance of synthetic resins used as a matrix of textile reinforcement. Hypothetical loss of interaction between materials after exceeding the glass transition temperature.
- Lack of knowledge of the use of non-flammable textile matrix materials and especially their behaviour at elevated temperatures

2. OBJECTIVES OF THE PH.D. THESIS

Main goal of the thesis

The main objective of the thesis was established based on the research gaps determined in the previous chapter. The thesis aims to extend knowledge about the behaviour of TRC exposed to fire and **IMPROVE THE BEHAVIOUR OF SLENDER STRUCTURES MADE OF TEXTILE-REINFORCED CONCRETE AT ELEVATED TEMPERATURES**. This main goal of the research work is divided into several subobjectives, which together fulfil the thesis's main goal. Each subobjective is described in the following subchapter.

Thesis subobjectives

The mentioned subobjectives are divided based on the literature research and the corresponding research gaps. A series of tests were carried out for each subobjective to investigate the related research question. The corresponding subobjectives are given in the following Table 2.

Table 2: Overview of the thesis subobjectives

Subobjective No.	Description of the subobjective
Subobjective I:	Experimental determination of the initial TRC mechanical conditions at ambient temperatures, i.e. determination of the bending capacity of TRC with a textile reinforcement, cohesion between the textile reinforcement with an epoxy resin matrix and HPC, and the influence of the textile reinforcement surface treatment.
Subobjective II:	Determination of the risk areas of TRC and the HPC used at elevated temperatures. Determination of the change in mechanical properties after fire exposure. Optimization of the materials used from the fire resistance point of view.
Subobjective III:	Increasing the passive fire resistance of TRC. Assessment of non-flammable materials for the matrix of textile reinforcement. Assessment of the available materials and their verification at ambient as well as elevated temperatures and their comparison with a reference from epoxy resin.
Subobjective IV:	Determination of the behaviour of real-scale structural members at elevated temperatures. Verification of the conclusion from intermediate-scale tests and design of additional fire-protection systems.

In some cases, selected subobjectives are directly connected to each other. Therefore, their detailed coordination was necessary for the pre-test phase of the research work. The association between the individual subobjectives and the related publications, attached in Annex A, is given in Figure 7.

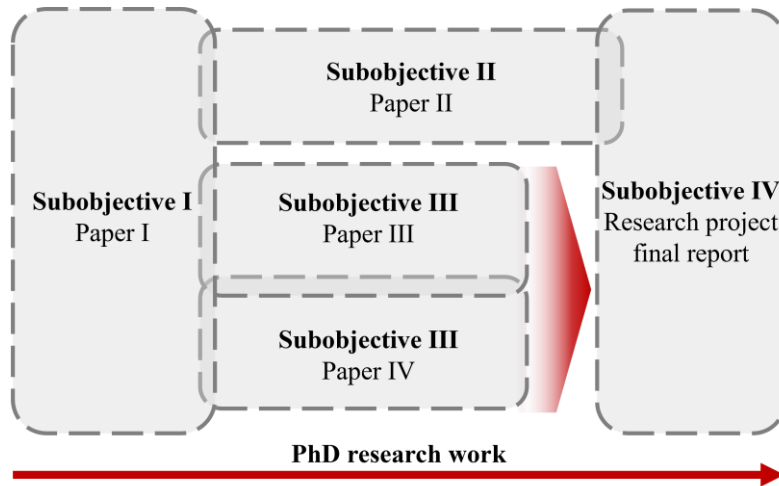


Figure 7: Scheme of the sequence of publications and linking of the subobjectives

Limitations of presented research

Due to the wide scope of the topic, the work focuses on the evaluation of slender structures, i.e. columns with a hollow cross-section. Furthermore, the work is defined by the use of carbon textile reinforcement with an epoxy resin matrix, i.e. a penetrated variant of textile reinforcement. However, due to the large number and types of materials, dealing with them would be very complicated and misleading. Therefore, the following parts were not included in the PhD thesis:

- Use of TRC for structural members such as ceilings, walls or shell members.
- Synthetic matrix materials of textile reinforcement other than epoxy resin.
- Apart from the materials described in *Paper III* [6] and *Paper IV* [34], other alternative materials of the textile reinforcement matrix are not considered.
- Other fire-protection systems, except for calcium-silicate boards and gypsum plasters used in real-scale fire tests as a part of the *Karbeton-II* research project [14]

3. OVERVIEW OF THESIS PUBLICATIONS

Thesis papers

This thesis is a compendium of four peer-reviewed publications, which have already been published in peer-reviewed journals. A summarization of the thesis papers is given in Table 3; the papers' full versions are appended in Annex A. The papers mentioned in this thesis, as well as the related test procedures, were designed in a subsequent sequence to fulfil the thesis's main goal as efficiently as possible. The sequence of the individual publications and the relations among them are shown in Figure 7.

Table 3: Overview of the thesis publications.

No. of paper	Name of the paper
Paper I	Vlach, T., Řepka, J., Hájek, J., Fürst, R. , Jirkalová, Z. and Hájek, P. Cohesion Test of a Single Impregnated Ar-Glass Roving in High-Performance Concrete. 2020. <i>The Civil Engineering Journal</i> .
Paper II ²	Fürst, R. , Vlach, T., Pokorný, M. and Mózer, V. Study of Behavior of Textile-Reinforced Concrete with Epoxy Resin Matrix in Fire. 2022. <i>Fire Technology</i> .
Paper III	Fürst, R. , Fürst, E., Vlach, T., Řepka, J., Pokorný, M. and Mózer, V. Use of Cement Suspension as an Alternative Matrix Material for Textile-Reinforced Concrete. 2021. <i>Materials</i> .
Paper IV	Fürst, R. , Hejtmánek, P., Vlach, T., Řepka, J., Mózer, V. and Hájek, P. Experimental Evaluation of Carbon Reinforced TRC with Cement Suspension Matrix at Elevated Temperature. 2022. <i>Polymers</i> .

Author's contribution to the papers

The author of the presented thesis actively worked on all four papers mentioned in Annex A – Appended Papers. The levels of contribution to each paper are given in Table 4. The entire work part of the included papers was performed with significant help of the people

² The article was submitted in 2020 and accepted in 03/2021. However, it was officially included in the journal Issue 14 in 06/2022.

mentioned as co-authors of the corresponding articles. The levels of responsibility are divided into the three following categories:

- Major The author’s responsibility was to do a major part of the work (equal or exceeding at least 2/3 of the responsibility and work effort for the part assessed)
- Medium The author’s responsibility was to do a significant part of the work (falling between 1/3 and 2/3 of the responsibility and work effort for the part assessed)
- Minor The author’s responsibility was minor for the point assessed and contained a small amount of the work duties (equal to or less than 1/3 of the responsibility and work effort for the part assessed)

The preparation of each article was divided into a total of six main parts, which are assessed individually in the following table.

Table 4: Author’s contribution to the papers incorporated in the PhD thesis

Number of the step:	Level of responsibility for the related work step			
	Paper I	Paper II	Paper III	Paper IV
1. Conceptualization of the tests	Minor	Major	Major	Major
2. Preparation of the specimens	Medium	Major	Medium	Minor
3. Performing the tests	Medium	Major	Medium	Medium
4. Data analysis	Minor	Major	Major	Major
5. Writing the original manuscript	Minor	Major	Major	Major
6. Paper final version preparation	Minor	Medium	Medium	Major

Related research projects and publications included in the thesis

Related research projects

The research work presented in this thesis was directly connected to two related research projects. First, the *Karbeton II* research project founded by the Technical Agency of the Czech Republic (TACR) for young research groups of the Zeta program, project number TJ02000119 [14]. The focus of this project was to develop the structural elements with hollow sections from HPC reinforced by a carbon reinforcement. The investigation was based on a previous research project where the behaviour of bend non-load-bearing structures was investigated [40]. The benefit coming from the intended research project was to develop a functional sample of a prefabricated new lightweight TRC column with

carbon reinforcement. This investigation also contained an investigation of the mechanical load-bearing capacity, as well as the fire-resistance class classification for structural column members. It was also investigated whether these structural members could be used without applying an additional fire-protection layer. The second research project is Application of alternative materials in textile concrete and their evaluation at room temperature and at elevated temperature, project number SGS21/094/OHK1/2T/11 [15].

Related publications included in the thesis

The author has also contributed to several publications related to the topic discussed in this thesis, whose list is given in the following Table 5. These publications include partially experimental conclusions written down in Czech. Therefore, these sources are included as supplementary documents only.

Table 5: Related thesis publications list

Character of the publication	Description of the related publication
Karbeton-II,	Interim report of work progress and achieved results for year 2019
TACR Zeta ³	Interim report of work progress and achieved results for year 2020

Author's other publications not included in the thesis

All parts of the ongoing research have been continuously presented at international conferences as well as in peer-reviewed journals. The summarizations of the publications which were not included in the thesis are provided in the following points:

Peer-reviewed journal papers:

- **Fürst, R., Häßler, D., Hothan, S.** Influence of the profile type and bar orientation on the performance of intumescent coatings applied to steel tension bars. *Fire Safety Journal*. 2022, 134, 103678. doi: 10.1016/j.firesaf.2022.103678.

³ Due to the size of the research team and the corresponding works distribution, the final contribution of all authors was balanced and the individual authors' contribution was not determined.

Peer-reviewed papers (non-impact):

- **Fürst, R.**, Vlach, T., Pokorný, M. Textile reinforced concrete and evaluation of its behavior at elevated temperatures. *TZB info*. 2020, ISSN 1801-4399.
- **Fürst, R.**, Pokorný, M., Vlach, T., Hejtmánek, P., Mózer, V. Column structures made from textile-reinforced concrete at elevated temperatures. *TZB info*. 2021, ISSN 1801-4399.
- Kafková, E., Vlach, T., Řepka, J., **Fürst, R.**, Hájek, P., Jirkalová, Z. Influence of scattered fibers on the mode of failure of textile concrete. *TZB info*. 2022, ISSN 1801-4399.

International conference papers and extended abstracts:

- **Fürst, R.**, Häßler, D., Hothan, S. European test standard for intumescent coatings applied to steel tension bars with solid section. Symposium Heißbemessung – Structural Fire Engineering 2022, Braunschweig.
- **Fürst, R.** et al. Nosné konstrukce z textilního betonu za zvýšené teploty. Extended abstract. 30th International Conference Fire Protection 2021, Ostrava, 2021-09-01/2021-09-02. ISBN 978-80-7385-247-4.
- **Fürst, R.**, Pokorný, M. Pasivní požární ochrana konstrukcí z textilního betonu. Extended abstract. 29th International Conference Fire Protection 2020, Ostrava, 2020-09-02/2020-09-03. ISBN 978-80-7385- 234-4.
- **Fürst, R.**, Pokorný, M. Požární specifika stavebních konstrukcí z textilních betonů 28th International Conference Fire Protection 2019, Ostrava, 2019-09-04/2019-09-05. ISBN 978-80-7385-221-4
- **Fürst, R.**, Pokorný, M. Požární specifika konstrukcí z textilního betonu. Advances In Fire & Safety Engineering - VIII. International Scientific Conference, Žilina, 2019-11-19/2019-11-20. Žilinská univerzita v Žilině, 2019. ISBN 978-80-554-1611-3.

4. METHODOLOGY, RESULTS AND DISCUSSION

This chapter describes the methodology of the procedures done in the experimental work. Subsequently, a general description of the papers is provided, as well as their relation to the selected subobjectives from Chapter 2, forming the main goal of the dissertation. Finally, test results are presented, including a general discussion.

Methodology

Once the main objective of the thesis and the partial subobjectives given in Chapter 2 were identified, a procedure for experimental tests was determined. The investigation was based on the multi-scale test procedure, in which the tests ranged from micro-scale tests of materials to tests of test members in a real scale. A schematic description of the content of the research works is given in Figure 8.

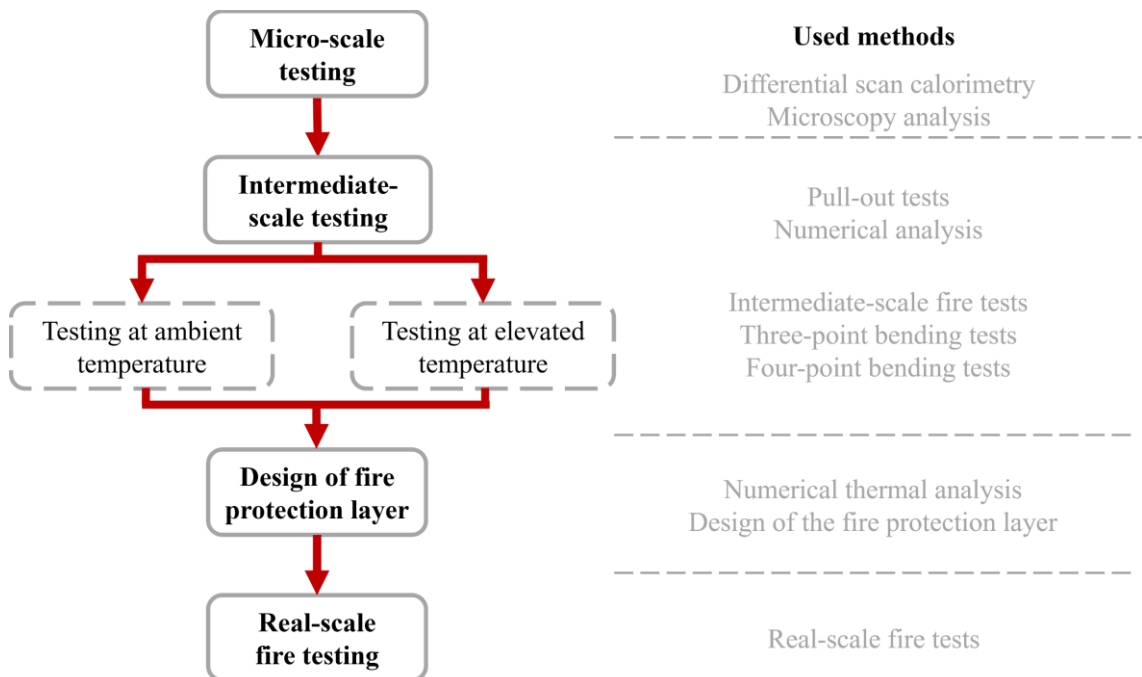


Figure 8: Scheme of the multi-scale testing of thesis experiments

Experimental test methods were carried out in accordance with the applicable legislation and standards for all the analyses at ambient and elevated temperatures. Table 6 summarizes the general principles of the tests performed based on the standards used. These standards are included in the table as well. The test methods are described in more detail in Annex A – Appended Papers.

Table 6: Description of the multi-scale testing

Micro-scale testing		
Micro-scale testing was used to determine detailed characteristics of the materials. Based on the results from these tests, the materials combination was established and verified for further testing.		
Method	Aim of the method used	Reference standard
Differential scanning calorimetry (DSC)	The DSC analysis was used to investigate the thermo-mechanical properties of the epoxy resins. Several different epoxy resins were tested for which the temperature phase states were determined. Based on the results, a suitable epoxy resin was identified for the mechanical tests that were to follow. An HP Phoenix 204 device was used for the DSC analysis, which measurement principle is based on the heat flux method.	ISO 11357-1
		ISO 11357-2
Microscopy analysis	In microscopic analysis, several cement suspensions were tested as a possible non-combustion material for the textile reinforcement matrix. Due to the inhomogeneous suspension structure, the investigation aimed to determine the size distribution of the individual particles in the suspension. Zeiss LSM 780 confocal microscope was chosen for analysis using the basic optical microscope settings and 100× magnification. All the samples analysed were taken from three independent replicates for each type of cement suspension.	ISO 8039 ISO 21073
Intermediate-scale testing		
Based on the results from microscopy tests, specimens for intermediate testing were designed. These specimens were subsequently tested to determine the mechanical properties of materials, such as bending and compressive strength and change in mechanical properties after fire exposure.		
Fire tests	Testing at elevated temperatures was performed in a furnace for intermediate tests miniFUR. Unloaded test specimens were exposed to elevated temperatures according to a standard temperature/time curve ISO 834 to simulate exposure conditions to a real fire. After fire exposure and visual assessment, the test specimens were subsequently mechanically tested to determine the change in their mechanical properties compared to reference specimens.	EN 1363-1

Three-point bending tests	The mechanical strength of the test specimens was determined based on mechanical experiments. These experiments were performed at ambient temperatures (reference specimens) and after fire exposure to determine the residual strength and the influence of elevated temperatures on the change in mechanical properties. The specimens varied according to the specific investigation. For the determination of tensile strength f_{cf} , three-point bending tests were performed with beam specimens $40 \times 40 \times 160 \text{ mm}^3$. Subsequently, compressive strength f_c was determined based on the tests of fragments from the beam specimens from three-point bending tests under one direction pressure. The bending strength was determined based on the four-point bending tests with plate specimens $100 \times 300 \times 30 \text{ mm}^3$.	EN 12390-3
Four-point bending tests		EN 12390-5
Compressive strength test		
Pull-out test	The developed pull-out method focused on the complete curve of bond behaviour with a simple interpretation and application of the results in the field of science and engineering and structure design. The ACI 440.3R-03 standard inspired this method. However, the specimen dimensions were modified due to the small cross-sectional area of the composite reinforcement in comparison with traditional FRP reinforcement. The resulting shape of the specimen was $100 \times 100 \times 20 \text{ mm}^3$ with one saturated textile yarn in the central axis of the specimen. The other aspects of the test set-up were similar to the traditional FRP cohesion test.	ACI 440.3R-03
Real-scale testing		
Real-scale tests aim to determine the behaviour of a structural member at elevated temperatures and verify the conclusions defined in the intermediate-scale tests.		
Real-scale testing of structural members	The real-scale tests aimed to verify the conclusions from the previously performed micro-scale and intermediate tests. Fire tests in real scale were performed in PAVUS a.s., an accredited fire laboratory, with column specimens with a hollow cross-section of $250 \times 250 \text{ mm}^2$. The specimens were protected by two different fire protection systems manufactured from gypsum plaster and calcium-silicate boards. During the fire tests, the temperatures on the textile reinforcement were measured, monitoring each time when the glass transition temperature of the epoxy resin was exceeded.	EN 1365-4 EN 1363-1

The measured data from the tests performed were statistically evaluated. For partial data assessment, the expanded measurement uncertainty was determined with an uncertainty coefficient $k_u = 2.0$ for the interval containing 95% of values. For the rest of the measured data, basic statistical evaluation was used based on the total number of the tests performed and the specimens tested. The entire statistical evaluation was performed in MS Excel 365 and GraphPad Prism 8.0.

Introduction to the appended publications and its relation to the subobjectives

This subchapter provides a general summarization of the paper's aims and their relation to the selected subobjectives from Table 2. Also a general description is given of the test set and of the intended goals that led to the fulfilment of the main goal of the thesis.

In the introductory part of the experimental investigation, the initial condition of the mechanical properties of TRC was determined. *Paper I* focuses on investigating the interaction between the impregnated textile reinforcement and HPC, and its determination by using the slightly modified pull-out test. The second aim of this article is to improve the interaction conditions between the reinforcement and HPC by using fine-grained silica sand applied on the surface of the composite reinforcement, similar to the traditional fibre-reinforced polymer reinforcement with commonly used diameters. To investigate the effect of this modification, four-point bending tests at ambient temperature were performed on plate specimens with variable amounts of textile reinforcement. Determination of the corresponding mechanical characteristics fulfilled goals of *Subobjective I* [12] and, at the same time, served as reference background for further tests.

Based on the results determined in the previous mechanical testing part, the behaviour of TRC at elevated temperatures was addressed in *Subobjective II*, based on the results given in *Paper II*. The main aim of this analysis at elevated temperatures was to assess the application of TRC consisting of HPC, textile reinforcement from carbon yarns and its epoxy resin matrix and determine its risk areas. For the investigation, beam and plate specimens were mounted at the front wall of the test fire furnace miniFUR and exposed to the standard temperature curve according to EN 1363-1 [41].

The influence of PP fibres in the HPC mixture was investigated to reduce the risk of concrete layers spalling. Directly after fire exposure, the visual assessment was done, and after that, residual mechanical properties were determined by bending and compressive tests. Furthermore, all the specimens exposed to elevated temperatures were compared with reference specimens. Based on this comparison, a change in the mechanical properties and residual bending strength was determined. In addition, the risk areas such as spalling of HPC, burning of the epoxy resin matrix and loss of interaction between materials were observed [25].

Paper III follows the conclusions from the intermediate tests at elevated temperatures [25] and focuses on substituting the flammable epoxy resin matrix, which was selected as the most critical part of TRC, with cement suspension [6]. In the first part of *Subobjective III*, microscopic research was carried out to determine the distribution of particle sizes in the cement suspension. Subsequently, five series of plate specimens differing in the type of the cement suspension used, as well as the method of textile reinforcement saturation, were designed and manufactured. Next, mechanical tests (four-point bending tests) were carried out to determine bending strength capacity. Finally, based on the results, the most effective type of cement suspension and the method of saturating the textile reinforcement were determined.

The work presented in *Paper IV* expands the previously performed mechanical tests at ambient temperatures of specimens with cement suspension and forms the second part of *Subobjective III* [34]. In addition, specimens with cement suspension matrix and epoxy resin were exposed to fire, and the residual tensile strength was tested. The conclusion of *Subobjective III* compares the flammable and non-flammable matrix of the textile reinforcement and the suitability of substituting the epoxy resin with cement suspension.

Conclusions from all the previous research parts were verified by testing specimens in a real scale, forming *Subobjective IV*. In total, two TRC columns were tested with hollow sections and the textile reinforcement matrix with epoxy resin. The test's main objective was to reach the intended fire-resistance time when the specimen did not lose its load-bearing capacity. However, due to the risk areas defined in *Paper II*, the design of an additional fire-protection layer was necessary. Two different materials, i.e. gypsum plaster and calcium-silicate boards, were used as a protection system. The adequate thickness of the fire-protection layers was defined based on the fine element thermal numerical analysis in the ANSYS software. For the hot design purposes, a critical design

temperature of the fire-protection layer was determined, the lower temperature point limit of the glass transition temperature interval being $T_g = 123$ °C. These temperature values were determined based on the results of the DSC analysis. The conditions of the numerical assessment were selected based on the results from the previous tests at ambient as well as elevated temperatures [12, 14, 25].

Results and discussion

The thesis contains in total four papers (*Paper I-IV*) and four related research subobjectives. This work deals with the experimental investigation of textile concrete and its fire resistance. First, *Paper I* describes the mechanical properties of TRC at ambient temperatures, which served as a basis for further tests. This part is followed by the intermediate fire testing, describing the risk areas of the TRC as a part of *Paper II*. Conclusions from testing at elevated temperatures served as a basis for *Paper III* and *Paper IV*, which focused on the substitution of the flammable matrix of textile reinforcement with cement suspension. Finally, all the results are verified on real-scale test specimens, where the conclusions discussed in this chapter were evaluated based on the results found in the experimental work.

The results presented in this subchapter cover examples of the results yielding significant conclusions only. All results, including a detailed description of the test specimens and test series, are detailed and discussed in the relevant articles in Annex A – Appended Papers.

Determination of mechanical properties of TRC at ambient temperature⁴

(Subobjective I)

The initial mechanical properties of TRC were determined based on the cohesion (pull-out) tests, which focused on analysing the different surface treatments of the textile, i.e. textile reinforcement with a smooth surface and textile reinforcement with a surface treated with silica sand. Pull-out tests in which the effect of the surface treatment was determined were followed by four-point tests that investigated the total bending strength of TRC. Conclusions, including the results of the mechanical tests performed at ambient temperatures, are summarized in the text below.

The results of the pull-out test are presented in Figure 9. Both diagrams show pull-out measured by the X-axis's potentiometer and the Y-axis's corresponding force. Pull-out tests proved little cohesion between the HPC part of specimens and textile reinforcement

⁴ The description of the elements tested and the interpretation of results were summarized based on the article *Cohesion Test of a Single Impregnated Ar-Glass Roving in High-Performance Concrete* [12].

with a smooth surface. Therefore, all rovings without surface treatment were pulled out of their HPC matrix and did not reach force values as the specimens with the treated surface of the textile reinforcement. Figure 9b shows a detailed view focused on the results at the beginning of the pull-out tests (the maximum X-axis value was limited to 100 μm). Specimens with treated textile reinforcement showed almost perfect bonding with the HPC. Therefore, all these specimens with surface treatment were broken before being pulled out. Finally, specimens with treated textile reinforcement showed better stability of the results because no sample shows significant deviations, as shown in Figure 9b.

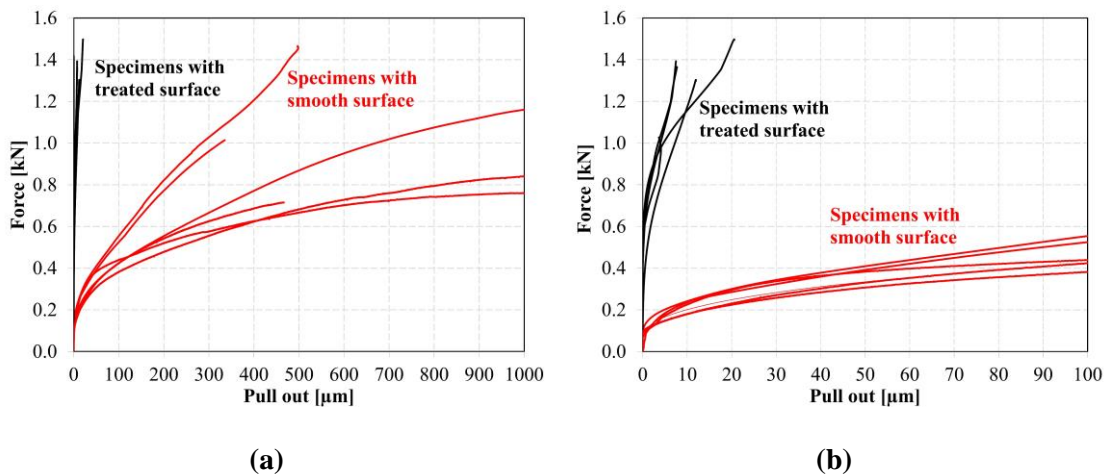


Figure 9: Results of the cohesion test (pull-out diagram):

(a) Difference between smooth and treated surface of the textile reinforcement; (b) Detailed view on the beginning of the pull-out test showing significant difference between smooth and treated textile reinforcement surface (limited X-axis).

Based on the pull-out tests, bending strength was determined by four-point bending tests to verify the influence of the yarn surface treatment on the resulting bending capacity. The four-point bending test was performed on small plate specimens $100 \times 360 \times 18 \text{ mm}^3$. Three variants with smooth surfaces and three with treated surfaces were manufactured. Plate specimens also differed in the total number of the textile reinforcements used. Detailed description of the specimens and the corresponding amount of the textile reinforcement is given in Table 7.

Table 7: Description of the specimens for four-point bending tests.

Variant [-]	Number of layers [pcs]	Number of yarns in one layer [pcs]
A	2	5
B	2	10
C	4	10

In the case of specimens with two layers of textile reinforcement and five yarns in the layer (Variant A), the first sudden drop in force represents the formation of the first crack, creating a plastic joint, followed by an opening of the crack and tensile activation of the reinforcement. Similar behaviour was also observed for specimens of Variant B, with two layers of reinforcement and ten yarns in each layer. The load-bearing capacity of the specimen before the first crack initiation is given only by the HPC's tensile strength without the reinforcement's contribution. After the initiation of the first crack, the specimens with smooth reinforcement typically formed one additional crack, each under one of the loading supports, after which the smooth reinforcement started slipping. Their behaviour under pressure was typical for slightly reinforced concrete structures with wide cracks opening. The specimens with the treated reinforcement surface formed more narrow cracks due to significantly better cohesion between the reinforcement and HPC. The pull of yarns was not that significant, and much faster reinforcement activation led to multiple cracking, which is characteristic of structures with higher amounts of reinforcement. More significant behaviour was observed in the case of specimens with two layers of reinforcement with ten yarns in each layer (Variant B). A higher amount of reinforcement led to a higher maximum value of reached force compared to the specimens from Variant A. The activation of the surface-treated 2×10 reinforcement was much faster than in the case of its smooth counterpart. The specimens with the treated surface also show higher ultimate reached force while having lower displacement at the time of their collapse. An example of the results of Variant B from four-point bending tests is given in Figure 10.

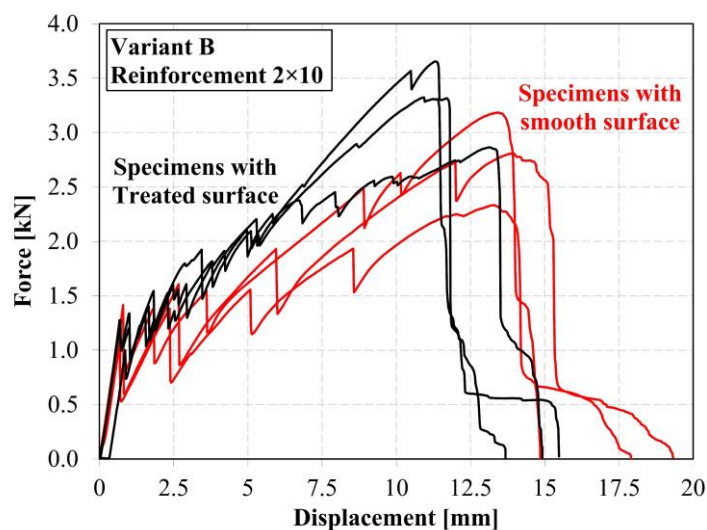


Figure 10: Example of the results from four-point bending test of specimens with 2×10 tensile reinforcement with and without surface treatment

Contrarily, specimens of Variant C with four layers and ten yarns in each layer showed that the amount of reinforcement is so high in the cross-sectional area of the specimen that the curves look similar. The positive effect of the surface treatment of the composite textile reinforcement with fine-grained silica sand is much less significant than in specimens with less textile reinforcement (variants A and B). Therefore, it is necessary to consider the optimal amount of textile reinforcement [12].

Establishing risk areas of textile-reinforced concrete at elevated temperatures⁵

(Subobjective II)

Based on the results from indicative fire tests [13], beam specimens were exposed to elevated temperatures, and a high risk of spalling was identified. Therefore, the first part investigated a change in mechanical properties (tensile and compressive strength) and the effect of different amounts of PP fibres in the concrete mixture. The residual strength was then compared with the reference specimens to determine the change in mechanical properties.

Figure 11a shows a decreasing trend in tensile strength compared to the reference specimens and the specimens exposed to elevated temperatures. The same trend is described in EN 1992-1-2 [35], which also only considers the decrease in tensile strength at elevated temperatures. On the other hand, several studies describe the behaviour of HPC at elevated temperatures in terms of the change in mechanical properties and conclude that its strength is increasing. The increase in tensile strength occurs in the interval between 100–370 °C [42]. In this range of temperatures, we can monitor the maximal increase in tensile strength by around 15% at 220 °C. However, when the temperature interval is exceeded, there is a rapid decrease in tensile strength. This interval was exceeded for the experimental specimens, so the tensile strength decreased compared to the references. The temperatures measured were around 247 °C on the unexposed surface during the fire experiment. Due to that, the tensile strength of the samples was lower than the tensile strength at ambient temperatures because the most significant part

⁵ The description of the elements tested and the interpretation of results were summarized based on the article *Study of Behavior of Textile-Reinforced Concrete with Epoxy Resin Matrix in Fire* [25].

of the specimens exceeded 370 °C. Therefore, the result was that tensile strength decreased approximately by 31%.

In contrast to tensile strength, there is a different temperature interval where the compressive strength increases [42]. This is due to the fact that the fire exposure was not long enough to exceed critical temperature in a major part of the specimen's body. Therefore, compressive strength is higher than the strength at a normal temperature, approximately by 22%. This behaviour was likely achieved by hydration of the remaining cement particle cores due to the evaporation of the free and partly also chemically bound water inside the specimens [43, 44]. The specimens were labelled as PP2, PP4, PP6 and PP8. The number in the series name corresponds to the amount of PP fibres used in the HPC mixture, i.e. PP2 – specimens with 2 kg·m⁻³ of PP fibres used in the HPC mixture, etc.

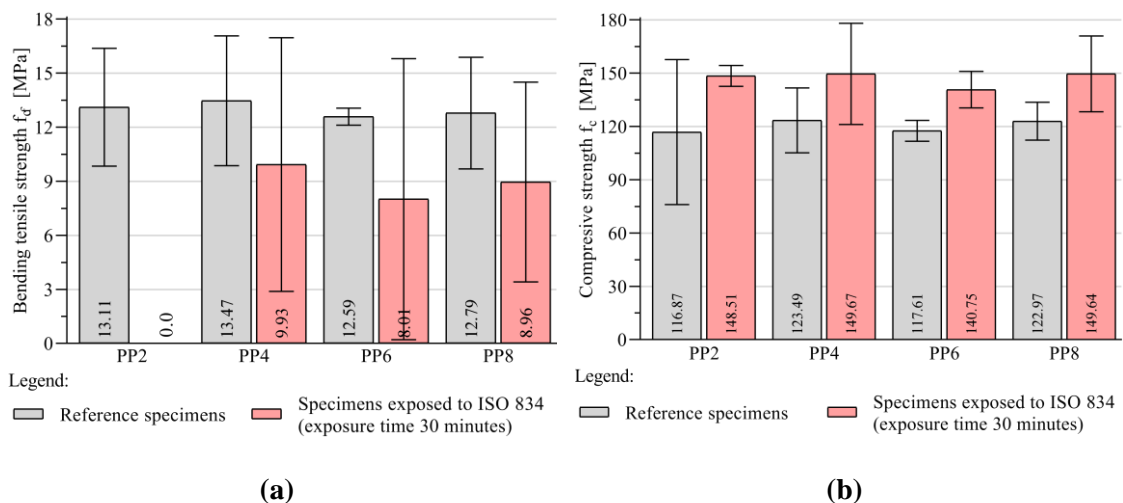


Figure 11: Change in mechanical properties of HPC: (a) bending tensile strength; (b) compressive strength

Note: For the PP2-specimens, the setting of the load force was too fast, and the press software could not evaluate the resulting bending tensile strength.

In the next step, TRC plate specimens were tested at elevated temperatures. In contrast to the tests presented in [12], textile reinforcement from carbon was chosen instead of glass textile reinforcement due to its generally higher temperature resistance (see Table 1 and [21]). Based on the literature and material research, the epoxy resin matrix was identified as a critical part of TRC due to its low temperature resistance. This was confirmed on a series of test specimens exposed to the ISO 834 standard temperature/time curve [41]. In the case of test specimens without the addition of PP fibres, there was a massive spalling of the concrete covering layers and direct exposure of the textile reinforcement to the fire. As a result of direct exposure, all experimental specimens started burning on their surface.

The burning persisted for about 3.5 minutes even though the experiment was stopped by switching off the gas supply to the furnace burner (see Figure 12).



Figure 12: Plate specimens without polypropylene fibres after the fire test

Also, specimens with PP fibres started burning despite the fact that the addition of PP fibres in the HPC mixture efficiently prevented spalling of the covering layer. Thanks to eliminating the spalling of the specimens, thus maintaining their integrity, the burning was reduced to 2.0 minutes after the fire test ended. The burning was caused by the burn-out of the PP fibres, which created a “pore bridge” and enabled the migration of the ER thermal decomposition products into the furnace where they were ignited, see Figure 13. In the follow-up visual analysis, it was evident that all of the ER matrices burned out in both specimen’s variant and created a cavity between the concrete and the tensile reinforcement.



Figure 13: Plate specimens with polypropylene fibres during the fire test

One of the causes of the ER burnout was the degradation of the textile reinforcement fibre and the resulting loss of bond between the HPC and the tensile reinforcement. In this case, only the reinforcement intersections (the overlap of fibre strings forming the mesh) could transmit the tensile tension. The absence of a textile reinforcement matrix significantly reduced load-bearing capacity, as shown in Figure 14. In the case of specimens exposed

to elevated temperatures, textile reinforcement was gradually pulled out due to the loss of interaction between materials.

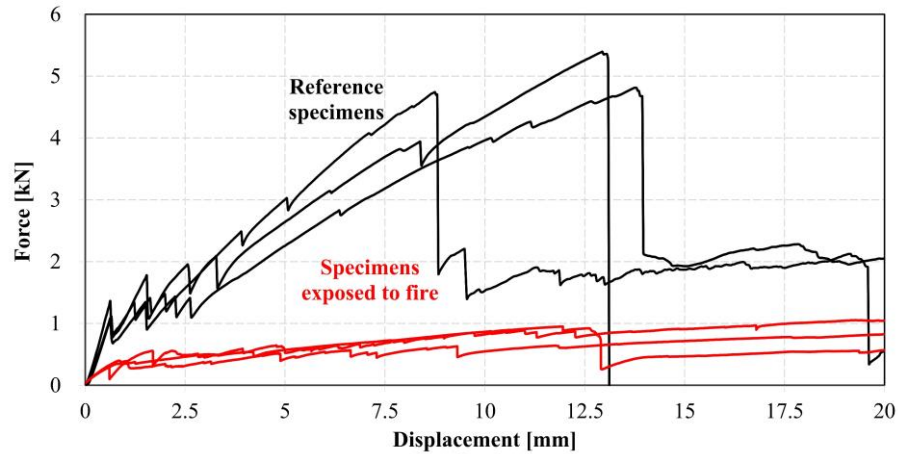


Figure 14: Comparison of the reference specimens and specimens exposed to fire

Substitution of the flammable epoxy resin matrix⁶

(Subobjective III)

In response to the tests at elevated temperatures and the observed low temperature resistance of the synthetic matrix and its influence on the load-bearing capacity of the TRC [25], an alternative material of a textile reinforcement matrix was verified. Cement suspension from CEM 42.5 R and CEM 52.5 R was chosen as a non-combustion replacement material.

Therefore, cement particles were imaged using confocal microscopy in the first part of the assessment. The distribution and size of the CEM 42.5 R and CEM 52.5 R particles were compared. The microscope photographs (see Figure 15) clearly show that CEM 52.5 R had an overall better distribution in cement suspension, while CEM 42.5 R contained more particles bound together in what is known as floccules, which may cause a problem of insufficient carbon filament saturation in comparison to individual filaments diameter of which is equal to approximately 7–10 μm . The size distribution of the cement particles differed for the two types of cement. CEM 52.5 R had a median particle size of 301.5 μm^2 (corresponding to the mean value of the length of one side of 9.8 μm), while the median

⁶ The description of the elements tested and the interpretation of results were summarized based on the article *Use of Cement Suspension as an Alternative Matrix Material for Textile-Reinforced Concrete* [6].

particle size in CEM 42.5 R was $397.8 \mu\text{m}^2$ (which was $11.3 \mu\text{m}$ in length). When also considering the formation of floccules in CEM 42.5 R, the results indicate an overall poorer probability of deep carbon fibre saturation.

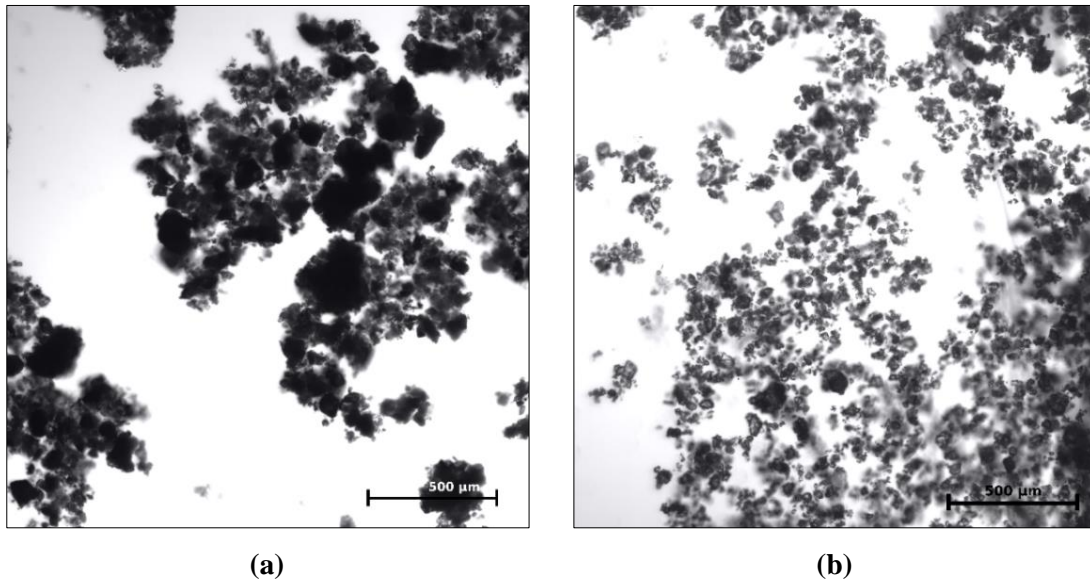


Figure 15: Microscope pictures of cement suspension:
 (a) CEM 42.5 R; (b) CEM 52.5 R.

Next, the hypothesis was put to test that the penetration of carbon roving strongly depends on the cement type and saturation method. In total, five series were manufactured, each with a different type of saturation material and method of saturation. The resulting percentage of saturation for each variant is given in Figure 16.

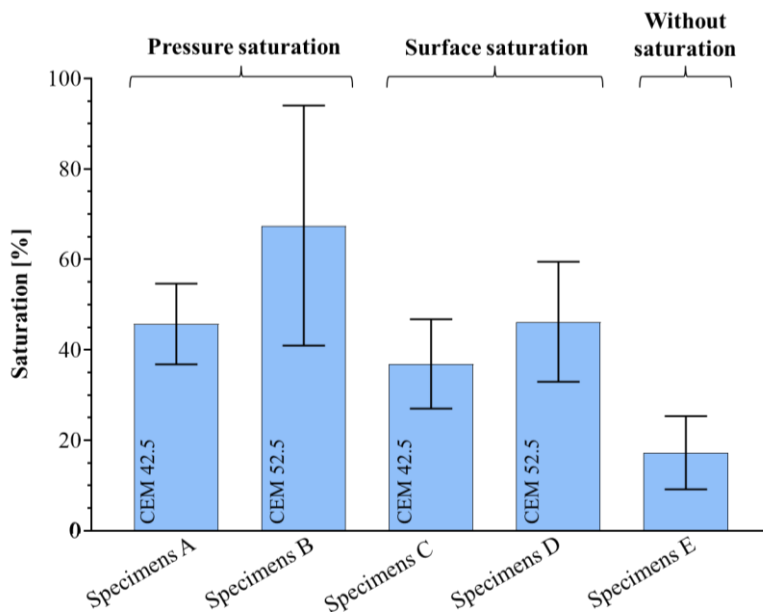


Figure 16: Assessment of the microscopic analysis of textile reinforcement percentage saturation

It is apparent from the visual and microscopy analysis when comparing the different methods of saturation and different types of cement that the best results were obtained in the series A and B samples (pressure saturation method) in contrast to specimens from series C and D, where surface saturation method was used. Furthermore, the greatest saturation depth was reached in series B samples (CEM 52.5 R), supporting the hypothesis that smaller particles penetrate the roving better in addition to combination with pressure saturation. A microscopy investigation determined that both the size of cement particles and the method of pressure saturation increased the saturation of cement CEM 42.5 R by 22%. In contrast, the increase in saturation between experimental samples C and D was only 9%, where surface penetration was used. Unfortunately, the series E specimens (natural penetration of carbon roving of HPC mixture) turned out to have insufficient number of particles penetrating the yarn core. Most of the HPC mixture particles were on the surface of the carbon roving only, and the saturation was inadequate. The reason for the poor saturation of the carbon fibres with the concrete mixture was the size of the particles in the mixture in contrast to the size of the individual fibrils of the carbon yarn (7–10 μm). Therefore, the HPC particles could not reach the core of the carbon roving.

The following mechanical test evaluation focused on verifying the influence of the cement suspension on performance by means of bending tests under four-point bending at ambient temperatures. Plate specimens with an epoxy resin textile reinforcement matrix were used as a reference to determine a change in mechanical properties, similar to [12]. Results from the mechanical analysis are given in Figure 17.

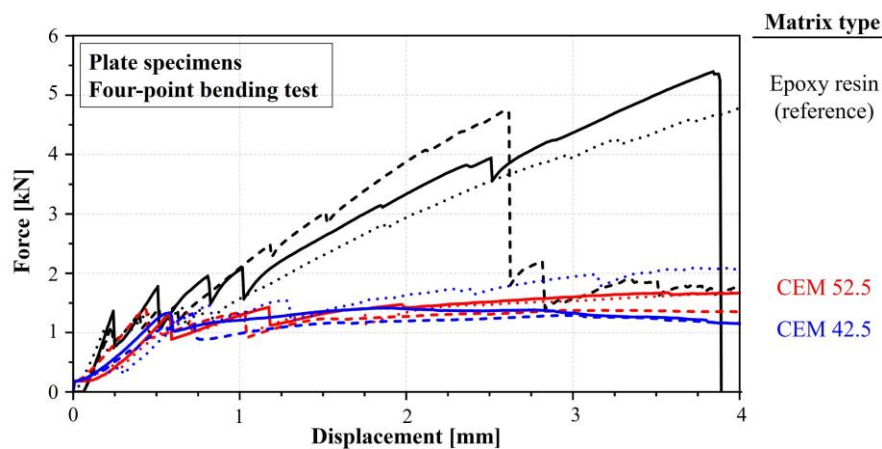


Figure 17: Evaluation of four-point bending tests of experimental specimens with different type of textile reinforcement matrix (pressure saturation)

Based on the results from the four-point bending tests, the textile reinforcement saturation with CEM 52.5 R proves to be a possible variant usable for replacing the combustible synthetic matrix of textile concrete. The tests performed confirmed the hypothesis that better mechanical behaviour occurs when a matrix with a smaller particle distribution is used. This was proven both on the basis of microscopic tests of cement suspension and fibre saturation in percent (Figure 15 and Figure 16) and on the basis of the results of mechanical tests presented in Figure 17. When the reference samples and series B specimens were compared (pressure saturation with CEM 52.5), it was clear that the specimens achieved approximately 30% efficiency of loading capacity compared to the reference specimens (specimens with ER matrix).

Verification of the cement suspension at elevated temperatures⁷

(Subobjective III)

The mechanical tests were divided into two main test packages. In the first test package, specimens at ambient temperatures were tested, and results from mechanical tests served as a reference. In the second test package, specimens were exposed to a standard temperature curve according to EN 1363-1. For these specimens, residual bending strength was subsequently determined. For each test package, specimens with three different covering layers and two different HPC mixtures were created. The concrete mixtures differed in the presence of PP fibres whose amount was determined based on previous fire tests in [25].

The bending strength of all the reference specimens was determined by four-point bending tests. Based on these mechanical tests, the negative influence of PP fibres in the HPC mixture was observed, especially in case of specimens with textile reinforcement saturated with cement suspension. Concurrently, the maximum measured bending strength value was approximately 24% less than for specimens without PP fibres, see Figure 18a. In contrast, in test specimens with an epoxy resin matrix, no significant effect was observed of PP on the attained bending strength, as was the case for samples with a

⁷ The description of the elements tested and the interpretation of results were summarized based on the article *Experimental Evaluation of Carbon Reinforced TRC with Cement Suspension Matrix at Elevated Temperature* [34].

cement suspension matrix Figure 18b. Simultaneously, a different pattern of specimen failure can be observed. In specimens with a cement suspension matrix (Figure 18a), the reinforcing carbon yarns were pulled out, and no progressive collapse occurred. On the contrary, the specimens with epoxy resin matrix were broken after reaching the tensile strength of carbon reinforcement (Figure 18b).

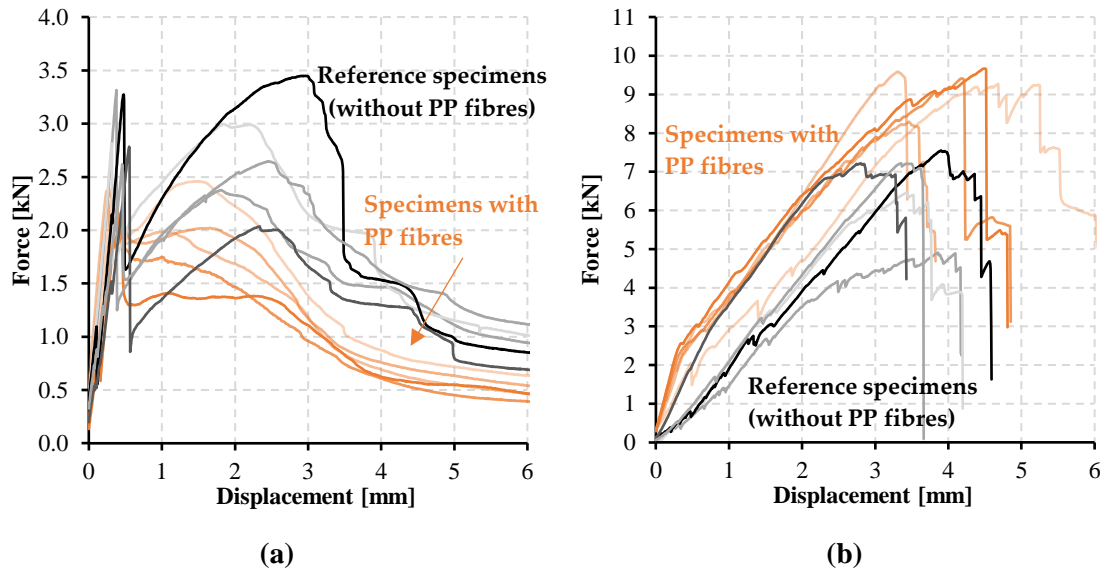
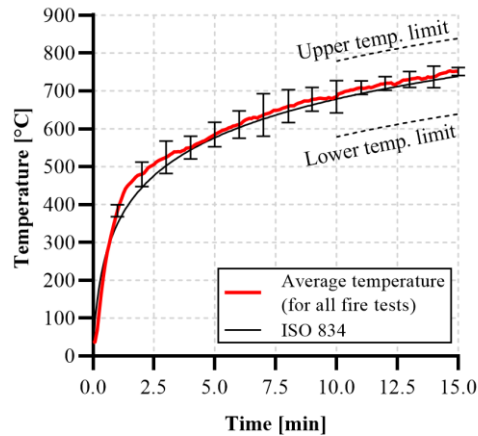


Figure 18: Bending strength of reference specimens with covering layer 0 mm:
(a) specimens with cement suspension matrix; (b) specimens with epoxy resin matrix

In the second test package, fire tests were performed. All specimens were mounted into the test furnace (see Figure 19a) and exposed to the standard temperature/time curve according to EN 1363-1. The temperature distribution in the furnace during the entire fire test is given in Figure 19b. A bigger difference between the actual measured gas temperature and the ISO temperature curve was observed between minutes 5 and 8. Nevertheless, the limits prescribed from minute 10 onwards were not exceeded. The individual temperature measured differs by a maximum of 45 K compared to ISO 834. For this reason, the temperature distribution in the test furnace was satisfactory for each fire test.



(a)



(b)

Figure 19: Instrumentation of the fire tests:

(a) furnace for intermediate fire tests miniFUR; (b) average temperature distribution in the furnace during fire tests

After fire exposure, the specimens with PP fibres added to the HPC mixture retained their integrity. However, all the specimens without PP fibres were destroyed due to the increased inner water vapour pressure and the closed pore structure of HPC in combination with the slender character of the specimens. Therefore, it was impossible to determine the residual bending strength of these specimens.

Different behaviour was observed for specimens with epoxy and cement matrix based on the visual analysis of specimens directly after the fire exposure. In addition, different behaviour was observed for test specimens with the addition of PP fibres using various materials of the textile reinforcement matrix. For specimens with cement suspensions, spalling of concrete layers did not occur in any test. Only transverse cracks were observed because of the fire exposure. Similar behaviour was observed for specimens with an epoxy resin matrix and no covering layer (0 mm). The absence of spalling may be due to the reinforcing layer being placed near the fire-exposed surface of the specimen and allowing additional reinforcement against spalling and, at the same time, it may be due to the migration of the epoxy resin thermal decomposition product out from the test specimen.

On the other hand, in the case of specimens with the epoxy resin matrix and covering layers of 5 mm and 10 mm, the separation of the entire area of the covering layers was observed. In most cases, the covering layers fell off, leaving the textile reinforcement exposed to fire. Therefore, it was not possible to determine the residual bending strength

for these specimens. After the fire exposure, based on the four-point bending tests, the residual bending strength of specimens exposed to elevated temperatures was determined. It was observed that the epoxy resin matrix completely burned out due to the direct fire exposure of the textile reinforcement or due to exceeding the ignition temperature of the epoxy resin when the covering layer did not spall.

On the contrary, the cement matrix was partially damaged on the surface, and the interaction between materials remains undisturbed to a certain extent. The specimens with a cement suspension matrix tested at elevated temperatures showed a similar trend of bending strength capacity as the reference specimens (Figure 20a). The results show that these specimens did not incur a significant decrease in mechanical bending strength as in the case of samples with the epoxy resin matrix. This was caused by the better temperature resistance of the cement suspension matrix material. Due to temperature effects, the bending strength decreased by approximately 40%. Simultaneously, the cement suspension samples showed a significant increase in ductility. Higher ductility was caused by the gradual pull-out of the individual filaments of the carbon yarn during the whole mechanical test. In contrast to the specimens with an epoxy resin matrix, the textile reinforcement did not drop out during mechanical tests, and no progressive break occurred.

In the tested specimens with an epoxy resin matrix, we observed a significant degradation of the epoxy resin due to the attained temperatures during the fire test. Therefore, a significant loss of mechanical properties of these specimens occurred (Figure 20b). During the fire tests, this matrix was burned out. Subsequently, the ability to homogenize the individual filaments in the textile yarn was infringed. In contrast to the reference specimens with an epoxy resin matrix, no progressive break occurred when the tensile strength of the textile reinforcement was reached. Specimens with the epoxy resin tensile reinforcement matrix exposed to elevated temperature were broken due to the pulling of the textile reinforcement or breakage due to absent interaction between the textile reinforcement and HPC – the textile reinforcement disengaged from HPC.

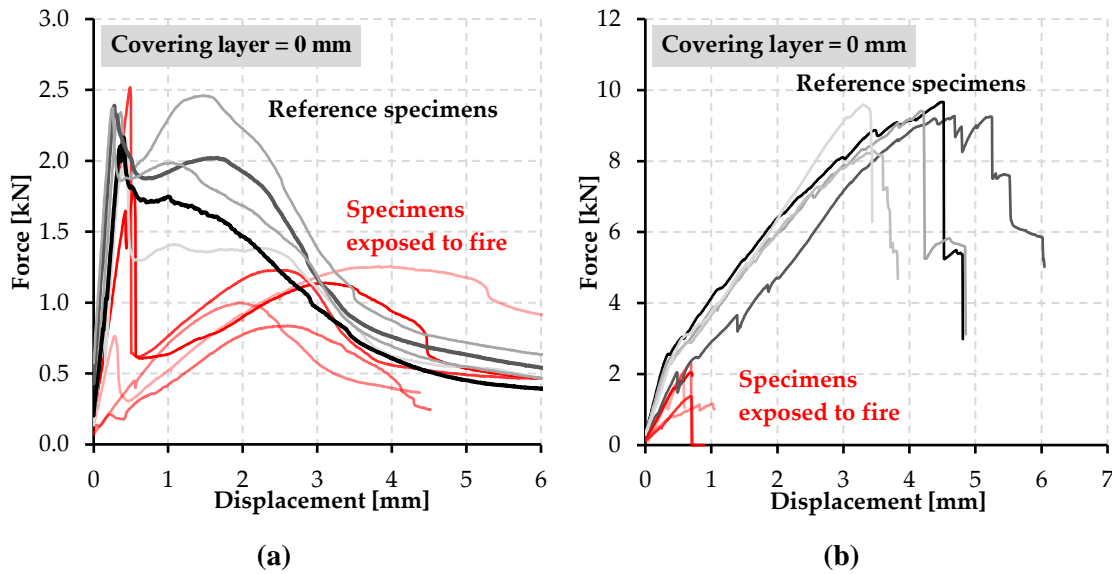


Figure 20: Residual bending strength of specimens exposed to elevated temperatures with covering layer of 0 mm:
(a) specimens with cement suspension matrix; (b) specimens with epoxy resin matrix

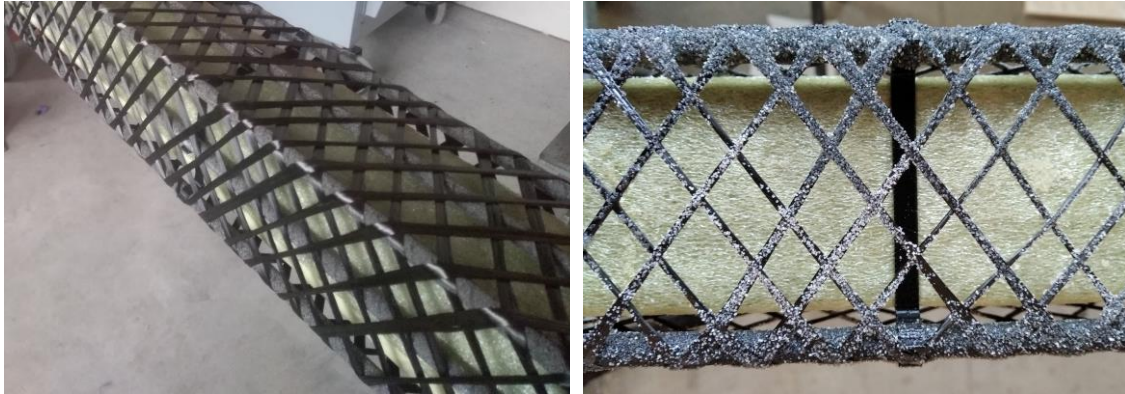
Validation of conclusion at the real-scale fire tests⁸

(Subobjective IV)

The conclusions presented in *Subobjective IV* are based on a two-year research project called *Karbeton-II* [14]. The project's main objective was to develop and verify the mechanical parameters of the TRC lightweight column structure [36, 37]. Moreover, the fire-resistance class of the manufactured load-bearing members was classified. The beginning of the development focused on the effective structural design, i.e. the shape and cross-section of the member, the amount of textile reinforcement and on determining the manufacturing procedure. In general, the research performed included other mechanical analysis, tests, investigations and design steps. However, this chapter presents selected analyses related to fire resistance and to the content of the thesis only.

⁸ The description of the elements tested and the interpretation of results were summarized based on the final report for the *Karbeton-II* research project, *TACR Zeta* [45, 46].

In the first part, the quantity of the material used for HPC mixture was optimized. Optimization aimed to achieve suitable mechanical parameters of HPC, i.e. compressive and tensile strength, modulus of elasticity and workability during the casting process. In the subsequent steps, the load-bearing capacity of the test specimens in the intermediate scale was tested. Then, based on the results, the most effective variant of textile reinforcement application was determined. The applied carbon textile reinforcement of the intermediate test specimen is given in Figure 21.



(a)

(b)

Figure 21: Prepared textile reinforcement for specimen $100 \times 100 \text{ mm}^2$ with $4 \times \text{ø}4 \text{ mm}$ CFRP rebars before HPC casting [14]:

(a) Before application of the epoxy resin matrix; (b) cured carbon reinforcement with treated surface based on the results from *Paper I*

Before the real-scale fire tests were carried out, an indicative fire test to verify the adherence of the selected fire-protection system was performed. Calcium-silicate boards [47] and gypsum plaster [48] were chosen as the fire protection systems. Since calcium-silicate boards can be mounted without anchoring them to the protected member, the effect of adherence does not play a role in this case. Therefore, an indicative fire test was performed only with gypsum plaster directly applied to the member's surface. In total, four specimens with treated member surface were created. Specimens for the unloaded indicative fire test had the shape of half of an axisymmetric column member designed for a real-scale test, shown in Figure 22.



Figure 22: One of the specimens with gypsum plaster for the indicative fire test

In total, four different specimens with different surface treatment were created:

- **Variant A:** without any surface treatment (a reference specimen);
- **Variant B:** with surface treatment with Knauf Betokontakt adhesive bridge [49];
- **Variant C:** with a Knauf Betokontakt adhesive bridge and steel mesh in the middle of the plaster layer (not anchored) [49];
- **Variant D:** with an adhesive bridge and steel mesh anchored by screws to the test specimen body [49].

Based on the fire test, the adherence between HPC and gypsum plaster in Variants A and B was observed to be insufficient and enable the creation of a cavity between the plaster and the protected member. The fire-protection layer did not fall off only due to the absence of the applied load-protection layer. On the contrary, the use of steel reinforcement in the gypsum plaster, i.e. Variants C and D, prevented the formation of a cavity between the materials and reached a slightly better insulation ability which was also proved based on the measured temperatures at the first layer of textile reinforcement. Altogether, they have proven to be an effective protection. To prevent damaging the specimen due to the anchoring of the steel reinforcing mesh of the plaster layer, Variant C, with the mesh not anchored to the test specimen surface, was selected for the real-scale test. Specimens with gypsum plaster after the unloaded indicative fire test are shown in Figure 23.

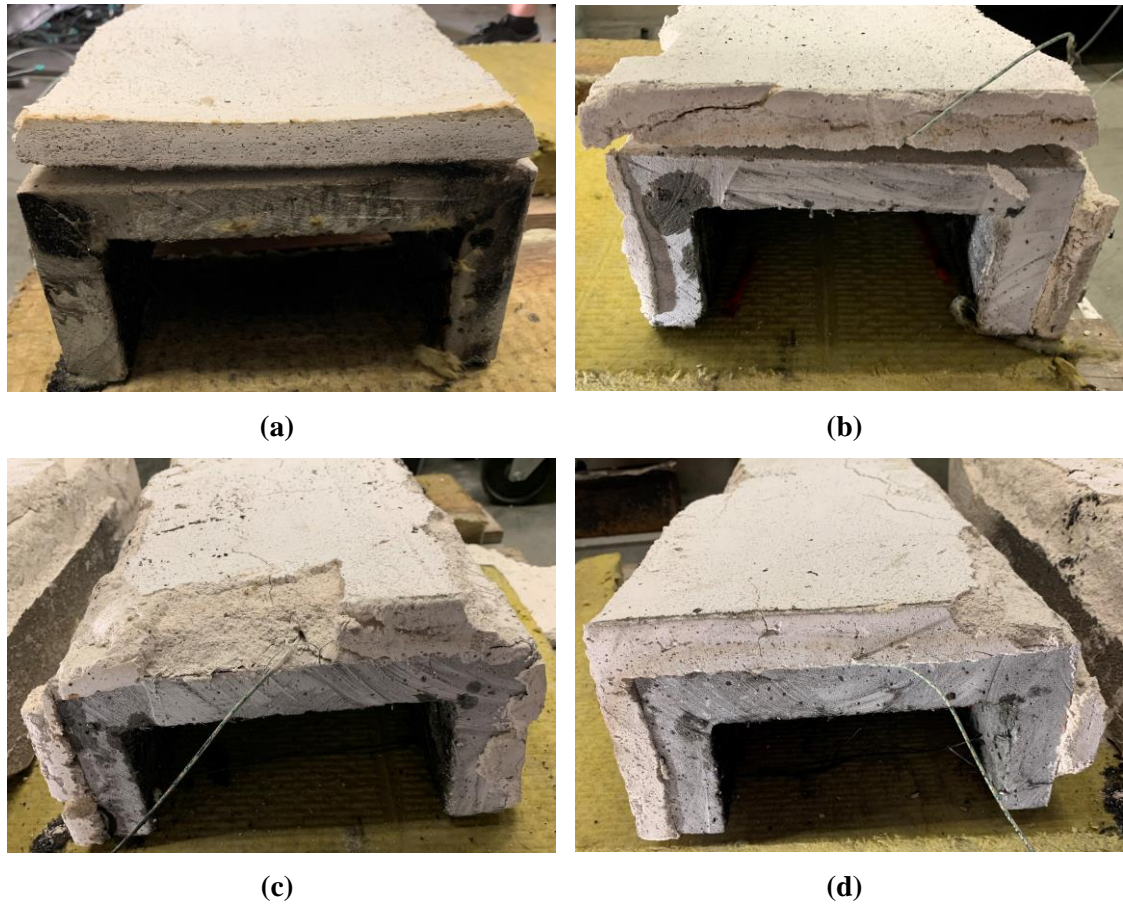
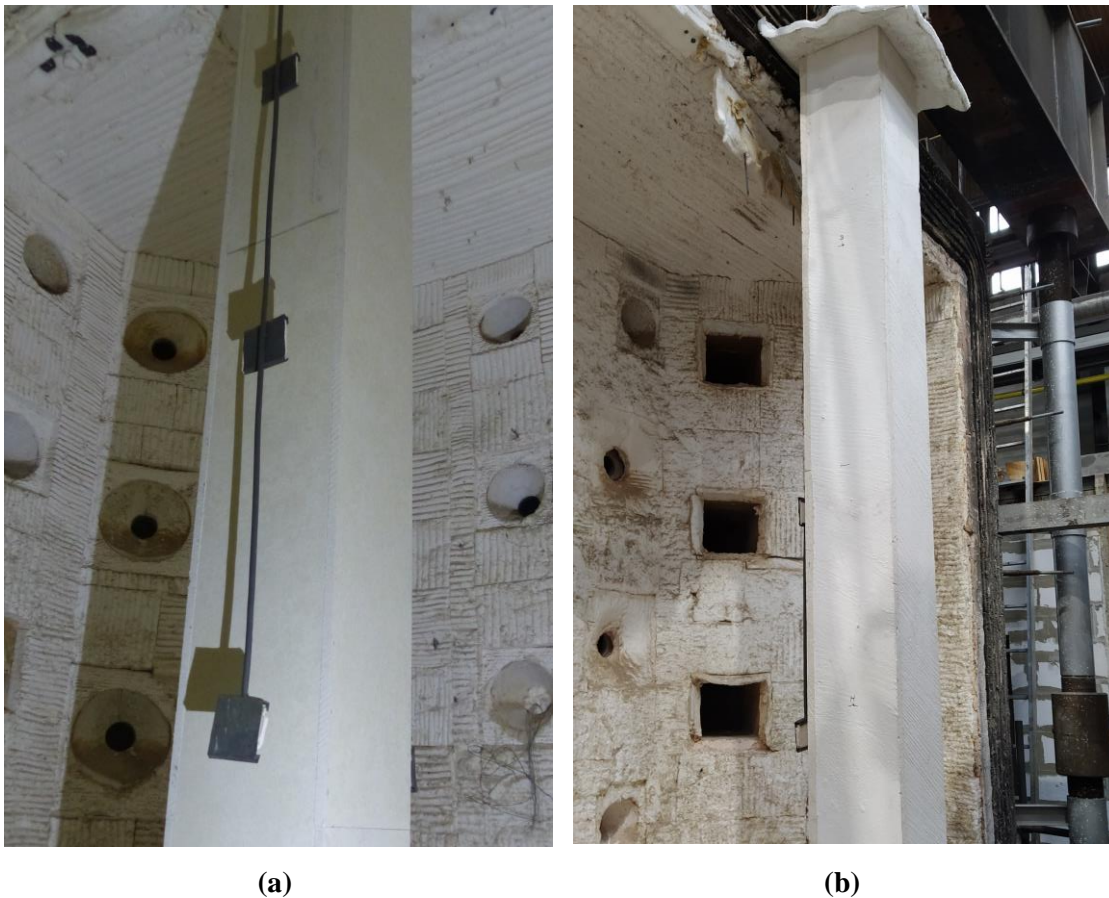


Figure 23: Specimens with gypsum plaster with thickness 30 mm after fire test:
(a) Variant A: without any surface treatment (reference specimen);
(b) with surface treatment with Knauf Betokontakt adhesive bridge;
(c) with a Knauf Betokontakt adhesive bridge and steel mesh in the middle of the plaster layer (not anchored);
(d) with an adhesive bridge and steel mesh anchored by screws to the test specimen body.

The first experiment was performed on smaller test specimens for column design optimization. Based on those results, columns and their possible fire protection was designed and performed with the following tests of mechanical and fire resistance. Experiments will be focused on the fire resistance of columns because it is the biggest obstacle for application in civil engineering before its certification.

Based on the individual analysis and tests performed, two real-scale columns with a height of $h = 3000$ mm, a cross-section of 250×250 mm² and a wall thickness of 33 mm were created. Both specimens were intended for a fire-resistance test in an accredited fire laboratory. Both real-scale fire tests were performed according to EN 1365-4 [50]. Based on the structural design, the loaded force was determined as 1000 kN with an eccentricity of 10 mm from the central axis of the specimen. The load was applied by a hydraulic

furnace loading system 30 minutes before the test and maintained at constant levels throughout the entire test. The fire tests started after the deformation was stabilised. The test specimens before the fire tests are shown in Figure 24.



**Figure 24: TRC column test specimens before the fire test with fire protection:
(a) Calcium-silicate boards Promatect-H; (b) Gypsum plaster Knauf Vermiplaster**

For both specimens tested, the design temperature was not exceeded during the intended duration of the fire test of 60 minutes. In the case of the calcium-silicate board system, Promatect-H, a local opening of a horizontal joint between the boards occurred during the fire test (Figure 25a). However, even this breach of the fire-protection layer did not cause a significant increase in temperatures inside the test body. In the case of the gypsum plaster protection layer, the development of hairline cracks over the entire surface of the test specimen was observed. Moreover, local falling off of the protective material at the corners of the cross-section occurred (see Figure 25b).

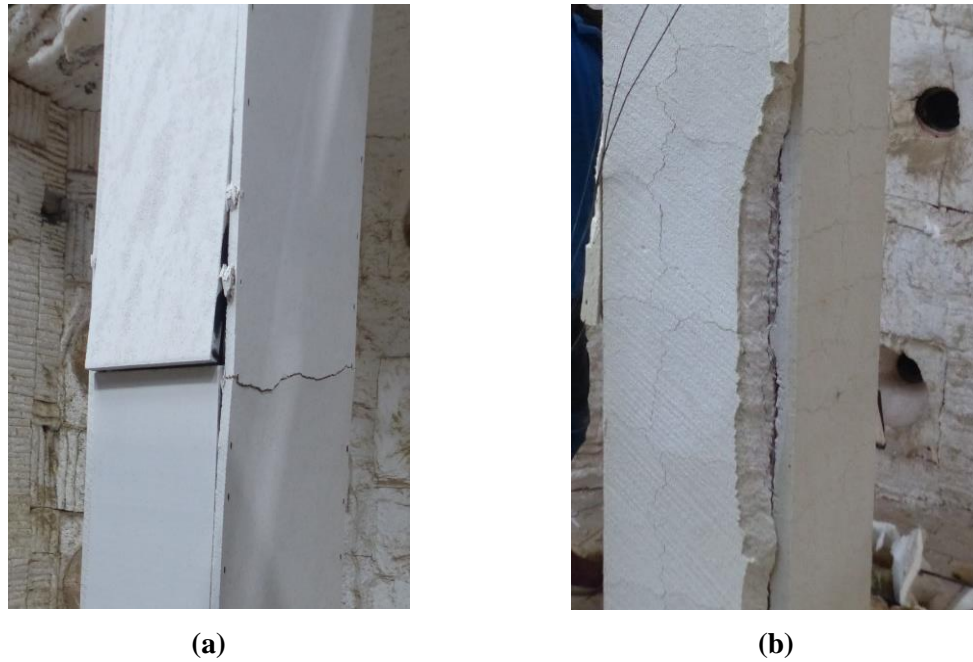


Figure 25: Test specimens and the damaged fire-protection layer after the fire test:
(a) Gypsum plaster Knauf Vermiplaster; (b) Calcium-silicate boards Promatect-H

During the entire test, no cavity was formed between the fire-protection layer and the column body. The absence of the cavity was caused due to the additional reinforcement of the plaster layer with a thin steel grid, based on a series of indicative fire tests, which were performed before the real-scale tests [45, 46]. There was therefore no condensation of water vapour at the interface of the materials. The rise of temperature on the first layer of the carbon reinforcement was almost linear throughout the entire duration of the fire test. Similar to the calcium-silicate board system, the critical design temperature was not exceeded. Therefore, the gypsum plaster also proved its insulation ability. For the temperatures measured on the first layer of textile reinforcement, see Table 8.

Table 8: The temperature of the test specimens reached at the first layer of the textile reinforcement

Fire protection system [-]	Time [min]				
	0	15	30	45	60
Promatect-H	11 °C	13 °C	33 °C	63 °C	91 °C
Vermiplaster	14 °C	33 °C	67 °C	89 °C	109 °C

The column protected by the calcium-silicate board system did not exceed the limit value of the vertical compression deformation limit of $C = 30$ mm, determined as $C = \frac{h}{1000}$ mm, and the compression rate of deformation $\frac{dc}{dt} = 9$ mm·min⁻¹, determined as $\frac{dc}{dt} = \frac{3 \cdot h}{1000}$ mm·min⁻¹ throughout the entire fire test, was as determined based on [50]. The test was

terminated after reaching minute 120 of the test, during which the limit values of deformation were not exceeded. Although the temperatures at the end of the fire test exceeded the critical temperature (T_g) on the first layer of the textile reinforcement, the pressure load was dominant due to the small eccentricity. The column did not collapse even though the epoxy resin matrix of the textile reinforcement was degraded due to the temperature increase. For this reason, the fire resistance could be officially classified as R 120 [51]. On the other hand, in the case of the specimen with the gypsum plaster protection system, a local break at the top corner occurred during the test's loading phase, see Figure 26.



Figure 26: Detail of local failure at the edge of the test specimen with Knauf Vermiplaster

It was caused due to a manufacturing imperfection of the textile reinforcement. A probable reason was insufficient textile reinforcement matrix saturation at the column's top corner, which could not transfer the transverse tensile forces without breaking during the load application. For this reason, applying adequate load was impossible and the entire fire test was without any load. Despite the absence of load, the fire test was carried out to observe the gypsum plaster's insulating ability and a temperature increase in the specimen. The temperatures measured were subsequently compared with temperatures from the test specimens with a calcium-silicate protection board system. However, based on the temperatures measured (see Table 8), it can be assumed that if there had been no significant damage to the fire-protection layer due to the applied load, there would have been no collapse, and the column would have retained its load-bearing capacity for the planned 60 minutes. The fire test was terminated in the planned time of 60 minutes, but due to the absence of load, it was impossible to classify the corresponding fire resistance.

5. CONCLUSIONS

The presented research aims to improve the TRC slender structures' behaviour exposed to elevated temperatures. This was achieved by performing a series of tests, including the findings from micro-scale tests (microscopic analysis, differential scanning calorimetry), intermediate-scale mechanical tests at ambient and elevated temperatures, and subsequently verified by real-scale fire tests on slender column structures with hollow sections.

Determination of TRC initial mechanical parameters

First of all, textile reinforcement in the form of a single impregnated textile yarn with a smooth and fine-grained silica sand-treated surface was tested by pull-out tests [12]. The tests showed that in contrast to specimens with a smooth surface, the specimens with treated surfaces reached the maximum tensile stress values in the composite reinforcement (Figure 9).

In the case of the test series with smooth surface yarn, it was observed that after the activation of the reinforcement at its full length, there was a very slow increase in force during the load application (Figure 9a). It was caused due to the deficient interaction between the textile reinforcement and HPC. The results imply that it is necessary to consider a larger anchorage length of the smooth composite reinforcement to provide a sufficient force transfer between materials.

Compared to the results given in Figure 9b, specimens with the treated surface of carbon yarn reached significantly higher contact stiffness. The treated surface of the reinforcement prevented slipping in HPC during load application, and therefore all specimens were broken before the carbon yarn was pulled out. Moreover, the results from the specimens with treated textile reinforcement surfaces showed a more stable trend of force/displacement curves (Figure 9b and Figure 10). The use of textile reinforcement with a treated surface appeared to be a better variant for the final production of TRC reinforcement.

Experimental evaluation of TRC risk areas at elevated temperatures

Following the tests performed at elevated temperatures, spalling of concrete layers and loss of interaction between materials were identified as highly problematic risk areas of TRC exposed to fire. The HPC higher spalling risk is associated with a low porosity of

the hardened material in comparison to concretes with standard compressive strengths. However, this issue becomes more important in the case of slender load-bearing members because the spalling of concrete layers can significantly weaken the constructions, potentially compromising their load-bearing capacity.

In the case of TRC, where the load-bearing wall of a structural member had a width of approximately 30 mm [22, 52], the spalling of concrete layers must be reduced. One possible solution to reduce the spalling of concrete layers is using polypropylene (PP) fibres in the HPC mixture. These fibres facilitate migration of water evaporation outside of the member and thus significantly reduce the risk of spalling [52]. Based on a series of several tests, the ideal amount of PP fibres in the HPC mixture was determined as $4 \text{ kg}\cdot\text{m}^{-3}$ [25]. Nevertheless, the presence of PP fibres in the HPC mixture leads to a decrease in the HPC mixture workability, which can lead to manufacturing imperfections. It was necessary to establish the right amount of PP fibres which would allow the casting of TRC without any manufacturing imperfections.

Specimens with an epoxy resin matrix contributed to the development of fire regardless of the occurrence of the spalling of concrete layers, i.e. whether PP fibres are present or not in the HPC mixture, respectively (Figure 12 and Figure 13). In the case of specimens with an HPC mixture where PP fibres were present, spalling was eliminated, but the burnt PP fibres formed a “pore bridge”, which allowed the migration of the thermal decomposition products of the epoxy resin. These decomposition products subsequently started burning at the surface of the specimens (Figure 13). Although specimens with PP fibres kept their integrity, loss of cohesion between the materials was observed. It was caused due to the low temperature resistance of the epoxy resin matrix because, firstly, these decomposition products started burning after the matrix thermal degradation and, secondly, the cohesion between HPC and the textile reinforcement was completely lost, which was determined based on mechanical tests (Figure 14). The residual bending strength of the specimens without PP fibres was not determined due to the massive spalling out of the concrete layers.

For further investigation, changes in the mechanical properties of HPC must also be considered. Based on the results of the mechanical tests, it was determined that the bending strength of HPC decreased by approximately 30% after exposure to elevated temperatures. On the contrary, the compressive strength increased by approximately 22% (Figure 11). The increase in HPC strength was experimentally demonstrated in [42, 44],

where the change in mechanical properties is associated with the temperature reached in the specimens. These experimental results contradict the conclusions of EN 1991-1-2 [52], which considers the loss of mechanical properties only, i.e. tensile and compressive strengths. The increased HPC compressive strength may be associated with a particular HPC mixture. For this reason, it is necessary to experimentally determine the change in mechanical strength for each concrete mixture to allow the effective design of TRC structures.

For the further design of TRC, it is essential to distinguish which type of construction is being assessed. The thesis particularly evaluates the use of TRC for columnar (vertical) structures, which are loaded primarily by pressure in combination with bending moment. Therefore, an increase in compressive strengths can contribute to load-bearing capacity of the member in the first part of the fire exposure. However, if TRC was used primarily for bent (horizontal) members, there would be a substantial loss of the concrete tensile strength. This could lead to under-reinforcement of the member and inappropriate structural design. In this case, it is necessary to consider the length of exposure to elevated temperatures, as all mechanical parameters may be reduced if the limit temperatures are exceeded. Otherwise, the procedure defined in EN 1991-1-2 [52] can be used, which only takes into account the decrease in the mechanical parameters of the HPC.

Use of alternative matrix of textile reinforcement

In response to the identified risk behaviour of synthetic resins at elevated temperatures, the use of non-flammable cement-based materials was verified. The aim was to propose a material alternative that would replace the flammable material in TRC and simultaneously achieve a suitable load-bearing capacity. Two different cement types were tested, CEM 42.5 and CEM 52.5, with two different penetration methods, i.e. surface saturation and pressure saturation. The microscopic tests revealed that CEM 52.5 has a higher quantity of smaller particles with an average size of 9 μm . This was in contrast to CEM 42.5, where the average size of particles reached approximately 16 μm (Figure 15) and particles' flocculation was observed (Figure 15b).

In the following mechanical tests, the ability of the textile reinforcement penetration by cement suspension and the related bending capacity was verified. This confirmed the assumption that materials with the most homogeneous structure possible were more suitable for achieving a higher degree of saturation in combination with the average size of the individual fibres in the bundle of textile reinforcement (Table 1). This trend was

also confirmed based on the results from the four-point bending tests (Figure 17). Furthermore, bending capacity was also linked to a percentage of saturation of the textile reinforcement which was defined based on the microscopy visual analysis in [6]. As part of the mechanical tests, two different HPC mixtures were assessed. The mixtures differed in the presence of PP fibres with the amount defined in [25]. However, according to Figure 18, it was figured out that the addition of PP fibres negatively affected the bending strength of the specimens with textile reinforcement and a cement suspension matrix. On the other hand, the presence of PP fibres had no reliable effect on the bending strength of the test specimens with epoxy resin.

Mechanical parameters of the non-flammable matrix at elevated temperatures

The suitability of cement suspension was also assessed at elevated temperatures (Figure 20). The test specimens with a textile reinforcement matrix of cement suspension experienced a decrease in bending strength of approximately 40% compared to the reference specimens, and the contribution to fire development was successfully eliminated. The load-bearing capacity decrease was linked to the degradation of the mechanical properties of the HPC as well as of the cement suspension due to the fire exposure. Compared to that, specimens with a textile reinforcement matrix from epoxy resins de facto lost their ability of cohesion between the reinforcement and the HPC due to the thermal degradation of the resins. Pulping of the reinforcement was observed, and the ability to intermediate interaction between materials was lost.

Real-scale tests of TRC

Conclusions from the previous experimental works presented in [6, 12, 25, 34] were verified based on tests at elevated temperatures in a real scale. In total, two TRC real-scale column specimens were created. For their manufacturing, the combination of HPC and carbon textile reinforcement impregnated with epoxy resin proved to be the best solution for structural member manufacturing. However, based on the conclusions from fire tests, risks were revealed, including restrictions on the use at elevated temperatures [13, 25, 34].

For this reason, additional protection layers from calcium-silicate boards and gypsum plaster were designed to prevent unwanted rises in temperature in the member (Figure 24). Based on the real-scale tests performed, the column structural member with a hollow section achieved fire resistance R 120 [51] with a fire protection layer from calcium-silicate board systems with a thickness of 2×20 mm (Figure 25). Therefore, based on the

experience with structural design and the officially determined fire-resistance class, the TRC column with a fire-protection layer could be used in civil engineering as the first example of this type of composite structural member.

Unfortunately, the column specimen with a gypsum fire protection system was damaged at its top part during the load phase of the fire test (Figure 26), making it impossible to determine the fire-resistance class according to [50]. However, a satisfactory temperature increase was observed based on the measured temperature data and their comparison with the temperatures from the specimens with calcium-silicate boards. The top specimen corner was damaged, probably due to the local textile reinforcement weakening. Considering this issue, it is necessary to verify the amount of the textile reinforcement in critical areas, i.e. at the top and bottom of a structural member, as well as the saturation state level. This applies even to cases of epoxy resin reinforcement, although it commonly reaches sufficient saturation ability. Alternatively, a slight over-reinforcement at the top and bottom parts of the vertical structural member may be suitable.

The tests performed focused on describing the behaviour of TRC exposed to fire. As a result, several problematic areas have been pointed out in order to be included in further assessment for use as a load-bearing construction material. In addition to the criteria necessary for the structural design, it is also essential to consider legislative restrictions that may apply to the combination of the materials used – especially flammable materials such as a synthetic resin matrix of textile reinforcement.

Legislative restrictions address mainly the risk of epoxy resin contribution to the development of fire. For example, in the Czech Republic, structures with flammable components contributing to the development of fire are considered to be equivalent to wooden columns. Due to this classification, these structural members are subject to strict restrictions, and their further use is excluded, for example, in buildings higher than 9 m [53, 54]. For this reason, it is necessary to explore further material optimization, as strict restrictions could fundamentally limit the use of TRC in civil engineering if flammable materials are used. In conclusion, once the identified challenges are fixed, TRC can be included in the most traditionally used reinforced concrete load-bearing structures.

6. FUTURE WORK (OUTLOOK)

Based on the work performed within this thesis framework, the following steps were suggested for further research, extending the knowledge about using TRC for load-bearing structural members. Possible subsequent steps in developing the TRC are divided into the following subchapters:

Determination of heat release rate of TRC

In [25] it was demonstrated that the use of synthetic resins as a matrix of textile reinforcement could contribute to the development of fire (Figure 12). Therefore, based on the national requirements, e.g. in the Czech Republic or Germany, this type of structure can be limited due to the use of flammable parts as an important part of construction, i.e. the part which contributes to load-bearing capacity. In accordance with the standard restrictions, TRC columns may be considered as structural members equal to vertical structures from plain wood. Therefore, it is recommended that the total heat release rate (HRR) of TRC be determined by e.g. cone calorimetry tests according to ISO 5660 [55]. Then, reliable comparisons and classifications of TRC members will be possible based on the results of this analysis compared to other materials.

Use of geopolymers as alternative matrix

Based on the results of the alternative cement-based textile reinforcement matrix materials tested, it would be appropriate to identify materials that achieve better mechanical properties than the results presented in [6, 34]. As a possible alternative, the use of fly ash-based geopolymers could be relevant for further testing.

It was found that the particle size of the applied matrix, in combination with the saturation method, affects the percentage of yarn saturation and the related mechanical properties. The geopolymer particle size is significantly smaller than cement particles. Moreover, geopolymers achieve excellent mechanical properties and temperature resistance [56]. Therefore, their use could be a way to substitute the combustible matrix of textile reinforcement while achieving better mechanical properties than cement suspension.

Use of intumescent coatings as an alternative fire protection

In one part of the *Karbeton II* research project [14], column specimens were tested with an additional applied layer of fire protection from calcium-silicate boards with a thickness of 40 mm and gypsum plaster with a thickness of 30 mm and exposed to a standard temperature curve. Unfortunately, the thickness of the protection layers was equal to or greater than the load-bearing wall (33 mm) of the column with the hollow section. Intumescent coatings (ICs) could be a potential solution, as they reach thicknesses of approximately from 1 to 5 millimetres after application [38]. Thanks to this, it would be possible to preserve the subtle character of constructions and thus significantly save additional materials used to protect TRC structures.

Real-scale fire test

It is necessary to extend the performed tests package in real scale of TRC structural members, as well as to determine the failure principles of TRC. At the same time, use of another fire protection systems, e.g. reactive fire-protection systems or verification of alternative matrix materials from geopolymers or different types of cement suspensions, other than those described in [6, 34] is planned. However, based on the test data, the use of columnar real-scale specimens turns out to be less suitable due to the use of risky materials, i.e. materials with low temperature resistance in the position of the shear or bending reinforcement. Therefore, it would be appropriate to change the character of the test specimen from members that are primarily loaded by pressure (columns) to members that are loaded mainly by bending (beams). In this case, observing the effect of the degradation of the mechanical properties of the materials used at elevated temperatures would be more effective

REFERENCES

- [1] Curbach, M., Fuchs H., Hegger, J. and Offermann, P. Sachstandbericht zum Einsatz von Textilien im Massivbau. Beuth Verlag, ISBN 978-3-410-65688-3. 1999. doi:10.2366/12477501
- [2] Scheerer, S., Chudoba, R., Garibaldi, M. P., ARIBALDI and M. Curbach, M. Shells Made of Textile Reinforced Concrete – Applications in Germany. *Journal of the International Association for Shell and Spatial Structures*. 2017, 58(1), 79–93. ISSN 1028365X, 19969015. doi:10.20898/j.iass.2017.191.846
- [3] Laiblová, L., Vlach, T., Michal Ženíšek, M., Řepka, J. and Hájek, P. Lightweight TRC Facade Panels with the LEDs. *Key Engineering Materials*. 2018, 760, 141–146. ISSN 1662-9795. doi:10.4028/www.scientific.net/KEM.760.141
- [4] Řepka, J., Vlach, T., Laiblová, L., Hájek, P., Ženíšek, M. and Kokeš, P. Thin Lightweight Panels Made of Textile Reinforced Concrete. *Solid State Phenomena*. 2017, 259, 238–243. ISSN 1662-9779. doi:10.4028/www.scientific.net/SSP.259.238
- [5] Raupach, J., Orlowsky, J., Büttner, T., Diltthey, U and Schleser, M. Epoxy-impregnated textiles in concrete – Load bearing capacity and durability. *ICTRC'2006 - 1st International RILEM Conference on Textile Reinforced Concrete*. RILEM Publications SARL. 2006, 77-88. ISSN 2351580087. doi:10.1617/2351580087.008
- [6] Fürst, R., Fürst, E., Vlach, T., Řepka, J., Pokorný, M. and Mózer, V. Use of Cement Suspension as an Alternative Matrix Material for Textile-Reinforced Concrete. *Materials*. 2021, 14(9). ISSN 1996-1944. doi:10.3390/ma14092127
- [7] Kulas, C., Solidian GmbH. Actual applications and potential of textile-reinforced concrete. *International Glassfibre Reinforced Concrete Association*. 2015, Dubai.
- [8] Tysmans, T., Adriaenssens, S., Wastiles, J. and Remy, O. Textile reinforced cement composites for the design of very thin saddle shells: A case study. *18th international conference on composite materials*. 2018, Athenes.
- [9] Ducháček, V. VŠCHT v Praze. Polymery: výroba, vlastnosti, zpracování, použití. Prague, Publisher VŠCHT, 2006. ISBN 978-80-7080-617-3.

- [10] Procházka, J., Štefan, R., Vašková, J., and CTU in Prague, Faculty of Civil Engineering. Navrhování betonových a zděných konstrukcí na účinky požáru. Prague, Publisher: CTU in Prague, 2010. ISBN 978-80-01-04613-5.
- [11] Peled, A., Bentur, A. and Mobasher, B. Textile reinforced concrete. London, Publisher: CRC Press, 2017. ISBN 9781315119151. doi:10.1201/9781315119151
- [12] Vlach, T., Řepka, J., Hájek, J., Fürst, R., Jirkalová, Z. and Hájek, P. Cohesion test of a single impregnated ar-glass roving in high-performance concrete. *Stavební obzor – Civil Engineering Journal*. 2020, 29(03), 358–369. ISSN 18052576. doi:10.14311/CEJ.2020.03.0032
- [13] Fürst, R. Fire specifics of building load-bearing structures of textile-reinforced concrete. Prague, 2019. Master thesis, Czech Technical University in Prague, Faculty of Civil Engineering.
- [14] Development of concrete lightweight columns with carbon reinforcement as element for load-bearing structures with loading and fire tests (Karbeton-II), Technology Agency of the Czech Republic, program for young researchers Zeta, Prague (2019-2021), PID: TJ02000119.
- [15] Application of alternative materials in textile concrete and their evaluation at room temperature and at elevated temperature. Grant Agency of the Czech Technical University in Prague, Prague (2020-2022). No.: SGS21/094/OHK1/2T/11
- [16] Walraven, J. and Stoelhorst, D. Tailor Made Concrete Structures. London, Publisher: CRC Press, 2008. ISBN 9780429103605. doi:10.1201/9781439828410
- [17] Kynclova, M., Fiala, C. and Hájek, P. High Performance Concrete as a Sustainable Material. *International Journal of Sustainable Building Technology and Urban Development*. 2011, 2(1), 63–68. ISSN 2093-761X, 2093-7628. doi:10.5390/SUSB.2011.2.1.063
- [18] Laiblová, L., Pešta, J., Kumar, A., Hájek, P., Fiala, C., Vlach, T. and Kočí, V. Environmental Impact of Textile Reinforced Concrete Facades Compared to Conventional Solutions—LCA Case Study. *Materials*. 2019, 12(19), 3194. ISSN 1996-1944. doi:10.3390/ma12193194
- [19] Portal, N. W. Usability of Textile Reinforced Concrete: Structural Performance, Durability and Sustainability. Goetheburg, 2015. Doctoral thesis, Chalmers University of Technology, Department of Civil and Environmental Engineering, division of Structural Engineering. ISSN 0346-718X.

- [20] Hegger, J., Will, N., Bruckermann, O. and Voss, S. Load-bearing behaviour and simulation of textile reinforced concrete. *Materials and Structures*. 2006, 39(8), 765–776. ISSN 1359-5997, 1871-6873. doi:10.1617/s11527-005-9039-y
- [21] Hegger, J and Voss, S. Investigations on the bearing behaviour and application potential of textile reinforced concrete. *Engineering Structures*. 2008, 30(7), 2050–2056. ISSN 01410296. doi:10.1016/j.engstruct.2008.01.006
- [22] Aïtcin, P. Česká komora autorizovaných inženýrů a techniků činných ve výstavbě and Česká betonářská společnost. High-Performance concrete. Prague, 2005. ISBN 978-80-86769-39-4.
- [23] Shah, H. A., Yuan, Q. and Photwical, N. Use of materials to lower the cost of ultra-high-performance concrete – A review. *Construction and Building Materials*. 2022, 327, 127045. ISSN 09500618. doi:10.1016/j.conbuildmat.2022.127045
- [24] Vlach, T. Adhesion of carbon and basalt composite reinforcement with UHPC. Prague, 2013. Master thesis, Czech Technical University in Prague, Faculty of Civil Engineering.
- [25] Fürst, R., Vlach, T., Pokorný and Mózer, V. Study of Behavior of Textile-Reinforced Concrete with Epoxy Resin Matrix in Fire. *Fire Technology*. 2022, 58(1), 53–74. ISSN 0015-2684, 1572-8099. doi:10.1007/s10694-021-01116-y
- [26] MasterFiber 012: Monofilní vlákno pro zabránění trhlinám na povrchu betonu vlivem plastického smršťování a sedání. Technical data sheet, 2021. Master Builders Solutions Deutschland GmbH.
- [27] SOLIDIAN. Leading in construction with non-metallic reinforcement. [online]. B.m.: Solidian GmbH, Germany. leden 2018. Dostupné z: https://www.solidian.com/fileadmin/user_upload/pdf/solidian_Image_broschure_en.pdf
- [28] Vlach, T., Laiblová, L., Řepka, J., Jiraklová, Z. and Hájek P. Experimental verification of impregnated textile reinforcement splicing by overlapping. *Acta Polytechnica CTU Proceedings*. 2019, 22, 128–132. ISSN 2336-5382. doi:10.14311/APP.2019.22.0128
- [29] Maxineasa, S. G., Taranu, N., Bejan, L. Isopescu, D. and Banu, O. M. Environmental impact of carbon fibre-reinforced polymer flexural strengthening solutions of reinforced concrete beams. *The International Journal of Life Cycle*

- Assessment*. 2015, 20(10), 1343–1358. ISSN 0948-3349, 1614-7502. doi:10.1007/s11367-015-0940-5
- [30] Carbon roving Tenax STS40 F13 24K 1600tex. Technical data sheet, 2010. Toho Tenax.
- [31] Deák, T. and Czigány, T. Chemical Composition and Mechanical Properties of Basalt and Glass Fibers: A Comparison. *Textile Research Journal*. 2009, 79(7), 645–651. ISSN 0040-5175, 1746-7748. doi:10.1177/0040517508095597
- [32] Černý, M., Glogar, P., Sucharda, Z., Chlup, Z. and Kotek, J. Partially pyrolyzed composites with basalt fibres – Mechanical properties at laboratory and elevated temperatures. *Composites Part A: Applied Science and Manufacturing*. 2009, 40(10), 1650–1659. ISSN 1359835X. doi: 10.1016/j.compositesa.2009.08.002
- [33] Isayev, A. Encyclopedia of Polymer Blends. Volume 3: Structure. Publisher: Wiley-VCH, 2016. ISBN 978-3-527-31931-2.
- [34] Fürst, R., Hejtmánek, P., Vlach, T., Řepka, J., Mózer, V. and Hájek, P. Experimental Evaluation of Carbon Reinforced TRC with Cement Suspension Matrix at Elevated Temperature. *Polymers*. 2022, 14(11), 2174. ISSN 2073-4360. doi:10.3390/polym14112174
- [35] EN 1992-1-2 Eurocode 2: Design of concrete structures, Part 1-2: General rules - Structural fire design. 2009.
- [36] Vlach, T., Jirkalová, Z., Hájek, J., Řepka, J., Fürst, R. and Hnidka, J. Load-bearing hollow column from high performance concrete with composite reinforcement and anti-fire plaster. Functional sample, 2021. Prague.
- [37] Vlach, T., Jirkalová, Z., Hájek, J., Řepka, J., Fürst, R. and Hnidka, J. Load-bearing hollow column from high performance concrete with composite reinforcement and anti-fire cladding. Functional sample, 2021. Prague.
- [38] Fire protection coating for concrete, HENSOTHERM ® 820 KS. Technical data sheet.
- [39] Müller, H. S., Haist, M. and Vogel, M. Assessment of the sustainability potential of concrete and concrete structures considering their environmental impact, performance and lifetime. *Construction and Building Materials*. 2014, 67, 321–337. ISSN 09500618. doi:10.1016/j.conbuildmat.2014.01.039
- [40] Advanced Concrete Elements with Woven Reinforcement (Karbeton-I), EU EFRR – Operační program Podnikání a inovace pro konkurenceschopnost, Prague (2016-2018), No.: CZ.01.1.02/0.0/0.0/15_019/0004908.

- [41] EN 1363-1, Fire Resistance Tests - Part 1, General requirements (2020).
- [42] Drzymala, T., Jackiewicz-Rek, W., Tomaszewski, M., Kús, A., Galaj, J. and Šukys, R. Effects of High Temperature on the Properties of High Performance Concrete (HPC). *Procedia Engineering*. 2017, 172, 256–263. ISSN 18777058. doi:10.1016/j.proeng.2017.02.108
- [43] Khouri, G. A., Anderberg, Y., Both, K., Fellingner, J., Majorana, C. and HØj, N. P. fib Bulletin No. 38 - Fire design of concrete structures - materials, structures and modelling. *The International Federation for Structural Concrete*, 2007. ISBN 978-2-88394-078-9. doi:10.35789/fib.BULL.0038
- [44] Naus, D. J. The Effect of Elevated Temperature on Concrete Materials and Structures - a Literature Review. Technical report, 2006. doi:10.2172/974590
- [45] Vlach. T. 2019, Interim report about work procedure and achieved results for 2019. No. Project: TJ02000119, Czech Technical University in Prague – University Centre for Energy Efficient Buildings.
- [46] Vlach. T. 2020, Interim report about work procedure and achieved results for 2020. No. Project: TJ02000119, Czech Technical University in Prague – University Centre for Energy Efficient Buildings.
- [47] PROMATECT®-H: Technical data sheet, Promat s.r.o. 2020. Online: <https://www.promat.com/siteassets/industry/downloads/technical-data-sheets-tds/calcium-silicates/eng/promat-promatect-h-product-data-sheet.pdf?v=49cca6/Download>
- [48] Požární ochrana uhlíkovvláknitých CFRP lamel omítkou Knauf Vermiplaster, Technical data sheet, Knauf Praha, spol. s.r.o. 2019. online: <https://www.knauf.cz/file/5010-knauf-tl-p901cz.pdf>
- [49] Betokontakt: Adhezní kontaktní penetrační můstek na betonový podklad před aplikací sádrových omítek. Technical data sheet, Knauf Praha, spol. s r. o. 2018. online: <https://www.knauf.cz/file/4697-bm-710-tl-cz-betokontakt.pdf>
- [50] EN 1365-4 - Fire resistance tests for loadbearing elements - Part 4: Columns, 2000
- [51] PAVUS, A.S. Protokol o zkoušce požární odolnosti č. Pr-21.2.059. B.m.: Požární zkušebna Veselí nad Lužnicí, zkušební laboratoř č. 1026 akreditovaná ČIA oznámená zkušební laboratoř pracoviště Veselí nad Lužnicí. 12. květen 2021
- [52] EN 1991-1-2: Eurocode 1: Actions on structures - Part 1-2: General actions - Actions on structures exposed to fire, 2004.

- [53] ČSN 73 0810 - Fire protection of buildings - General requirements. ÚNMZ - Úřad pro technickou normalizaci, metrologii a státní zkušebnictví. 2016
- [54] ČSN 73 0802 ed. 2 - Fire protection of buildings - Non-industrial buildings. ÚNMZ - Úřad pro technickou normalizaci, metrologii a státní zkušebnictví. 2020
- [55] ISO 5660-1: Reaction-to-fire tests — Heat release, smoke production and mass loss rate — Part 1: Heat release rate (cone calorimeter method) and smoke production rate (dynamic measurement). 2015
- [56] HLAVÁČEK, P. Engineering properties of alkali activated composites. Prague, 2014. Doctoral thesis, Czech Technical University in Prague, Faculty of Civil Engineering.

LIST OF TABLES

Table 1: Comparison of mechanical properties and melting points of selected textile reinforcement materials.....	5
Table 2: Overview of the thesis subobjectives.....	11
Table 3: Overview of the thesis publications.....	13
Table 4: Author’s contribution to the papers incorporated in the PhD thesis.....	14
Table 5: Related thesis publications list.....	15
Table 6: Description of the multi-scale testing	18
Table 7: Description of the specimens for four-point bending tests.	24
Table 8: The temperature of the test specimens reached at the first layer of the textile reinforcement	41

LIST OF FIGURES

Figure 1: Schematic TRC load-bearing member with hollow section.....	2
Figure 2: Comparison of the concretes with different water/cement ration [22].....	4
Figure 3: Variants of the carbon textile reinforcement with schematic yarn cross-section:	6
Figure 4: Change of the epoxy resin phase states [9].....	7
Figure 5: Variants of applied fire protection systems on a TRC hollow section column:	9
Figure 6: Reaction of the intumescent coating and foam forming.....	9
Figure 7: Scheme of the sequence of publications and linking of the subobjectives.....	12
Figure 8: Scheme of the multi-scale testing of thesis experiments.....	17
Figure 9: Results of the cohesion test (pull-out diagram):.....	24
Figure 10: Example of the results from four-point bending test of specimens with 2×10 tensile reinforcement with and without surface treatment.....	25
Figure 11: Change in mechanical properties of HPC:	27
Figure 12: Plate specimens without polypropylene fibres after the fire test.....	28
Figure 13: Plate specimens with polypropylene fibres during the fire test.....	28
Figure 14: Comparison of the reference specimens and specimens exposed to fire.....	29
Figure 15: Microscope pictures of cement suspension:	30
Figure 16: Assessment of the microscopic analysis of textile reinforcement percentage saturation.....	30
Figure 17: Evaluation of four-point bending tests of experimental specimens with different type of textile reinforcement matrix (pressure saturation)	31
Figure 18: Bending strength of reference specimens with covering layer 0 mm:	33
Figure 19: Instrumentation of the fire tests:.....	34
Figure 20: Residual bending strength of specimens exposed to elevated temperatures with covering layer of 0 mm:	36
Figure 21: Prepared textile reinforcement for specimen 100×100 mm ² with 4× ø4 mm CFRP rebars before HPC casting [14]:	37
Figure 22: One of the specimens with gypsum plaster for the indicative fire test.....	38
Figure 23: Specimens with gypsum plaster with thickness 30	39
Figure 24: TRC column test specimens before the fire test with fire protection:.....	40
Figure 25: Test specimens and the damaged fire-protection layer after the fire test:	41

List of figures

Figure 26: Detail of local failure at the edge of the test specimen with Knauf Vermiplaster
..... 42

ANNEX A – APPENDED PAPERS

Note:

All publications are appended in full and actual version to date 02/2023.

Citations of publications in the attached papers are independent of the numbering of the references in the text part of the thesis.

List of appended papers:

- Paper I Vlach, T., Řepka, J., Hájek, J., **Fürst, R.**, Jirkalová, Z. and Hajek, P. Cohesion Test of a Single Impregnated Ar-Glass Roving in High-Performance Concrete. *The Civil Engineering Journal*, 2020, 2020(3), 358-369. ISSN 1805-2576. doi:10.14311/CEJ.2020.03.0032
- Paper II **Fürst, R.**, Vlach, T., Pokorný, M. and Mózer, V. Study of Behavior of Textile-Reinforced Concrete with Epoxy Resin Matrix in Fire. *Fire Technology*, 2022, 58(1), 53-74. ISSN 0015-2684. doi:10.1007/s10694-021-01116-y
- Paper III **Fürst, R.**, Fürst, E., Vlach, T., Řepka, J., Pokorný, M. and Mózer, V. Use of Cement Suspension as an Alternative Matrix Material for Textile-Reinforced Concrete. *Materials*, 2021, 14(9), ISSN 1996-1944. doi:10.3390/ma14092127
- Paper IV **Fürst, R.**, Hejtmánek, P., Vlach, T., Řepka, J., Mózer, V. and Hájek, P. Experimental Evaluation of Carbon Reinforced TRC with Cement Suspension Matrix at Elevated Temperature. *Polymers*, 2022, 14(11), ISSN 2073-4360. doi:10.3390/polym14112174

PAPER I

Cohesion Test of a Single Impregnated Ar-Glass Roving in High-Performance Concrete

Authors: Tomáš Vlach, Jakub Řepka, Jakub Hájek, Richard Fürst,
Zuzana Jirkalová, Petr Hájek.

Journal: The Civil Engineering Journal

Publisher: Czech Technical University in Prague

Volume and number: 3/32

Year of publication: 2020

Number of pages: 12 pages

DOI: 10.14311/CEJ.2020.03.0032

COHESION TEST OF A SINGLE IMPREGNATED AR-GLASS ROVING IN HIGH-PERFORMANCE CONCRETE

Tomáš Vlach, Jakub Řepka, Jakub Hájek, Richard Furst, Zuzana Jirkalová and Petr Hájek

University Center for Energy Efficient Buildings of CTU in Prague, Buštěhrad, Třinecká 1024, Czech Republic; tomas.vlach@cvut.cz; jakub.repka@cvut.cz; jakub.hajek@cvut.cz; richard.furst@cvut.cz; zuzana.jirkalova@cvut.cz; petr.hajek@cvut.cz

ABSTRACT

The development of light and very thin concrete building structures and demand for extremely thin elements in design are inter alia reasons for the development of composite materials as non-traditional reinforcement. Composite materials are currently used as reinforcement mostly in the form of fiber reinforced polymer bars similar to traditional steel reinforcement bars, but the last decade sees also rise in the use of technical textiles. This article is focused on the interaction between impregnated textile reinforcement and high-performance concrete matrix and its easy determination using originally modified pullout test. The second aim of this article is improvement of interaction conditions between reinforcement and cementitious matrix using fine-grained silica sand applied on the surface of the composite reinforcement similarly to the traditional fiber reinforced polymer reinforcement with commonly used diameters. To investigate an effect of this modification a bending test was performed on small thin concrete slabs with different amounts of reinforcement.

KEYWORDS

Concrete, High performance concrete, Textile reinforcement, Cohesion, Interaction, Roving, Alkali resistant glass, Surface treatment

INTRODUCTION

Textile reinforced concrete (TRC) is a new composite material made of high-performance concrete (HPC) reinforced with technical textiles. The properties of this material are still intensively researched and its use is steadily growing. The basic principle is identical to the traditional steel reinforced concrete. HPC has great mechanical properties regarding compression and textile reinforcement has similarly good parameters in tension. With proper utilization of the HPC properties it is possible to use lesser amount of concrete in comparison with traditional concrete for elements with similar load-bearing capacity which in turn leads to more environmentally effective elements [1]. The technical textiles used as reinforcement are chemically resistant and non-corrosive and these characteristics can be further improved by using epoxy resin or materials. The TRC elements therefore do not need as massive concrete cover of reinforcement as in the case of traditional reinforced concrete with steel reinforcement affected by corrosion. The most commonly used technical textiles as reinforcement are alkali-resistant glass, carbon, basalt and aramid.

This article is focused on the interaction of impregnated textile reinforcement in HPC matrix and its easy determination using originally modified pull-out test. In addition, this experiment was supplemented by the bending test performed on thin slabs to further verify and test the different amounts of reinforcement in cross-sectional area. This issue is relatively thoroughly dealt with in the case of fiber reinforced polymer (FRP) reinforcement with conventional diameters. Testing

methods, interaction and methods for its improvement were already successfully proposed and measured. There are many articles and standards all around the world. Impregnated technical textiles using epoxy resin for homogenization are basically also FRP material with considerably smaller diameter, but standards for element design and the effect of interaction with the cement matrix have not been issued yet. There is also no standard with defined procedures to measure the interaction conditions.

Some articles about the interaction conditions of textile reinforcement were already published. This article is focused only on impregnated technical textiles. Portal [2] states that there is no standard methodology for measurement and evaluation of the TRC pull-out test. The pull-out test was set by the Krüger [3] and Lorenz and Ortlepp [4] asymmetric test. In their experiment samples of 400 x 100 x 15 mm were reinforced using one layer of technical textile. Various anchoring lengths were selected for the characterization of interaction conditions and also the moment of breaking point of textile reinforcement in the sample [5].

Banholzer [6] developed a one-sided test that is used for detection of broken light-fiber filaments. A sample is manufactured with dimensions of 10 x 10 mm and length of 30 mm using epoxy resin with a bundle of fibers in the middle of this prism. The fibers inside are therefore sufficiently protected against the steel jaws of the testing machine. The sample with epoxy prism is then embedded into the concrete matrix with dimensions of 50 x 50 mm and length of also 30 mm. During the testing procedure the sample of reinforcement is pulled out of the concrete part using a supported steel plate with displacement speed of 0.1 mm/min until the maximum displacement of 1.7 mm.

Very interesting testing methodology is also described in [5] with whole fabrics, not a single roving. This case also includes the effect of PP and PVA fibers that are used during the weaving of technical textile for yarn joining. These fibrils connect the whole fabric before the process of impregnation. The principle is analogous to the previously described testing methodology with a single roving. A portion of technical textile is inserted into the HPC specimen during the concreting with free length of fabric to be fixed into the testing machine. The fabric fixed into the testing machine is then pulled out from the concrete specimen using a steel frame as a support for the concrete part.

MATERIALS AND PREPARATION OF SPECIMENS

Concrete

The HPC mixture used in this experiment was developed at the Faculty of Civil Engineering, Czech Technical University in Prague (FCE CTU) for various applications [7]. This mixture was designed using mainly local sources of raw materials. It is a self-compacting fine-grained concrete and its composition is presented in Table 1. The HPC mixture used in this experiment was without any types of fibers. Water cement ratio was 0.25 and the water binder ratio was 0.20 for this mixture. Compressive strength tested on cubes with sides of 100 mm was equal to 140.5 MPa according to the standard CSN EN 12390-3. Tensile strength while bending tested on beams with dimensions of 160 x 40 x 40 mm was equal to 15.4 MPa according to standard CSN EN 12390-5. The same HPC recipe has been also used for several applications and research activities at the CTU like waffle and solid experimental facade elements [8] or in [9], [10]. Using the same concrete mixture allows the results to be compared with each other during the continuous process of alternative reinforcement development.

Tab. 1 - High-performance concrete mix composition

Component	Unit	HPC
Cement I 42.5R	[kg/m ³]	680
Technical silica sand	[kg/m ³]	960
Silica flour	[kg/m ³]	325
Silica fume	[kg/m ³]	175
Superplasticizers	[kg/m ³]	29
Water (12°C)	[kg/m ³]	171
Total	[kg/m ³]	2340

Composite reinforcement

The technical textile reinforcement was produced from AR-glass fibers homogenized with epoxy resin. Rovings of AR-glass fibers were chosen from other types of technical textiles such as carbon, basalt or aramid due to the lower elasticity modulus, more visible interaction conditions and also due to economic aspects. Used rovings were from the company Cem-FIL® with a length weight (titer) of 2400 g/km (= 2400 tex), specific gravity of 2680 kg/m³, tensile strength of 1700 MPa and modulus of elasticity of 72 GPa according to the technical data sheet.

Epoxy resin SikaFloor-156 from the company Sika was used for the homogenization of the rovings. Basic parameters of pure resin are tensile strength in bending of 15 MPa and modulus of elasticity of 2.0 GPa. Specific gravity of the material is 1100 kg/m³ according to the technical data sheet. This resin has excellent penetrating properties due to its low viscosity and is therefore very suitable for roving homogenization. The epoxy resin accounted for about 65% of the cross-section of the impregnated roving due to the experimental manual nature of its production in the lab.

Part of the textile reinforcement was produced with a smooth surface formed by the epoxy resin, while the other part was created with surface modification utilizing fine-grained silica sand. This surface treatment ensures better interaction conditions between composite reinforcement and the cementitious matrix and was inspired in surface modification of the FRP bars with higher diameter. The application of this type of surface treatment in the case of textile reinforcement was described by Shi-ping [11] and the suitable size of silica sand grains was defined by previous author's research [12].

Specimen preparation

The specimens were prepared for two types of experimental verification of the composite reinforcement performance. The first experiment designed for determination of basic material interaction conditions was a pull-out test performed with a single impregnated roving with smooth surface in comparison with a roving with surface treatment using fine-grained silica sand. The second experiment was a four-point bending test performed as the most common way of loading for TRC applications. Molds for all TRC specimens were prepared individually using a system of laminated chipboards. One mold was made for five identical specimens for the pull-out test and the other one for three TRC panels for the four-point bending test.

The developed pull-out test method for single impregnated roving was originally inspired by American standard for testing of FRP reinforcements ACI 440.3R-03 "Guide test methods for fiber reinforced polymers (FRPs) for reinforcing or strengthening concrete structures" with modified

specimen dimensions. The concrete part of specimens had constant dimensions of 100 x 100 mm with thickness related to the composite reinforcement diameter. First experiments were performed with the thickness close to the mentioned ACI standard with respect to the ratio to the other two dimensions, so the first thickness was 100 mm [13]. Especially in the case of single thin impregnated roving with the surface treatment the composite roving was usually broken before the start of slipping along the cementitious matrix. That leads to the thickness optimization using easy calculations. The resulting optimal thickness of the specimens for the used AR-glass roving 2400 tex with the diameter of approximately 2.0 mm was calculated to 20 mm.

The single roving homogenized by epoxy resin was fixed in the middle of the mold before the concreting of HPC part. A small cone made of silicone was installed on the composite roving inside the mold on the side where the composite reinforcement was fixed in the testing machine to prevent pulling of a shear cone from the HPC during the test procedure. This HPC shear cone would negatively affect results and cause skips on the measured curve. The anchoring length of each single impregnated roving was measured as the length of the roving inside a mold before concreting without the silicone cone. This length was also controlled after the pull-out test was performed by breaking of the HPC part and measuring the actual length. Mold was not treated with a demolding oil to prevent the contamination of the surface of the composite reinforcement.

The side of composite reinforcement fixed in testing machine was provided with epoxy sleeve enveloping it. Composite reinforcement has high tensile strength but is very fragile, so the epoxy sleeves were there to prevent damage of the impregnated rovings due to them being fixed in the testing machine. The epoxy sleeves replaced previously used steel ones [14], which made preparation of the specimens and manipulation with them much easier.

After initial preparations, the concreting was performed using self-consolidating HPC. The preparation of specimens is presented in Figure 1. Altogether 12 specimens were prepared - 6 specimens with the smooth surface and 6 specimens with the surface modification using fine-grained silica sand. The surface modification is visible in Figure 1.

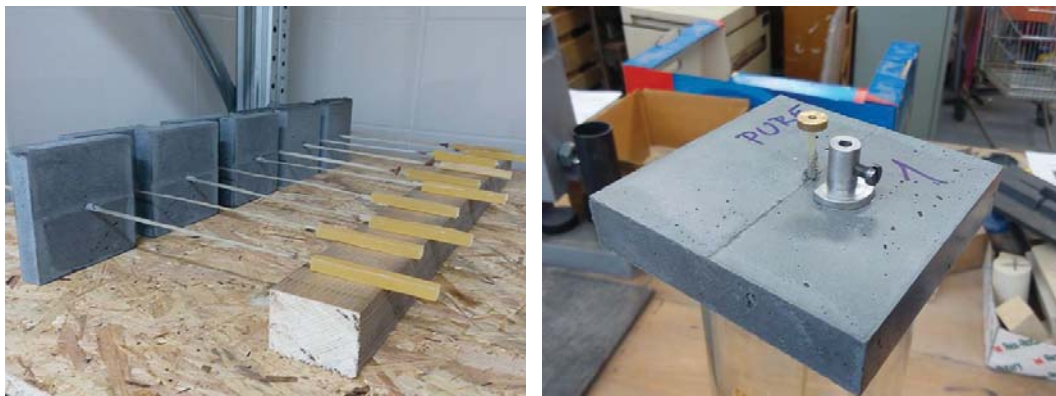


Fig. 1 – Specimens preparation for the pull-out test.

Specimens for the four-point bending test were prepared in the form of small slabs with the dimensions of 100 x 360 x 18 mm. Reinforcement grids made of the impregnated AR-glass rovings were prepared in two different densities with 5 and 10 rovings per 100 mm specimen width and were cut to fit the intended specimen dimensions. The slabs were prepared in three variants. One with two 5 roving layers (2x5), second with two 10 roving layers (2x10) and third with four 10 roving layers (4x10). The last variant represents the maximum amount of textile reinforcement that allowed for proper concrete distribution throughout the specimens. All variants were prepared with a smooth surface and also with a surface modification, three specimens for each variant.

The casting process was performed layer by layer. That means a layer of HPC with a controlled thickness to ensure the proper concrete cover, then a TR was inserted, then a middle portion of HPC, another TR, and an upper layer of HPC in the case of specimens with two reinforcement grids and similarly in the case with four. The concrete cover layer was designed with a thickness of 4 mm and due to the chosen concreting process, no spacers were used. Specimens were not vibrated to prevent movement of the composite reinforcement to the HPC surface, the concrete HPC mixture was self-consolidating as mentioned above. The preparation of the specimens for the flexural test is presented in Figure 2.

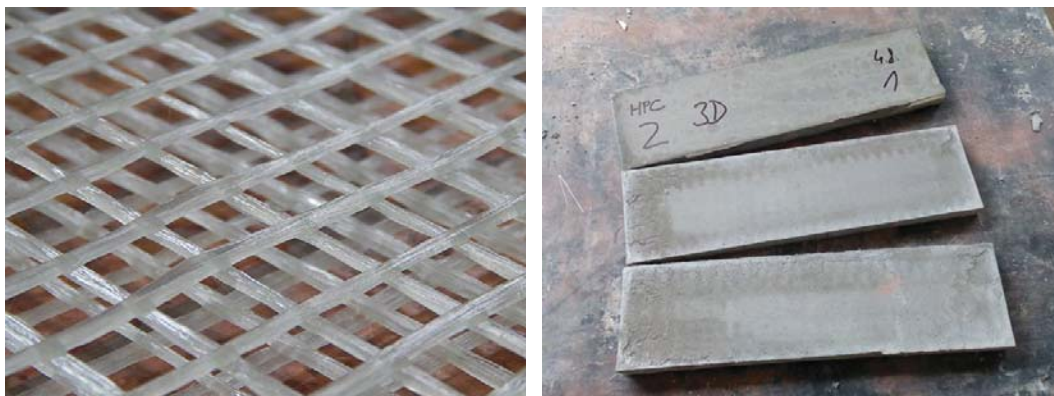


Fig. 2 – Specimens preparation for the four-point bending test.

All specimens were demolded one day after the casting process and were stored in constant conditions for another 27 days. The panels were stored in water tank and constant temperature of 22 °C. The specimens created for pull-out test were placed in air-conditioned environment with constant humidity of 60%. Dimensions and weight of the specimens were measured before testing.

EXPERIMENTS

Cohesion test

The developed pull-out method was focused on the complete curve of bond behaviour with a simple interpretation and application of results in the field of science as well as in the field of engineering and structures designing. As mentioned above this method was inspired by the ACI 440.3R-03 standard, but specimen dimensions were modified due to the small cross-sectional area of the composite reinforcement in comparison with traditional FRP reinforcement. Other aspects of the test set up were very similar to the traditional FRP cohesion test. Epoxy sleeves were installed only on one side of the rovings because of the safe and stable fixing to the testing machine without any damages to the roving filaments. Concrete part had constant dimensions of 100 x 100 mm and optimized thickness of 20 mm for single AR-glass impregnated roving with titer 2400 tex in this experiment. A view of the developed testing set up inspired by ACI standard is presented in Figure 3.

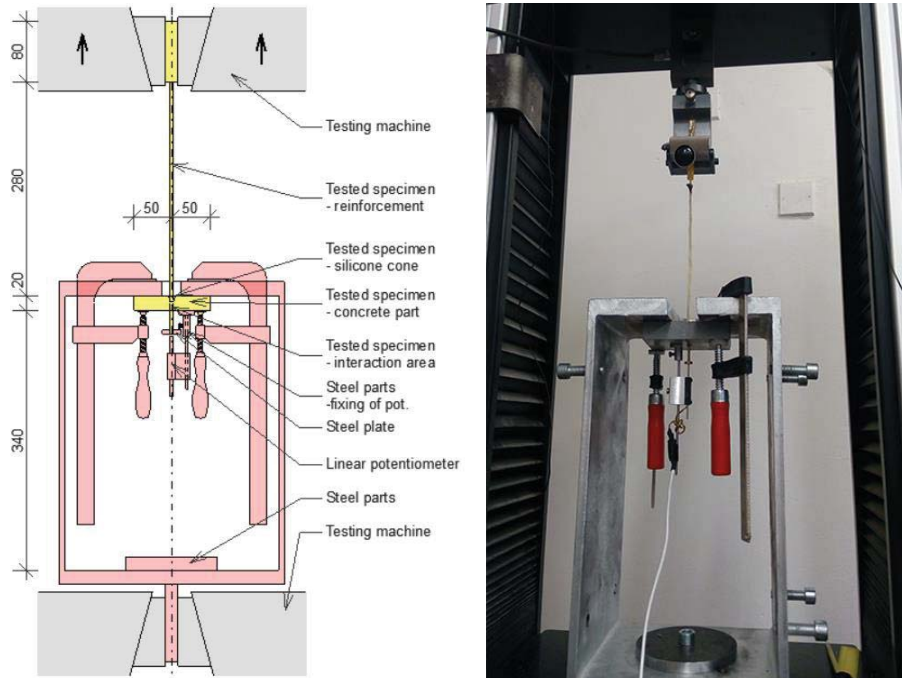


Fig. 3 – Basic scheme of own developed pull out test method inspired by ACI standard and picture of the actual setup.

Time, force, crosshead displacement and pull-out of the reinforcement were measured during the test procedure inspired by the ACI standard for a simple and direct determination of bond behaviour. Pull-out was measured on the free end of the impregnated roving by a potentiometer. The concrete part was equipped with a steel element made precisely by a lathe attached to the concrete by epoxy resin and the potentiometer was fixed in this steel part by a bolt. A circular rigid steel plate was similarly attached at the free end of the reinforcement which protruded from the concrete part by approximately 20 mm to provide stable contact area for the potentiometer. Considering the steel plate, the maximum theoretical pull-out value was around 15 mm. Detailed view of the potentiometer and its fixing on the HPC part is presented in Figure 4. The speed of loading was constant at 2.0 mm/min according to the prescribed tensile stress increment of approximately 2.0 MPa/s in ACI 440.3R-03 standard.



Fig. 4 – Detailed view of the bottom part of the concrete specimen with installed potentiometer and support constructions for the pull-out values measurement.

The results of the pull-out test are presented in Figure 5 and Figure 6 in the form of two graphs. Both graphs show pull out measured by the potentiometer on the X axis and corresponding force on the Y axis. Figure 5 shows overall comparison of specimens with smooth composite reinforcement and those with the surface treatment made of fine-grained silica sand. The test proved that there was little cohesion between HPC matrix and composite reinforcement with smooth surface as all rovings without surface treatment were pulled out of their HPC matrix. Figure 6 presents more detailed view focused on the specimens with impregnated rovings treated with fine-grained silica sand which showed almost perfect bonding with the HPC matrix. All impregnated rovings with surface treatment were broken before they could be pulled out. Another advantage of the surface treatment of the reinforcement is the stability of the results because no sample shows significant deviations as shown in Figure 6. Also, the maximum tensile strength of the impregnated rovings was without any negative caused by the embedded grains of silica sand. The presented curves of pull-out can be used for example for non-linear numerical modelling of crack development and crack opening of TRC elements using analytical methods or other numerical software.

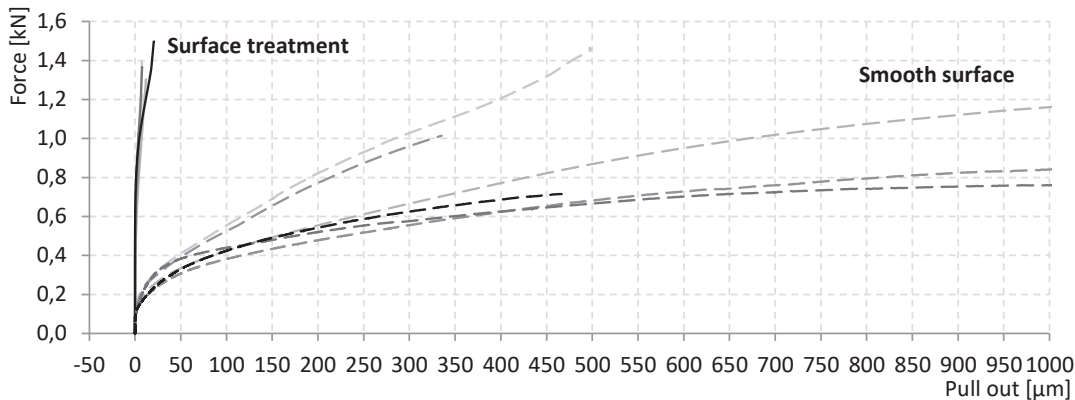


Fig. 5 – Results of pull-out test presented in the form of force – pull-out diagram using data from the testing machine and potentiometer showing rapid difference between the smooth surface and specimens with the surface modification.

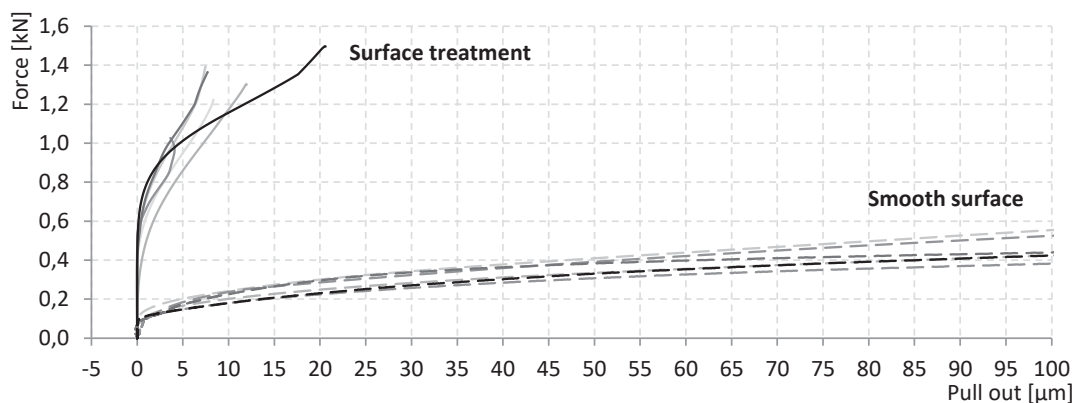


Fig. 6 – Results of pull-out test presented in the form of force – pull-out diagram using data from the testing machine and potentiometer. Detailed view on the beginning of the pull-out test with limited X axis showing rapid difference between the smooth and treated surface.

Four-point bending test

The four-point bending test was performed on small slabs with dimensions of 100 x 360 mm with constant thickness of 18 mm. Concrete cover of the composite reinforcement was designed to only 4 mm and was achieved by controlled application of HPC layers. The specimens were not vibrated to prevent the reinforcement movement to the HPC surface due to the lower density of the composite reinforcement compared to HPC. Three specimens were created for each group with the same designed amount of reinforcement. Six sets of samples were prepared in total.

Three variants with smooth surface and three with surface treatment using fine-grained silica sand were created. The first group contained two identical layers of composite reinforcement. One layer had 5 parallel impregnated rovings in the longitudinal direction with grid spacing of 22 mm. Grid spacing of rovings in transverse direction was 24 mm. The second group was also made with two identical layers of pre-prepared textile reinforcement but with 10 impregnated rovings in longitudinal direction spaced 10 mm from each other. The last third group of specimens was made with four layers of reinforcement with 10 impregnated rovings in longitudinal direction similar to the previous group. This combination of 4 layers with 10 rovings in each layer was the maximum possible amount of composite reinforcement for these specimen dimensions and composite reinforcement production technology, especially for the specimens with surface treatment. A view of the test setup and typical crack development is shown in Figure 7.



Fig. 7 – Typical crack development of 2x5 reinforcement with smooth surface on the left and 4x10 reinforcement treated with fine-grained silica sand on the right side.

Testing was performed with axial distance of supports of 300 mm and 100 mm in the case of loading supports. All supports had curvature with 15 mm radius. Monitored parameters during the testing procedure were magnitude of the reaction on the load cell and displacement of crosshead of the testing machine. Four-point bending test was performed on MTS 100 testing machine with controlled constant load increment of 2.0 mm per minute [12], [15], [16].

The results are presented in Figure 8, Figure 9 and Figure 10 in the form of force – displacement graph, because presentation of flexural stress on the y axis is not relevant after the initiation of the first crack in the HPC part despite the fact that it is commonly used. Always two graphs are presented side by side where the left side represents specimens with smooth composite reinforcement and the right side represents specimens with composite reinforcement with surface treatment.

Specimens with only two layers of textile reinforcement with five rovings in each layer are shown in Figure 8. The first sudden drop on the curve represents the formation of the first crack, creating a plastic joint, followed by an opening of the crack and an activation of the reinforcement. The load-bearing capacity of the specimen before the first crack initiation is given only by the tensile strength of the concrete without the contribution of the reinforcement. The small difference in this value between the samples with smooth reinforcement on the left and the samples with

surface treated reinforcement on the right is due to a slight inconsistency in specimen thickness which varied from the intended 18 mm.

After the initiation of the first crack the specimens with smooth reinforcement typically formed one additional crack, each under one of the loading supports, after which the smooth reinforcement started slipping. Their behaviour under pressure was typical for a slightly reinforced concrete structures with wide cracks opening. The specimens with the surface treated reinforcement formed multiple more narrow cracks, due to significantly better interaction conditions between reinforcement and cementitious matrix. The pull-out was not that significant and much faster reinforcement activation lead to the multiple cracking, which is characteristic for structures with higher amount of reinforcement [12], [16].

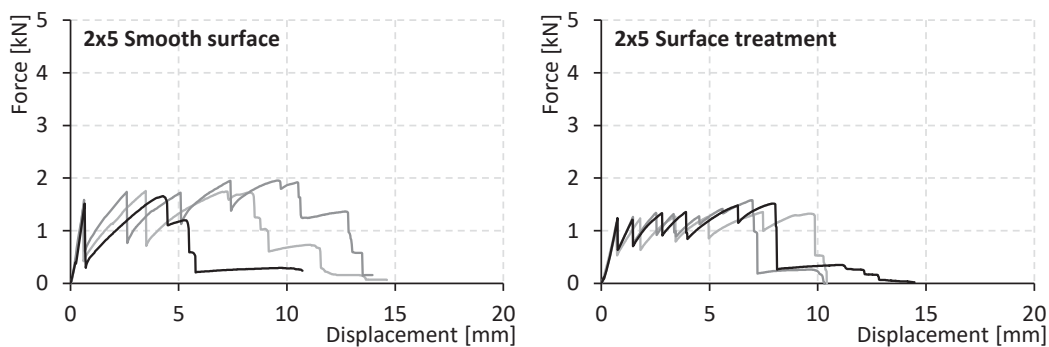


Fig. 8 – Force – displacement curves from the four-point bending test of specimens reinforced with 2x5 impregnated rovings with and without surface modification.

Very similar trend is presented in Figure 9 in the case of more heavily reinforced specimens with 10 rovings in each layer of reinforcement. Higher amount of reinforcement logically led to the higher maximum value of reached force in comparison to the specimens with 2x5 reinforcement. The specimens with smooth reinforcement on the left side show similar crack development as the specimens in Figure 8 on the right side with 2x5 reinforcement treated with fine-grained silica sand. The activation of surface treated 2x10 reinforcement is again much faster than in the case of its smooth counter-part. The specimens with surface modification also show higher ultimate reached force while also having lower displacement in the time of their collapse.

Figure 10 shows that the amount of reinforcement is so high in the cross-sectional area of the specimen that curves look more or less similar. The positive effect of the surface modification of composite textile reinforcement with fine-grained silica sand is much less significant in comparison with Figure 8 and Figure 9.

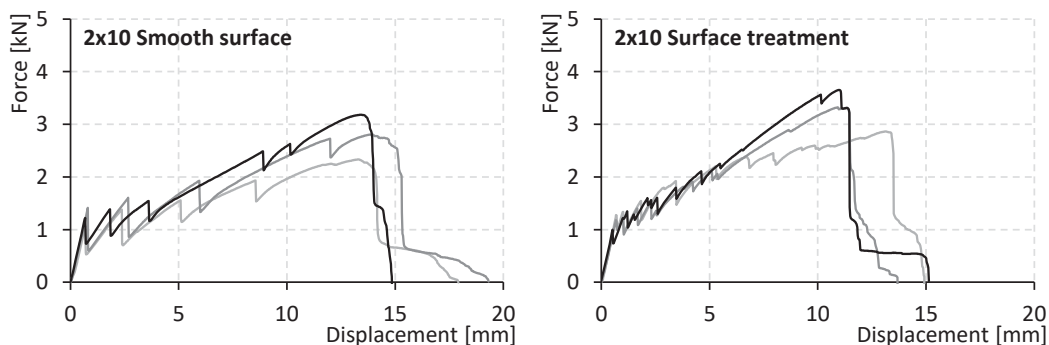


Fig. 9 – Force – displacement curves from the four-point bending test of specimens reinforced with 2x10 impregnated rovings with and without surface modification.

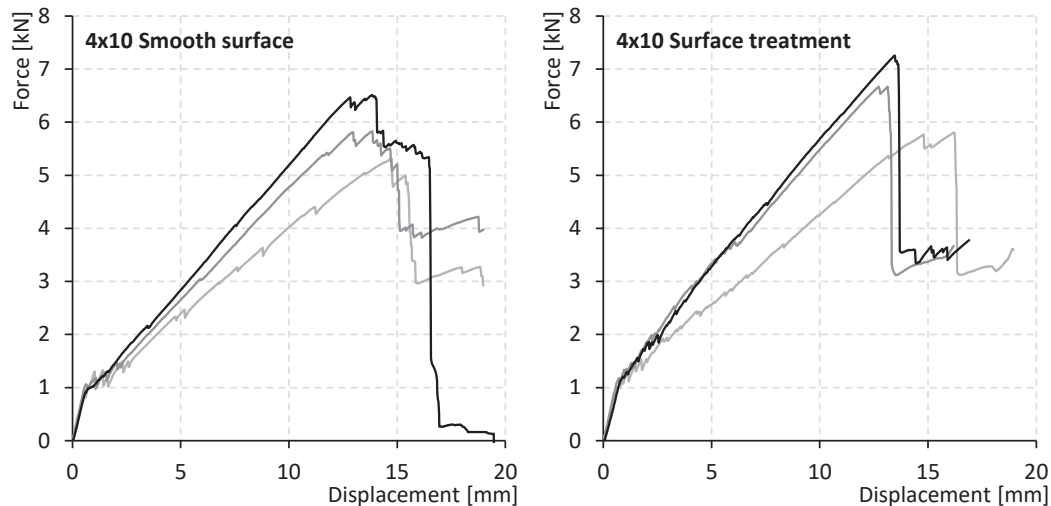


Fig. 10 – Force – displacement curves from the four-point bending test of specimens reinforced with 4x10 impregnated rovings with and without surface modification.

CONCLUSION

During the testing procedure of the own developed pull-out test method, the composite textile reinforcement in the form of a single impregnated roving with surface treatment made with fine-grained silica sand reached the maximum values of tensile stress in the composite reinforcement corresponding to the results of tensile test presented in a previous research. That means that the surface treatment using fine-grained silica sand has no significant negative effect on the tensile strength of the impregnated roving. The impregnated individual rovings were in most cases damaged (in the case of impregnated rovings with smooth surface after significant pull-out) where they were in contact with the surrounding HPC prism due to the fact that the reinforcement was pressed by the irregular contact area of the HPC during the process of reinforcement activation. The fibers near the surface of the textile reinforcement were therefore subjected to higher tensile stress, which leads to the weakening of the reinforcement and subsequent breaking of the roving in this area. Epoxy resin impregnation of the individual rovings however provides sufficient protection of AR-glass fibers in HPC matrix from premature damage for both smooth and modified reinforcement. The HPC part of tested specimens showed no signs of damage.

The difference between specimens with and without surface treatment is also clearly visible. The curves representing typical samples with smooth surfaces show a rapid pull-out of the reinforcement from the part of the HPC sample with higher pull-out values and lower corresponding force. After activation of the reinforcement in its full length, there is a very slow increase in force during the loading process due to poor interaction of both materials. This result signifies the need of large anchorage length of the smooth composite reinforcement required for the load transfer in the actual TRC element. The curves representing typical samples with surface modification provide much better results with higher contact stiffness. Grains of fine silica sand allow almost no slipping due to the high surface roughness.

The contact area of the reinforcement and cementitious matrix is constant in this method, due to the composite reinforcement passing completely through the HPC prism. The pull-out is measured by a potentiometer placed on the free end of the reinforcement protruding from the HPC prism which ensures activation of the reinforcement in its whole length.

Textile reinforcement with surface treatment provides significantly better results regarding the crack formation and development as was also demonstrated by flexural bending test performed on small slabs using different variants and amounts of composite textile reinforcement. Better

bonding conditions lead to a very short anchorage length for reinforcement activation without a significant loss of force due to the loading process controlled by constant increment of displacement. The ultimate bending strength was also a little higher. The most visible difference in the results is at the beginning of the curve during the process of reinforcement activation in the case of 2x10 impregnated rovings with smooth surface and with surface treatment. The surface treatment is therefore very effective and can also have economic benefits by saving reinforcement material.

It is also obvious from the presented figures that with a higher amount of textile reinforcement a bending behaviour similar to that of elements made of traditional materials and with traditional diameters of reinforcement can be achieved. This means that after the first initiation of cracks, there is no massive opening of cracks. This effect was achieved with a roving material made of alkali-resistant glass, which has a modulus of elasticity slightly higher than the HPC used. After impregnation with epoxy resin, the composite reinforcement as a whole even has a similar modulus of elasticity. It explains why such a large amount of composite reinforcement was needed to achieve those results during the bending test.

ACKNOWLEDGEMENTS

This work has been supported by the Ministry of Education, Youth and Sports within National Sustainability Programme I (NPU I), project No. LO1605 - University Centre for Energy Efficient Buildings – Sustainability Phase.

REFERENCES

- [1] L. Laiblová *et al.*, „Environmental Impact of Textile Reinforced Concrete Facades Compared to Conventional Solutions—LCA Case Study”, *Materials*, roč. 12, č. 19, Art. č. 19, led. 2019.
- [2] N. Williams Portal, I. Fernandez Perez, L. Nyholm Thrane, a K. Lundgren, „Pull-out of textile reinforcement in concrete”, *Constr. Build. Mater.*, roč. 71, s. 63–71, lis. 2014.
- [3] M. Krüger, „Vorgespannter textilbewehrter Beton (Prestressed textile reinforced concrete)”, *Philos. Dr. Thesis Stuttg. Univ. Stuttg. Fak. Bau- Umweltingenieurwissenschaften Diss*, 2004.
- [4] E. Lorenz a R. Ortlepp, „Bond Behavior of Textile Reinforcements - Development of a Pull-Out Test and Modeling of the Respective Bond versus Slip Relation”, in *High Performance Fiber Reinforced Cement Composites 6*, G. J. Parra-Montesinos, H. W. Reinhardt, a A. E. Naaman, Ed. Springer Netherlands, 2012, s. 479–486.
- [5] W. Brameshuber, *Report 36: textile reinforced concrete-state-of-the-art report of RILEM TC 201-TRC*, roč. 36. RILEM publications, 2006.
- [6] B. Banholzer, „Bond behaviour of a multi-filament yarn embedded in a cementitious matrix”, PhD Thesis, Bibliothek der RWTH Aachen, 2004.
- [7] M. Kynclova, „Environmentally effective waffle floor structures from fibre concrete”, prezentováno v International PhD Symposium in Civil Engineering, Technical University of Denmark, Lyngby, 2010.
- [8] T. Vlach, P. Hájek, C. Fiala, L. Laiblová, J. Řepka, a P. Kokeš, „Waffle Facade Elements from Textile Reinforced High Performance Concrete”, *Proc. HiPerMat*, 2016.
- [9] C. Fiala *et al.*, „Construction and Static Loading Tests of Experimental Subtle Frame from High Performance Concrete for Energy Efficient Buildings”, *Solid State Phenomena*, 2017.
- [10] A. Chira, A. Kumar, T. Vlach, L. Laiblová, a P. Hajek, „Textile-reinforced concrete facade panels with rigid foam core prisms”, *J. Sandw. Struct. Mater.*, roč. 18, č. 2, Art. č. 2, bře. 2016.
- [11] S. Yin, M. Na, Y. Yu, a J. Wu, „Research on the flexural performance of RC beams strengthened with TRC under the coupling action of load and marine environment”, *Constr. Build. Mater.*, roč. 132, s. 251–261, úno. 2017.
- [12] T. Vlach, L. Laiblová, M. Ženíšek, A. Chira, A. Kumar, a P. Hájek, „The Effect of Surface Treatments of Textile Reinforcement on Mechanical Parameters of HPC Facade Elements”, in *Key Engineering Materials*, 2016, roč. 677, s. 203–206.
- [13] T. Vlach, M. Novotná, C. Fiala, L. Laiblová, a P. Hájek, „Cohesion of Composite Reinforcement Produced from Rovings with High Performance Concrete”, *Appl. Mech. Mater.*, roč. 732, s. 397–402, 2015.

- [14] V. Tomáš *et al.*, „Comparison of Different Methods for Determination of Modulus of Elasticity of Composite Reinforcement Produced from Roving”, *Adv. Mater. Res.*, č. 1054, Art. č. 1054, 2014, Viděno: úno. 27, 2017.
- [15] L. Laiblová, T. Vlach, M. Ženíšek, A. Kumar, a P. Hájek, „Comparison of Different Types of Glass Reinforcement for HPC Facade Elements from Mechanical and Economical Aspects”, *Key Engineering Materials*, 2017.
- [16] T. Vlach, L. Laiblová, M. Ženíšek, J. Řepka, a P. Hájek, „Soft Insert for Support Modeling of Slightly Textile Reinforced Concrete”, *Key Engineering Materials*, 2018.

© 2020. This work is published under <https://creativecommons.org/licenses/by/4.0/> (the “License”). Notwithstanding the ProQuest Terms and Conditions, you may use this content in accordance with the terms of the License.

PAPER II

Study of Behavior of Textile-Reinforced Concrete with Epoxy Resin Matrix in Fire

Authors: Richard Fürst, Tomáš Vlach, Marek Pokorný, Vladimír Mózer

Journal: Fire Technology

Publisher: Springer

Volume and number: 58/1


Year of publication: 2022


Number of pages: 22


DOI: [10.1007/s10694-021-01116-y](https://doi.org/10.1007/s10694-021-01116-y)



Study of Behavior of Textile-Reinforced Concrete with Epoxy Resin Matrix in Fire

Richard Fürst ^{*}, Fire Laboratory, University Centre for Energy Efficient Buildings, CTU in Prague, Prague, Czech Republic

Tomáš Vlach , Composite Material Laboratory, University Centre for Energy Efficient Buildings, CTU in Prague, Prague, Czech Republic

Marek Pokorný  and Vladimír Mózer , Fire Laboratory, University Centre for Energy Efficient Buildings, CTU in Prague, Prague, Czech Republic

Received: 28 May 2020/Accepted: 2 March 2021/Published online: 30 May 2021

Abstract. Textile-reinforced concrete is currently most frequently used for non-load-bearing structures, but there is a vision for also using it in load-bearing construction elements. In recent years, this construction material has been subjected to detailed examination. Different combinations of materials for potential use in textile-reinforced concrete have been described. These differ in the type of concrete mix and the composition of the textile reinforcement. The aim of this work is to test the application of a specific textile-reinforced concrete, consisting of high-performance concrete, textile reinforcement from carbon fibers and its epoxy resin matrix, at an elevated temperature. The combination of these materials makes it possible to produce subtle load-bearing structures with excellent mechanical properties. The critical issue is the behavior of these structures when exposed to fire. A series of medium-scale fire condition experiments were carried out with a temperature load based on the ISO 834 curve, followed up by mechanical tests. The aim of these experiments was to describe critical areas of textile-reinforced concrete in fire and to propose possible solutions. In an indicative fire experiment, experimental samples displayed massive spall of concrete layers, and interaction between materials was lost due to the low temperature resistance of the epoxy resin. Concurrently, the optimal quantity of polypropylene fibers was experimentally determined. This paper presents an experimental demonstration of the problematic aspects of textile-reinforced concrete and subsequent recommendations for future work with practical application in the design of load-bearing structures.

Keywords: Textile-reinforced concrete, High-performance concrete, Carbon fibers, Epoxy resin, Load-bearing structures, Fire

1. Introduction

The construction of buildings is currently evolving due to the more frequent use of alternative materials, increased visual quality and architectural design of structures. At the same time, importance is being placed on sustainability in civil engi-

*Correspondence should be addressed to: Richard Fürst, E-mail: richard.furst@cvut.cz



neering, especially reducing the materials used with respect to their carbon footprint. This means maximizing performance and saving primary raw material resources. Therefore, alternative composite materials with excellent material properties are being used more frequently. This fact is followed by several studies which have characterized the environmental impact of the new composite materials. These studies describe the life cycle cost and environmental impact, especially for structures from HPC [1, 2] or particularly from TRC [3]. Based on the findings from these studies, materials with higher mechanical qualities achieve lower environmental impact values, primarily because of their efficiency and saving of material. From the point of view of textile reinforcement, it is appropriate to use either basalt or carbon fibers since basalt fibers need much less energy for their production than other textile materials. Finally, the environmental impact and carbon footprint of carbon fibers is the lowest of all the alternatives [4] in comparison with other materials.

This work describes the development of a composite material based on HPC and textile reinforcement, i.e. textile-reinforced concrete (TRC). The material presented in this paper was developed at the Czech Technical University (CTU) in Prague, Faculty of Civil Engineering, and at the University Center for Energy Efficient Buildings (UCEEB) at CTU in Prague. In general, TRC is a combination of high-performance concrete and textile reinforcement with a matrix most frequently consisting of synthetic resins. Thanks to the outstanding mechanical qualities of the material, it is possible to realize subtle constructions or constructions with non-standard shapes as shell structures, or thin-walled structures (Fig. 1) [5–7]. TRC was by far the most frequently used material for non-load-bearing structures such as facade panels or design members [8]. Currently, several studies describe possible ways for using TRC in load-bearing structures. One of the advantages of TRC as a material for load-bearing structures is its flexible textile reinforcement. Owing to the high resistance of the textile reinforcement to atmospheric corrosion, it is possible to consider the covering layer of TRC only with respect to the interaction between materials. Therefore, it is possible to propose a



Figure 1. Example of the reinforcement mesh and structures made out of TRC: (a) carbon fiber reinforcement in the form of an L-angle with impregnation from the epoxy resin; (b) example of non-load-bearing structures made out of textile-reinforced concrete.

covering layer of around 5–10 mm [9], which is quite different from the situation for traditional reinforced concrete. At the same time, the realization process, e.g. the HPC production method or the covering layer guarantee, is extremely difficult and therefore this construction material is intended exclusively for prefabrication [10, 11]. However, for further development of TRC it is necessary to achieve a deeper understanding based on basic research, which should proceed alongside assessment of TRC on the effects at elevated temperatures.

With this combination of materials, it is necessary to consider the behavior of the individual components exposed to elevated temperatures. The behavior of TRC at elevated temperatures has been described in several studies that dealt with temperatures ranging around 700°C [12–14]. Due to the standard temperatures during fire (exceeding 1000°C), it is necessary to investigate such situations, especially when TRC contains flammable materials in the textile reinforcement matrix. For future research at elevated temperatures, it is appropriate to focus on experiments where the experimental samples shall be loaded according to the standard temperature curve ISO 834 as per [15].

In general, the design of load-bearing structures impacted by fire is driven by maintaining their mechanical properties for the required time of fire resistance. This means that the construction element should not be deformed over the load-bearing capacity limit of the structure, or even collapse during the fire. If the structural element has not only a load-bearing but also a fire-separating function, it must at the same time retain its integrity and insulating ability [16]. Generally, structures which are loaded only in compression do not exist due to the imperfection of the structure. Therefore for bend structures, it is necessary to ensure the transfer of tensile tension generating the bending moments (see Fig. 2) by which the bend structures are dominantly loaded. This is especially the case of subtle structural elements. If this capability fails, progressive collapse of the structure occurs, due to the absence of yield strength of the carbon material. This must be avoided in designing load-bearing structures.

For a TRC structure made from high-performance concrete (HPC) and textile reinforcement with epoxy resin (ER) matrix, the structure is significantly weaker if the interaction between the tensile reinforcement (carbon fiber) and HPC is impaired. The interaction is provided by the textile reinforcement matrix, which enables the activation of all fibers (homogenization) in the carbon yarn and thus allows the use of the entire tensile capacity. The temperature limit (where the total loss of interaction between materials occurs) is the so-called glass transition temperature. This is the temperature where the elastic modulus rapidly decreases, and the deformation sharply increases (see Fig. 3).

Therefore, it is necessary to prevent the temperature increase over the ER glass-transition temperature value. Traditional reinforced concrete structures (with steel reinforcement) have a covering layer in the range of 10 to 40 mm, serving primarily as a protection against atmospheric corrosion. In comparison, textile reinforcement has excellent resistance to atmospheric corrosion. Therefore, it is possible to design TRC construction elements only with respect to the interaction between materials, thus minimizing the covering layer to 5–10 mm [9]. However, these solutions negatively affect the temperature resistance of the overall TRC structure

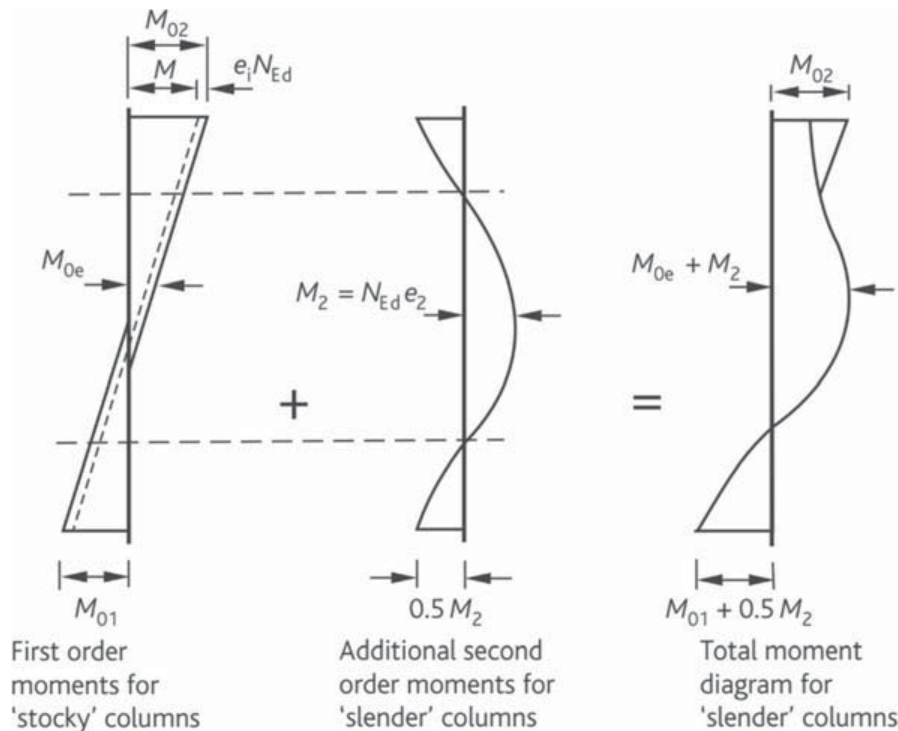


Figure 2. Bending moment loading of a bend structure (column) [17].

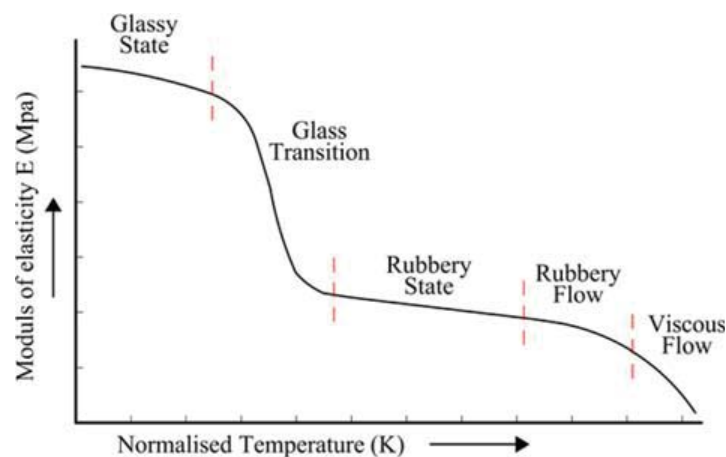


Figure 3. Epoxy resin phase states [18].

because this cover layer does not provide sufficient protection of ER from elevated temperatures.

For the development of TRC, HPC has been used, having better standard mechanical properties. HPC is used for its compressive strength, better workability, modulus of elasticity and waterproofing properties. Production of HPC is possible by using plasticizers, which enable use of less water during preparation and

thus achieve higher compressive strength. Because less water has been used in the concrete mixture, the final hardened construction element has significantly lower porosity, with greater compressive strength.

From the point of view of fire resistance, HPCs [19] have worse fire resistance compared to standard concrete. It is primarily impacted by the absence of pores caused by the small water coefficient. As a result, HPC is not able to provide migration of water vapor pressure through the pores to the external environment. The absence of pores can be substituted by adding polypropylene (PP) fibers to the concrete mixture. These fibers evaporate at a relatively low temperatures (170°C, according to [20]) and allow water vapor to migrate out of the concrete structure. Despite some negative aspects, HPC is still one of the best variants for subtle TRC construction elements. However, it is necessary to consider its behavior at elevated temperatures during the design.

2. Methods and Materials

In this chapter, the test samples used in experiments are described. The mechanical properties of materials are also described, including the procedure of experimental sample preparation.

2.1. Test Samples and Materials Used

Two variants of the experimental samples for exposure to elevated temperatures were prepared. The first variant was a beam with dimensions of $40 \times 40 \times 160$ mm for the standard bending and compression tests according to the standard of [20, 21] without textile reinforcement. The second variant was a plate designed with dimensions of $100 \times 18 \times 360$ mm and provided with two layers of textile reinforcement. For the following thermal analysis, wire thermocouples were placed inside the samples, near to the exposed side of the samples (for more details see Fig. 4).

The standard beam and plate samples according to [20, 21] were used in our experiments. The samples were tested for changes in their mechanical properties:

- without exposure to elevated temperatures—reference
- following exposure to elevated temperatures—ISO 834 for 15 and 30 min

The HPC mixture used for the preparation of experimental samples was developed for different applications under previous research projects at CTU in Prague [23]. The quantities of each material in the concrete mixture are described in Table 1. The production of HPC was carried out according to the prescribed procedure, where the cured concrete has the following material properties:

- Compressive strength **115.0** MPa
- Tensile strength **11.5** MPa
- Modulus of elasticity **49.5** GPa

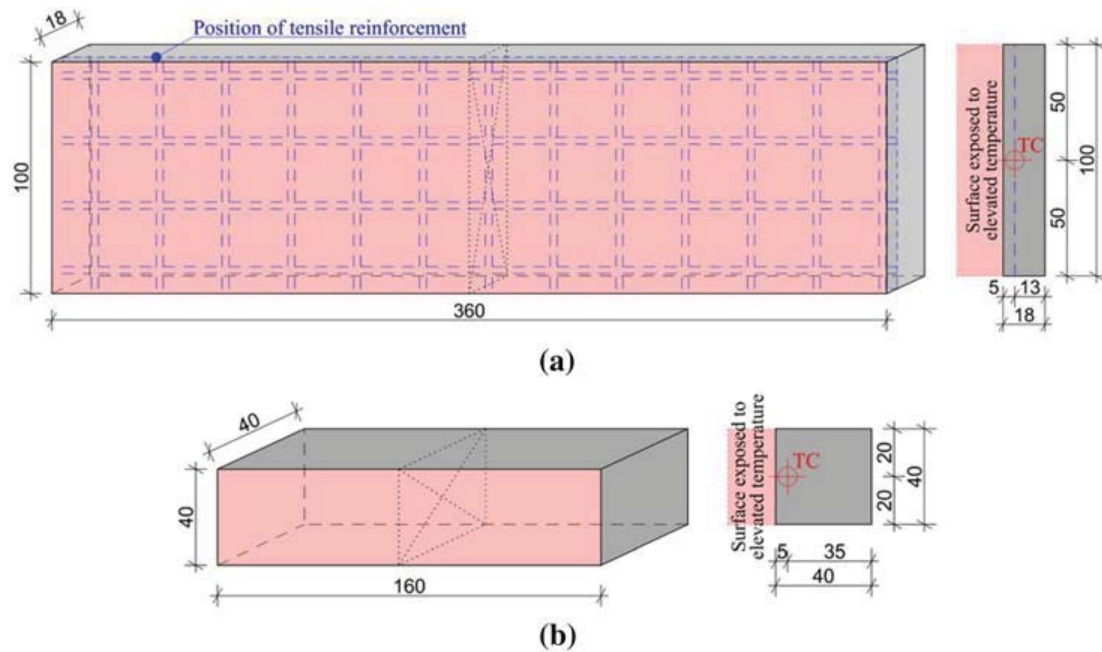


Figure 4. Axonometry and cross section of experimental samples and position of reinforcement mesh: (a) experimental plate sample of TRC; (b) experimental sample from HPC. Note: During the fire experiment, the temperature on the unexposed side was measured as well—in the picture, the position of the thermocouple on the unexposed side was not described.

**Table 1
Mixture of HPC [23]**

Mix content	Quantity (kg m^{-3})
Cement I 42, 5R	680
Silica sand	960
Silica flour (ground quartz)	325
Silica fume (microsilica)	175
Superplasticizer	29
Water	171
Total	2420

For the preparation of TRC samples, tensile reinforcement of carbon fibers was used. Fibers were impregnated with epoxy resin—a commercially available product named **Solidian GRID Q142/142-CCE-25XYZ**. All necessary material properties are described in Table 2.

Each of the experimental samples has been conditioned for 28 days in a lime-water bath according to [25]. After this time, fire experiments were performed.

Table 2
Material Properties of Carbon Mesh Used [24]

<i>Geometry textile reinforcement</i>		
Yarn material	Carbon	–
Impregnation material	Epoxy resin	–
Yarn axis distance	25	mm
Cross-section of the strand	3.62	mm ²
Cross-section of the reinforcement	142	mm ² m ⁻¹
<i>Material properties</i>		
Tensile strength of the yarn	> 4.0	N mm ⁻²
Resisting force	440	kN m ⁻¹
Modulus of elasticity	> 220.0	N mm ⁻²

2.2. Fire Exposure

The fire experiments were performed in a mobile fire furnace called miniFUR developed by FireLAB at the University Center for Energy Efficient Buildings, CTU in Prague. The furnace serves for medium-scale experiments and can achieve the temperature curve according to ISO 834 (see Fig. 6). The furnace is heated with cement-fiber boards and has a steel load-bearing structure. Ventilation of the furnace is ensured naturally, with two air inlets at the bottom of the furnace and two exhaust vents. The required temperature is achieved by burning of propane 2.5 with a net calorific value of 46.4 MJ kg⁻¹ (according to the technical data-sheet of the propane), distributed through a 300 × 100 × 100 mm gas burner located in the central axis of the furnace (see Fig. 5).

For monitoring and adjusting the course of temperature, we have installed eight thermocouples. Four are placed under the ceiling of the furnace and four above

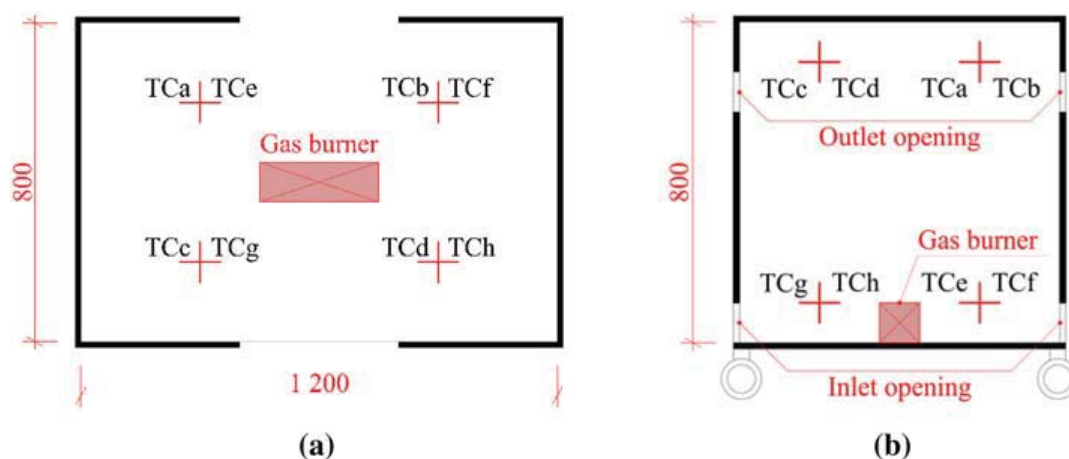


Figure 5. Position of gas burner and thermocouples in the fire furnace burning space: (a) plan view of the furnace; (b) cross-section through the furnace center.

the floor (see Fig. 5). The reproducibility of the fire experiments showed that it is possible to repeatedly achieve temperatures in the burning space of the furnace near the ISO 834 temperature curve [16] for up to 45 min (see Fig. 6).

The ISO 834 exposure was selected since it represents the standard thermal exposure during fire resistance tests. Other heating regimes were also considered. The use of the standard ISO 834 temperature curve allowed observation of the onset and extent of spalling, which becomes more severe with steeper temperature increases in the initial phases of heating, when the sample is at or close to room temperature.

The experimental samples were always placed in the upper part of the furnace, where the highest gas temperature is achieved. The samples were attached to the front walls made from aerated concrete blocks with a thickness of 100 mm (see Fig. 7). The space between the concrete wall and the experimental samples was filled with slightly expanding sealant. This sealant prevents exposure of samples to heat from more than one side.

2.3. General Description of Performed Mechanical Tests

The experimental samples were left to cool for 24 h after the fire experiment. The cooling process was not recorded. When the temperature of the samples was stabilized, the mechanical compression and tensile tests were carried out according to [21, 22]. All these mechanical tests were compared with reference samples to observe the change in mechanical properties.

2.3.1. Bending Tensile Strength (Three-Point Bending) Bending tensile strength was determined on beam samples with dimensions of 40 × 40 × 160 mm. In the next step, the tensile strength was calculated using the formula

$$f_{cf} = \frac{3 \cdot F_t \cdot l}{2 \cdot d_1 \cdot d_2^2}$$

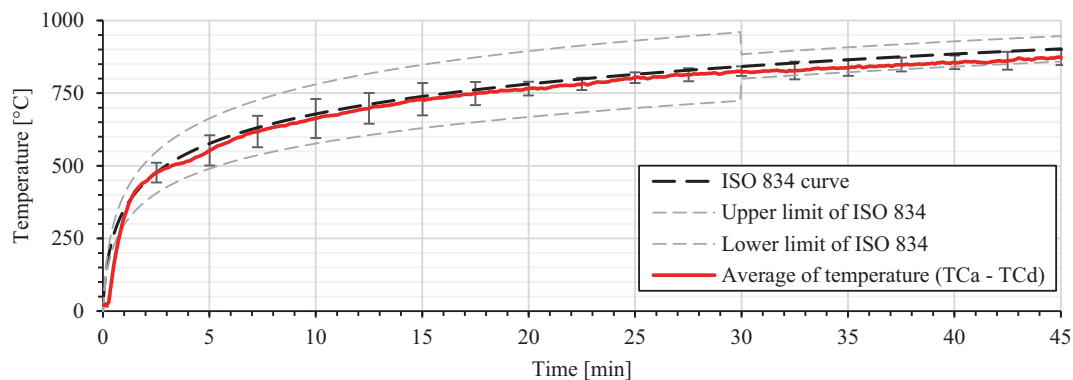


Figure 6. Temperature curve in the burning space during the fire experiment for 45 min.



Figure 7. Attaching of experimental samples to the front wall of the concrete brick furnace: (a) beam samples; (b) plate samples.

where f_{cf} represents bending tensile strength [MPa], l distance between supports [mm] and d_1 and d_2 represent the width of samples [mm]. The result values were rounded to the nearest 0.1 MPa (see Fig. 8).

2.3.2. Compressive Strength Test One of the beam samples broke during the three-point bending test and was used for the subsequent compression test. The samples were equally loaded in the compression until their explosive failure. In the next step, the compression strength was calculated using the formula:

$$f_c = \frac{F_t}{A_c} = \frac{F_t}{d_1 \cdot d_2}$$

where f_c represents compression strength [MPa], F_t maximum load value during the compression test and the product of d_1 , d_2 dimensions represents the cross-sectional area of the sample [mm]. The result values were rounded to the nearest 0.5 MPa (see Fig. 9).

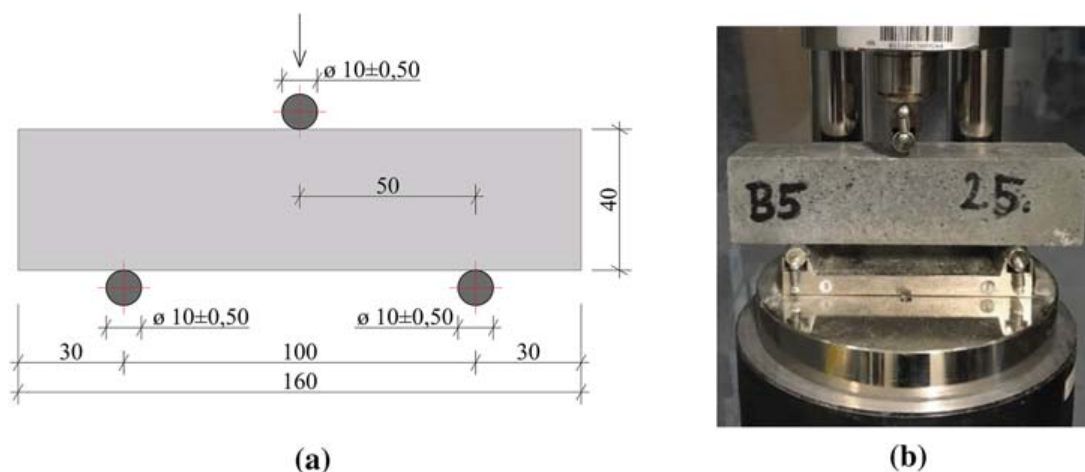


Figure 8. Tensile bending strength tests (three-point bending): (a) mechanical test scheme; (b) experimental sample in the mechanical press.

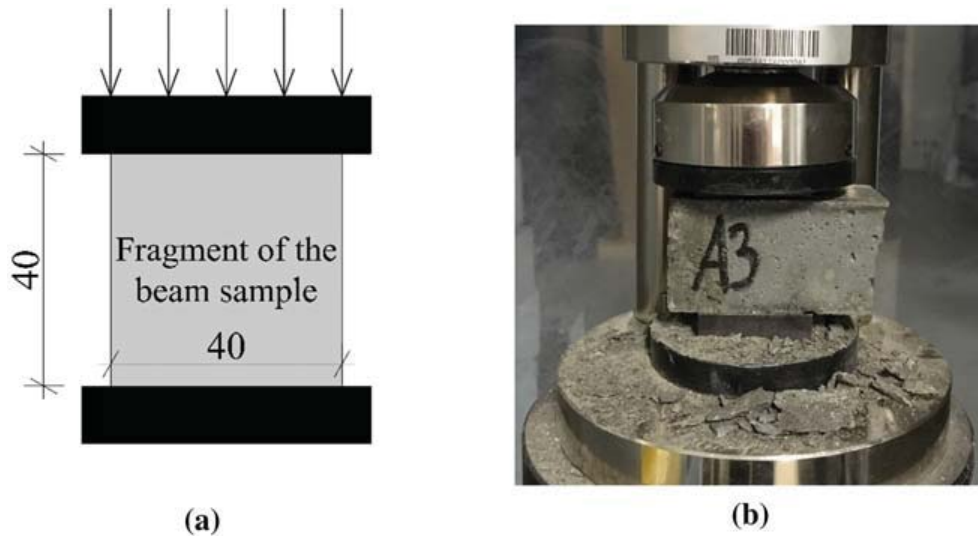


Figure 9. Compressive strength test: (a) mechanical test scheme; (b) part of beam sample in mechanical press.

2.3.3. Bending Tensile Strength (4-Point Bending) Verification of the plate samples' loss of mechanical properties was determined using the four-point bending test (loading by two loads, see Fig. 10). The samples have been loaded until failure. We have measured the maximum value of force achieved before the sample failed. The plate samples were placed in a mechanical tester and loaded at 2 mm min^{-1} . The load transfer from the press to the test samples is ensured by a spherical component (joint) with three degrees of freedom. This solution eliminates geometrical imperfections occurring during the production of samples.

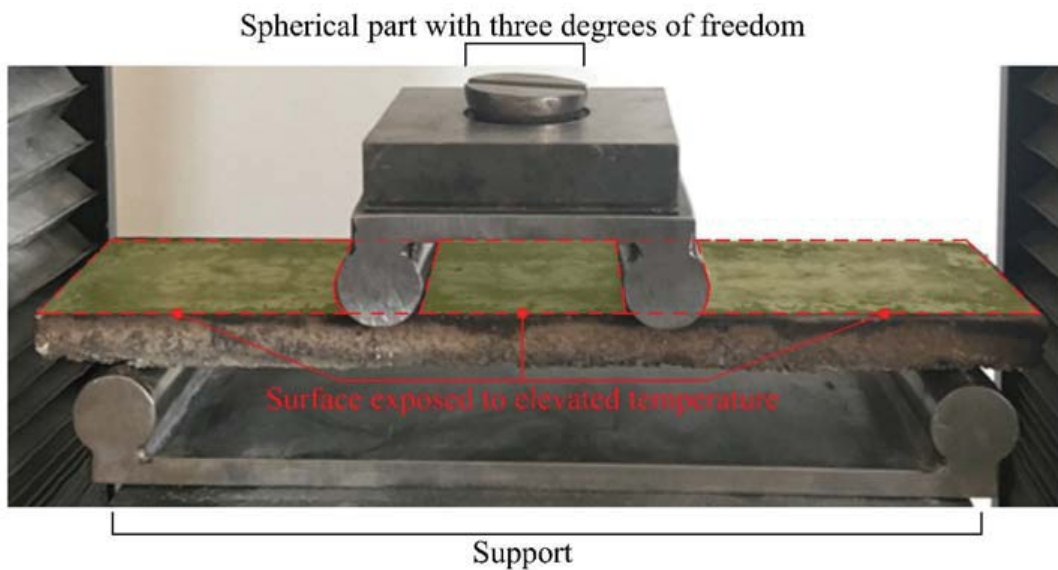


Figure 10. Experimental plate sample in the mechanical four-bending press.

2.4. Production of Test Samples for Partial Experiments

Within the experimental part of this work, a series of medium-scale fire experiments and mechanical tests were carried out. This chapter describes the procedure of preparing the experimental samples.

2.4.1. Experimental Samples for Indicative Fire Experiment For the indicative fire tests two series of plate samples were produced from TRC with (series D) and without (series C) added PP fibers according to [16]. Both variants of samples were reinforced with carbon mesh. The dimensions of the plate samples (after the concrete had hardened) are described in Table 3. Each sample was measured using a laser caliper at both ends and in the center. These values were averaged, and the resulting value served as the representative thickness. These values were further used in the evaluation of mechanical tests. Dimensions of the samples exposed to fire were measured after the experiment.

2.4.2. Experimental Samples for Fire Experiment with Determination of Quantity of PP Fibers in Concrete Mixture The experimental samples were produced from HPC with a different quantity of PP fibers in the concrete mixture. The original quantity of PP fibers was chosen from Eurocode 2 [16], where the application is described for reinforced concrete structures. For HPC and analogically for TRC structures, similar positive performance can be expected as for the reinforced concrete structures. However, due to the thickness of the TRC structures, particularly their covering layers, these structures are considerably more sensitive to the spalling of concrete layers. The quantity of PP fibers was determined as the minimum amount described in Eurocode 2 [16], i.e. 2 kg m^{-3} . Subsequently, the quantity of PP fibers in the concrete mixture was increased in multiples, see Table 4. Overall, we created 12 experimental samples, as well as 12 reference samples.

The preparation of each experimental sample was carried out according to the prescribed procedure [21]. The concrete mixture was prepared for each sample ser-

Table 3
Dimension of Plate Samples

Sample	Description of sample	Size
		Ø thickness mm
C1	TRC sample exposed to temperature according to ISO 834	19.46
C2		17.67
C3		18.77
D1	TRC sample with PP fibers exposed to temperature according to ISO 834	19.07
D2		20.57
D3		19.91

The length and width of the test sample was constant, i.e. equal to 360/100 mm due to the precise dimensions of the mold

Table 4
Quantity of PP Fibers in Concrete Mixture

Sample	Volume of concrete mixture l	Quantity of PP fibers in concrete mixture kg m ⁻³	Weight of PP fibers g
PP2	3	2	6
PP4	3	4	12
PP6	3	6	18
PP8	3	8	24

ies separately. The samples were labeled and conditioned in a water bath for 28 days before the fire experiment. During the fire experiment, we measured the temperature inside the furnace, inside of the test specimen (5 mm from the exposed side) and on the unexposed side of the experimental samples. The dimensions of the samples are described in Table 5.

3. Results and Discussion

In general, the measurements and recorded data contain an error manifested as the deviation between the actual (real) measurement value and the recorded value. In order to reliably record the measured data, we have determined the expanded measurement uncertainty by using the expansion coefficient K_u equal to 2 (to include approximately 95% of the values [26]).

3.1. Results of Indicative Experiment

The initial ambient temperature during the experiment was 20°C. Due to the massive spalling of concrete layers of the C series (plate samples without PP fibers), we had to stop the experiment after 15 min instead of the planned 30 min. The reason for the end of the experiment before the set time was to keep a sufficient mass of the experimental sample to be able to test the loss of mechanical properties. The furnace used during the experiment is shown in Fig. 11. The temperature inside the furnace was within the limits of the ISO 834 curve (see Fig. 12) during the whole experiment.

In the plate samples (C-series), massive spalling of concrete layers occurred and as a result, the textile reinforcement was exposed to flames. We could not determine the thickness of the spalled layers because a major part of the experimental samples were destroyed due to the elevated temperatures. As a result of exposing the textile reinforcement to fire, all experimental samples started burning on their surface. The burning persisted for about 3.5 min, even after then the experiment was stopped by switching off the gas supply to the furnace (see Fig. 13). The positive effect of PP fibers for high-temperature resistance has been extensively discussed in the literature and experimentally demonstrated, however, due to the

Table 5
Dimension and Weight of Experimental Samples with Different
Quantity of PP Fibers

Sample	Description of sample	Size of sample		Weight
		$\varnothing d_1$	$\varnothing d_2$	m
		mm	mm	kg
PP2-1	Reference sample	40.13	40.11	0.566
PP2-2		40.06	40.08	0.571
PP2-3		39.98	40.47	0.57
PP2-4	Sample exposed to temperature according to ISO 834	39.98	39.41	0.576
PP2-5		40	40.33	0.586
PP2-6		39.87	40.44	0.58
PP4-1	Reference sample	39.87	39.98	0.58
PP4-2		40.22	40.89	0.568
PP4-3		40.01	40.58	0.579
PP4-4	Sample exposed to temperature according to ISO 834	39.98	40.87	0.573
PP4-5		40.01	40.96	0.599
PP4-6		39.94	41.01	0.583
PP6-1	Reference sample	40.08	40.9	0.56
PP6-2		39.97	39.96	0.571
PP6-3		40.1	40.92	0.574
PP6-4	Sample exposed to temperature according to ISO 834	40.03	39.92	0.581
PP6-5		39.94	39.97	0.579
PP6-6		40	40.7	0.579
PP8-1	Reference sample	39.92	40.41	0.564
PP8-2		39.99	41.78	0.567
PP8-3		39.85	41.37	0.58
PP8-4	Sample exposed to temperature according to ISO 834	40.04	40.72	0.581
PP8-5		40.31	40.64	0.576
PP8-6		40	40.25	0.57

subtle character of TRC structures, it is necessary to minimize the effect of concrete layer spalling down to the lowest possible level.

In contrast to the C-samples, the D-sample concrete layers did not detach, and the samples maintained their integrity. These samples also started burning similarly to the C-samples, but the D-series samples only burned around 2 min after the experiment was ended. The cause of this behavior was the burn-out of the PP fibers, thus creating a “pore bridge” and enabling the migration of ER thermal decomposition products into the furnace where they were ignited. In the follow-up visual analysis, it was evident that all of the ER matrix burned out and created a cavity between the concrete and the tensile reinforcement.

One of the causes of the ER burnout was degradation of the textile reinforcement fiber and the resulting loss of bond between the HPC and the tensile reinforcement. In this case, only the reinforcement mesh intersections (the overlap of fiber strings forming the mesh) could transmit the tensile tension. The C-samples



Figure 11. Medium-scale fire furnace (miniFUR) during the indicative fire experiment.

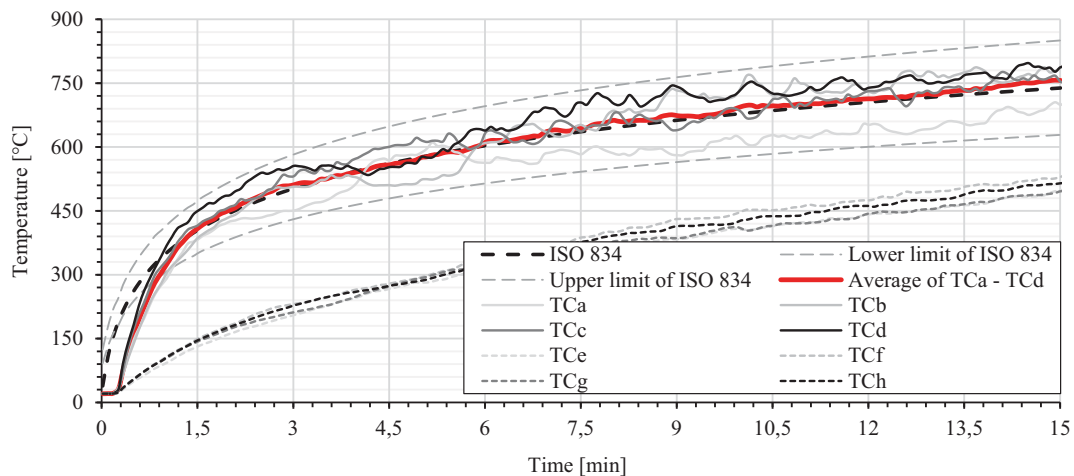


Figure 12. Temperature curve inside the furnace during the indicative fire experiment; TCa-TCd = temperature measured by thermocouples in the furnace upper part; TCe-TCh = lower part of the furnace.

were not tested in the subsequent mechanical tests (tensile strength at four-point bending) due to the destruction of experimental samples during the fire experiment. For the results of the reference and D-samples from the four-point bending mechanical test, see Fig. 14. The tensile strength of D-samples was measured up to the first crack. The measured value was around 0.28 kN for D-samples and 1.3 kN for reference samples. The mechanical test was terminated for samples exposed to elevated temperatures after exceeding the maximum specified deformation—20 mm. Conversely, the mechanical test of the reference samples was performed after exceeding the tensile strength and their sudden failure.



Figure 13. View through the ventilation opening of the experimental samples' burning surface in the furnace: ignition of C-sample, without PP fibers (left) and D-sample with PP fibers (right), after the end of the indicative experiment.

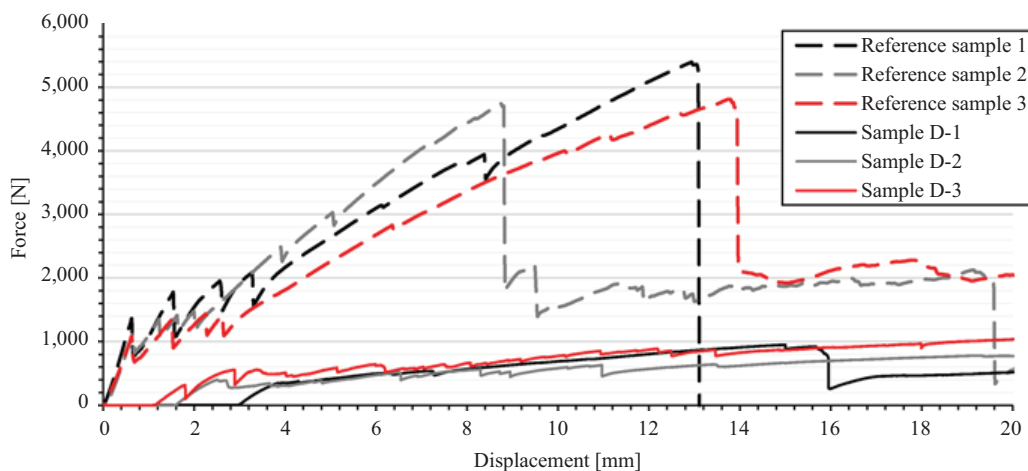


Figure 14. Comparison of reference and D-series plate samples.

3.2. Results of Fire Experiment with PP Fibers in Concrete Mixture

The experimental samples with PP fibers retained their integrity and therefore the total length of the fire experiment was 30 min.

Visual comparison of the individual samples showed the positive effect of a higher quantity of PP fibers. In this chapter, only sample series PP2 and PP4 are compared (see Fig. 15). The other series of samples were not compared, because there was no spalling of concrete layers. Depth of the spall of concrete layers was measured with a laser meter.

For the PP2 experimental series, PP fibers were used in a concentration of 2 kg m^{-3} , but spalling occurred on all sample surfaces with an average thickness of 2.63 mm (Fig. 15). When the quantity of PP fibers was increased to 4 kg m^{-3} , only limited local spalling of concrete layers occurred. Other series with a quantity of PP fibers higher than 4 kg m^{-3} , (6 and 8 kg m^{-3}) did not spall, however,

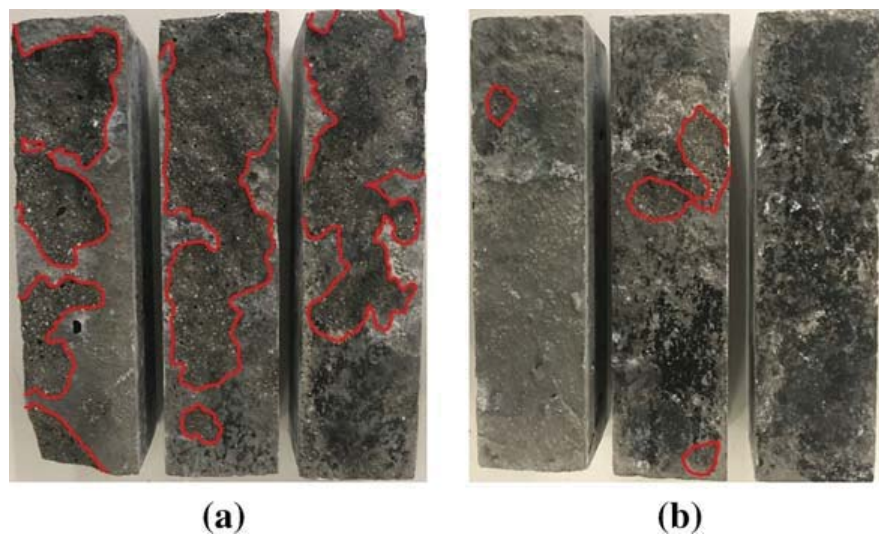


Figure 15. Comparison of concrete layer spall value of experimental samples after 30 min of exposure: (a) PP2-series samples; (b) PP4-series samples. Red-bordered parts represent the spalled parts of experimental samples (Color figure online).

applying more PP fibers would be expensive. The parameters of spalled layers and weight loss of the individual test samples are described in Table 6.

For realization of subtle structures from TRC it is necessary to consider the risk of the concrete layers spalling. The covering layer in TRC is usually very thin (about five millimeters) so undesired exposure of the textile reinforcement and

**Table 6
Value of Concrete Layers Spall and Weight Loss of Experimental Samples Exposed to ISO Curve**

Sample	Weight of experimental samples before fire experiment	Loss of weight after fire experiment	Average value of spall of concrete layers
	g	g	mm
PP2-1	537.6	28.4	2.64
PP2-2	532.6	38.4	2.51
PP2-3	525.2	44.8	2.73
PP4-1	532.6	47.4	–
PP4-2	553.4	14.6	–
PP4-3	548.8	30.2	–
PP6-1	541.6	18.4	–
PP6-2	529.4	41.6	–
PP6-3	539.6	34.4	–
PP8-1	540	24	–
PP8-2	536.4	30.6	–
PP8-3	530.4	49.6	–

possible damage of the structure could occur due to spalling in the exposed area. For this reason, the protection which prevented spalling on the concrete layer surface is considered to be a satisfactory result. In the subsequent phase, a mechanical test of the tensile and compressive strength was performed. According to [27] we can observe that the variable value of mechanical properties depends on the temperature reached. Thermal-graphic analysis (Fig. 16) was performed from the measured temperatures. From these pictures, we can observe the part of beam samples which showed an increase or decrease in mechanical properties. For detailed measured values see Figs. 17 and 18

Figure 16 shows that the greater part of the samples achieved less tensile strength due to the temperature increase. In the case of tensile strength, the temperature range where the samples achieve higher values of tensile strength is narrower than in the case of compressive strength [27]. The temperatures between measured points were interpolated.

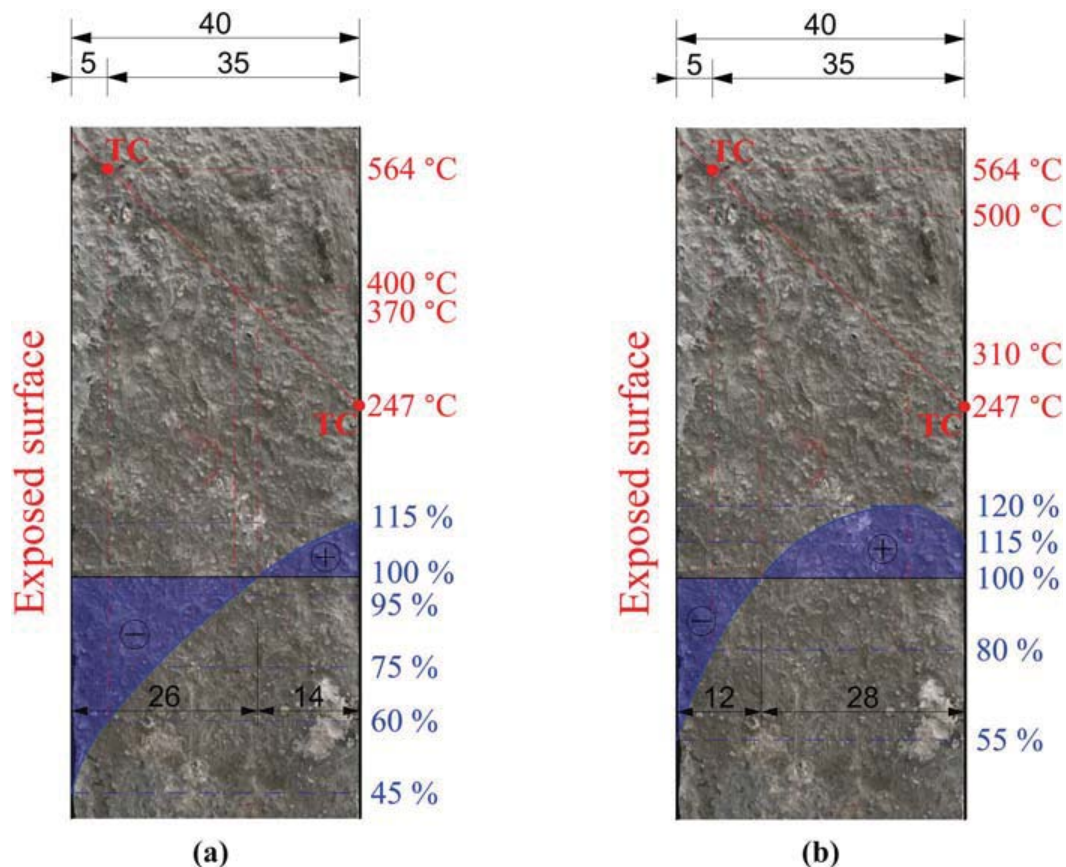


Figure 16. Thermal-graphic analysis of experimental beam samples PP4: (a) bending tensile strength; (b) compressive strength; TC—position of thermocouple; blue color—strength value, where 100% corresponds to strength at 20°C; red color—temperature reached; (+)—part of sample where the strength is higher than strength at normal temperature; (—) —part of sample where the strength is lower than strength at normal temperature (Color figure online).

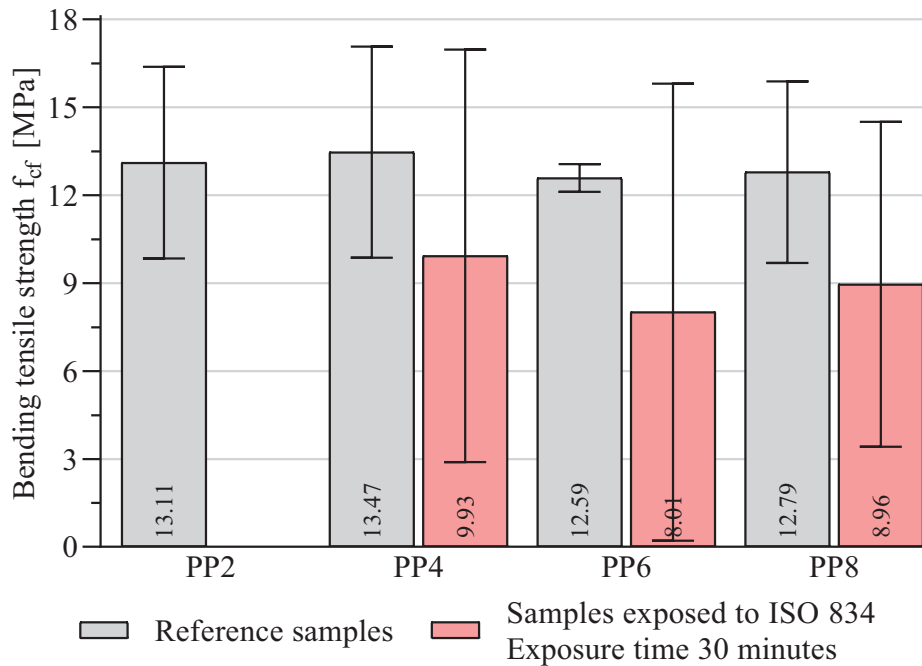


Figure 17. Comparison of bending tensile strength of reference samples and samples exposed to temperature according to ISO 834.

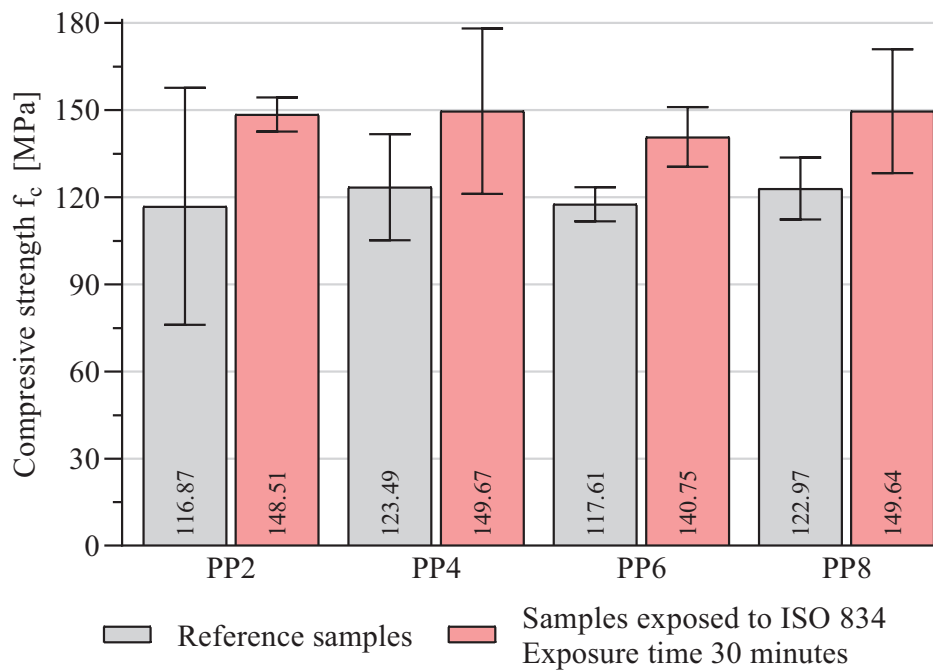


Figure 18. Comparison of compressive strength of reference samples and samples exposed to temperature according to ISO 834.

In Fig. 16 it is possible to see a decreasing trend of tensile strength compared to the reference samples and samples exposed to elevated temperatures. The same trend is described in EN 1992-1-2, which also only considers the decrease of tensile strength at elevated temperatures. On the other hand, there are several studies which describe the behavior of HPC at elevated temperatures concerning the change of mechanical properties. The increase of tensile strength occurs in the interval between 100 and 370°C [27]. In this range of temperatures, we can monitor the maximal increase of tensile strength around 15% at 220°C. However, when the temperature interval is exceeded, there is a rapid decrease of tensile strength. For the experimental samples, this interval was exceeded, and therefore the tensile strength decreased compared to the reference samples. Measured temperatures during fire experiment were around 247°C on the unexposed surface. Due to that, the tensile strength of the samples was lower than tensile strength at normal temperatures, because most of the samples exceeded 370°C (Fig. 16). Therefore the result was that tensile strength decreased approx. by 31%. For the PP2-samples, the setting of the load force was too fast, and the press software could not evaluate the resulting bending tensile strength. Practically immediately, the sample failed, and therefore these values are considered as zero.

For compressive strength, there is a similar trend in an increase of compressive strength. In contrast to tensile strength, there is a different temperature interval where the compressive strength increases. This interval is bordered by an upper value of 500°C [27]. The fire exposure was not long enough to exceed this temperature in the major part of the sample body. Therefore the result of compressive strength is higher than the strength at a normal temperature approximately by 22%. This was likely achieved by hydration of the remaining cement particle cores due to the evaporation of the free and partly also chemically bound water inside the sample. Similar observations were made in [28–30].

4. Conclusion

The aim of this paper was to investigate the behavior of textile-reinforced concrete (TRC) at elevated temperatures according to the standard temperature curve (ISO 834). Experiments were performed in a furnace for medium-scale fire experiments. Experimental samples were made from high-performance concrete (HPC) with tensile reinforcement by carbon fibers. These tensile reinforcements have a matrix of an epoxy resin (ER). The samples had the shape of a small beam (160 × 40 × 40 mm) and plate (100 × 360 × 18 mm), exposed on one side to the elevated temperatures for 15 and 30 min. The next step was to compare the change of mechanical properties in reference samples and samples exposed to elevated temperatures. The compressive strength and bending tensile strength of three- and four-point bending was investigated. In the first experimental part, an indicative fire experiment was performed describing problematic areas of TRC in the plate sample form. Spalling of concrete layers and loss of interaction between materials due to the low temperature resistance of ER are the high-risk problematic areas. In the second experimental part, experiments investigating solutions for

improvement of elevated-temperature resistance were performed. These solutions include the addition of polypropylene fibers (PP) to the concrete mixture.

The indicative fire experiment was performed as an informative experiment to describe the problematic areas of the TRC structure with HPC. The experiment revealed two basic problems. The first one was the high risk of spalling of concrete layers, where the whole covering layer of experimental samples spalled out in samples without PP fibers. Due to the extent of damage, these samples could not be further mechanically tested. The second one was the loss of interaction due to the low temperature resistance of the ER. There was no spalling of concrete layers in this series because 2 kg m^{-3} of PP fibers was added according to [16]. Therefore we were able to carry out the four-point bending test. From the mechanical tests we consider that the ability of plate samples to transmit tensile tension is completely lost (Fig. 14). During these tests, there was no progressive rupture as in the reference samples, because the textile reinforcement was complete without matrix, and the individual fibers of reinforcement mesh were pulled out. The interaction was lost due to the low temperature resistance of the ER. At the same time, during the fire experiment it was possible to observe the formation of pores, because the PP fibers burn out. After that, the products of thermal decomposition of the ER burn on the surface of the sample (Fig. 13).

In the follow-up experiment, the optimal quantity of PP fibers was experimentally verified. The criteria for determining the quantity of fibers were: the value of spalling of concrete layers, change of the mechanical properties of the experimental samples and, finally, the economic advantage. The optimum amount of 4 kg m^{-3} was experimentally established, where the spalling of concrete layers was only in the local surface part of samples (Fig. 15). The samples were subjected to mechanical testing according to [21, 22]. Following the performed studies [27, 31] we saw a similar trend of tensile and compressive strength. In contrast to EN 1991-1-2, where only the decrease of tensile and compressive strength is considered, we observed an increase of compressive strength by approximately 22%, following the ISO 834 of 30 min. On the contrary, the tensile strength decreased by approximately 30% more than the strength of the reference sample, because the temperature interval where the strength increases is narrower than in the case of compressive strength (Fig. 17, 18). However, in the case of tensile strength, which is primarily transmitted by tensile reinforcement, an increase in compressive strength is more important compared to the decrease in tensile strength.

For follow-up work, it would be particularly useful to investigate the behavior of the ER at elevated temperatures. This may have the negative effect of unwanted spalling of concrete layers due to ER evaporation and contributing to a pore pressure increase in TRC construction elements. The choice of an ER with elevated temperatures resistance could prevent this negative behavior. Another variant of TRC structure protection is the design of additional fire protection. For an efficient design, it is necessary to perform a detailed temperature analysis and describe the behavior of the individual components at the elevated temperatures of materials from which is the TRC composed. At the same time we should research more deeply the fact that the structures made of TRC with epoxy resin matrix can burn on their surfaces. This fact can affect the application of these

structures in civil engineering, because there may be requirements so that the structure does not release heat. Therefore the amount of heat released should be determined, for example, by calorimeter analysis.

Acknowledgements

This work has been supported by the Ministry of Education, Youth and Sports under the National Sustainability Programme I, project No. LO1605.

References

1. Kynclova M, Fiala C, Hajek P (2011) High performance concrete as a sustainable material. *Int J Sustain Build Technol Urban Dev* 2:63–68. <https://doi.org/10.5390/SUSB.2011.2.1.063>
2. Laiblová L, Pešta J, Kumar A, Hájek P, Fiala C, Vlach T, Kočí V (2019) Environmental impact of textile reinforced concrete facades compared to conventional solutions—LCA case study. *Materials* 12:3194. <https://doi.org/10.3390/ma12193194>
3. Portal NW (2015) Usability of textile reinforced concrete: structural performance. *Durab Sustain* 3914:130
4. Portal NW, Lundgren K, Wallbaum H, Malaga K (2015) Sustainable potential of textile-reinforced concrete. *J Mater Civ Eng* 27:04014207. [https://doi.org/10.1061/\(ASCE\)MT.1943-5533.0001160](https://doi.org/10.1061/(ASCE)MT.1943-5533.0001160)
5. Tysmans T, Adriaenssens S, Wastiels J, Remy O (2011) Textile reinforced cement composites for the design of very thin saddle shells: a case study 6
6. Walraven JStoelhorst D((2008) Tailor made concrete structures: new solutions for our society (Abstracts Book 314 pages + CD-ROM full papers 1196 pages). CRC Press, Boca Raton. [10.1201/9781439828410](https://doi.org/10.1201/9781439828410)
7. Kulas C (2015) Actual applications and potential of textile-reinforced concrete
8. Laiblová L, Vlach T, Ženíšek M, Řepka J, Hájek P (2018) Lightweight TRC facade panels with the LEDs. *Key Eng Mater* 760:141–146. <https://doi.org/10.4028/www.scientific.net/KEM.760.141>
9. Solidian (2018) Leading in construction with non-metallic reinforcement
10. Hegger J, Will N, Bruckermann O, Voss S (2006) Load-bearing behaviour and simulation of textile reinforced concrete. *Mater Struct* 39:765–776. <https://doi.org/10.1617/s11527-005-9039-y>
11. Hegger J, Voss S (2008) Investigations on the bearing behaviour and application potential of textile reinforced concrete. *Eng Struct* 30:2050–2056. <https://doi.org/10.1016/j.engstruct.2008.01.006>
12. Reinhard HW, Kruger M, Raupach M (2008) Behavior of textile-reinforced concrete in fire. *ACI Spec Publ*, SP250, 99–100
13. Buttner RM, Orlowsky J, Raupach M (2014) Fire resistance tests of textile reinforced concrete under static loading—results and future developments. In: Fifth international RILEM workshop high perform. Fiber Reinforced Cement Composites HPRFRC5
14. Fürst R (2019) Fire specifics of building load-bearing structures of textile reinforced concrete (Diploma thesis). CTU in Prague, Prague

15. Kapsalis P, Tysmans T, Verbruggen S, Triantafyllou T (2018) Preliminary high-temperature tests of textile reinforced concrete (TRC). In: Proceedings, vol 2, p 522. <https://doi.org/10.3390/ICEM18-05416>
16. EN 1992-1-2—Eurocode 2: design of concrete structures—part 1–2: general rules—structural fire design, 2006
17. EN 1992-1-1: Eurocode 2: design of concrete structures—part 1–1: general rules and rules for buildings, 2006
18. Isayev AI (2016) Encyclopedia of polymer blends. Volume 3: structure. Wiley-VCH, Weinheim
19. Aitcin P-C (2005) Česká komora autorizovaných inženýrů a techniků činných ve výstavbě, Česká betonářská společnost, 2005. High Performance Concrete. Pro Českou komoru autorizovaných inženýrů a techniků činných ve výstavbě (ČKAIT) a Českou betonářskou společnost vydalo Informační centrum ČKAIT, Prague
20. MasterFiber 012, Technical data sheet: Monofilament fibre to prevent cracks on the concrete surface due to plastic shrinkage and settling [WWW Document], 2017. BASF. https://assets.master-builders-solutions.basf.com/cs-cz/basf-masterfiber%20012-tl.pdf?__hstc=829422.9ef1a35fe0d1675bce73e857272c47df.1589198101020.1589198101020.1589198101020.1&__hssc=829422.3.1589198101020&__hsfp=4227766293. Accessed 18 Mar 2020
21. EN 12390-3: Testing hardened concrete—part 3: compressive strength of test specimens, 2009
22. EN 12390-5: Testing hardened concrete—part 5: flexural strength of test specimens. B.m, 2009
23. Vlach T (2013) Adhesion of carbon and basalt composite reinforcement with UHPC (Diploma thesis). CTU in Prague, Prague
24. Technical data sheet: Solidian GRID Q142/142-CCE-25, 2018
25. EN 12390-2: Testing hardened concrete—part 2: making and curing specimens for strength tests, 2019
26. Rabinovich SG (2010) Measurement errors and uncertainties: theory and practice. AIP Press, Springer, New York
27. Drzymała T, Jackiewicz-Rek W, Tomaszewski M, Kuś A, Gałaj J, Šukys R (2017) Effects of high temperature on the properties of high performance concrete (HPC). *Procedia Eng* 172:256–263. <https://doi.org/10.1016/j.proeng.2017.02.108>
28. Kupilík V (2006) Stavební konstrukce z požárního hlediska. Grada, Praha
29. Khouri GA, Anderberg Y, Both K, Fellinger J, Majorana C, Høj NP (2007) fib Bulletin 38. Fire design of concrete structures, fib Bulletins. fib. The International Federation for Structural Concrete. <https://doi.org/10.35789/fib.BULL.0038>
30. Naus DJ (2006) The effect of elevated temperature on concrete materials and structures—a literature review. (No. ORNL/TM-2005/553, 974590). <https://doi.org/10.2172/974590>
31. Kupilík V (2009) Fire protection of construction. Hungary

PAPER III

Use of Cement Suspension as an Alternative Matrix Material for Textile-Reinforced Concrete

Authors: Richard Fürst, Eliška Fürst, Tomáš Vlach, Jakub Řepka,
Vladimír Mózer

Journal: Materials

Publisher: MDPI

Volume and number: 14/9

Year of publication: 2021

Number of pages: 18

DOI: [10.3390/ma14092127](https://doi.org/10.3390/ma14092127)

Article

Use of Cement Suspension as an Alternative Matrix Material for Textile-Reinforced Concrete

Richard Fürst ^{1,2,3,*} , Eliška Fürst ^{4,5} , Tomáš Vlach ^{2,6} , Jakub Řepka ^{2,6} , Marek Pokorný ^{1,2} 
and Vladimír Mózer ^{1,2} 

- ¹ Fire Laboratory, University Centre for Energy Efficient Buildings of Czech Technical University in Prague, Třinecká 1024, 273 43 Buštěhrad, Czech Republic; marek.pokorny@cvut.cz (M.P.); vladimir.mozer@cvut.cz (V.M.)
 - ² Faculty of Civil Engineering, Czech Technical University in Prague, 166 29 Prague 6, Czech Republic; tomas.vlach@cvut.cz (T.V.); jakub.repka@cvut.cz (J.Ř.)
 - ³ Federal Institute for Materials Research and Testing (BAM), Division 7.3-Fire Engineering, Unter den Eichen 87, 12205 Berlin, Germany
 - ⁴ Institute of Organic Chemistry and Biochemistry of the Czech Academy of Sciences, Flemingovo n. 2, 16610 Prague 6, Czech Republic; eliska.fuerst@mdc-berlin.de
 - ⁵ Allosteric Proteomics, Max Delbrück Center for Molecular Medicine, Robert-Rössle Straße 10, 13125 Berlin, Germany
 - ⁶ Laboratory of Composite Structures, University Centre for Energy Efficient Buildings of Czech Technical University in Prague, Třinecká 1024, 273 43 Buštěhrad, Czech Republic
- * Correspondence: Richard.furst@cvut.cz; Tel.: +49-30-8104-4775



Citation: Fürst, R.; Fürst, E.; Vlach, T.; Řepka, J.; Pokorný, M.; Mózer, V. Use of Cement Suspension as an Alternative Matrix Material for Textile-Reinforced Concrete. *Materials* **2021**, *14*, 2127. <https://doi.org/10.3390/ma14092127>

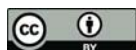
Academic Editor: Dario De Domenico

Received: 15 March 2021

Accepted: 20 April 2021

Published: 22 April 2021

Publisher's Note: MDPI stays neutral with regard to jurisdictional claims in published maps and institutional affiliations.



Copyright: © 2021 by the authors. Licensee MDPI, Basel, Switzerland. This article is an open access article distributed under the terms and conditions of the Creative Commons Attribution (CC BY) license (<https://creativecommons.org/licenses/by/4.0/>).

Abstract: Textile-reinforced concrete (TRC) is a material consisting of high-performance concrete (HPC) and tensile reinforcement comprised of carbon roving with epoxy resin matrix. However, the problem of low epoxy resin resistance at higher temperatures persists. In this work, an alternative to the epoxy resin matrix, a non-combustible cement suspension (cement milk) which has proven stability at elevated temperatures, was evaluated. In the first part of the work, microscopic research was carried out to determine the distribution of particle sizes in the cement suspension. Subsequently, five series of plate samples differing in the type of cement and the method of textile reinforcement saturation were designed and prepared. Mechanical experiments (four-point bending tests) were carried out to verify the properties of each sample type. It was found that the highest efficiency of carbon roving saturation was achieved by using finer ground cement (CEM 52.5) and the pressure saturation method. Moreover, this solution also exhibited the best results in the four-point bending test. Finally, the use of CEM 52.5 in the cement matrix appears to be a feasible variant for TRC constructions that could overcome problems with its low temperature resistance.

Keywords: textile-reinforced concrete; non-combustibility; cohesion; high-performance concrete; carbon fibers; cement matrix

1. Introduction

Textile-reinforced concrete (TRC) is a construction material currently used for non-load bearing structures [1–5] and facade panels, but it could potentially be used in load-bearing construction elements [6,7]. In load-bearing structures, marginal TRC application issues arise from the ability to withstand high temperatures during fire. In previous work the main weakness of TRC was identified as the behavior of the homogenized carbon-fiber reinforcement with epoxy resin matrix at elevated temperatures [8,9]. Fire experiments showed that the load-bearing capacity of TRC at elevated temperatures depends on the interaction between the textile reinforcement and high-performance concrete (HPC). Since epoxy resins used in this variant of TRC have low resistance to higher temperatures [10–13], this study focused on the identification of an alternative available material for the homogenization of textile reinforcement before installation in concrete.

The traditional variant of carbon TRC is composed of impregnated carbon roving HPC with a synthetic resin matrix [14]. By replacing the steel reinforcing elements (rebars, wires etc.) of standard reinforced concrete structures with impregnated carbon roving, corrosion protection is not required and the covering layer can be significantly reduced. The combination of HPC with carbon-fiber reinforcement allows for subtler structural elements. A cross-section indicating general composition of a TRC structure, a hollow column, is shown in Figure 1.

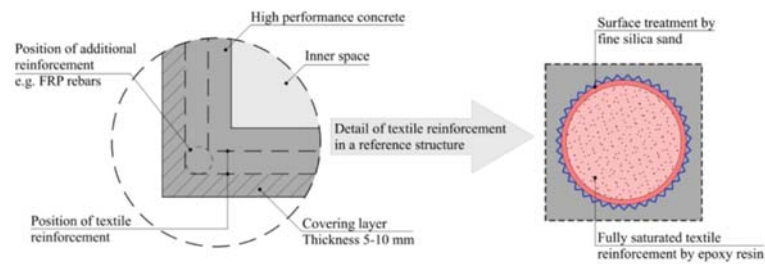


Figure 1. Composition of a TRC structural column.

Carbon-fiber roving impregnation brings higher load-bearing capacity due to the increased tensile load distribution across the entire cross-section of the carbon fiber strand. The epoxy resin which is used as impregnation material, however, increases the brittleness of the composite. Synthetic-based materials are increasingly being used in modern construction, often in the form of synthetic epoxy resins and adhesives. However, in load-bearing structures, this material can negatively affect their mechanical properties from the fire safety perspective. For these structures, it is necessary to determine their behavior at elevated temperatures, and identify appropriate protective measures based on these findings. In composite structures, their load-bearing capacity depends on the interaction between the synthetic materials and textile reinforcement.

In general, the synthetic resins consist of a two-component resin and a hardener. According to the specified preparation instructions, resins change their structure from a free molecular arrangement to a stable, crosslinked mesh-state. After crosslinking, the epoxy resin acquires its final mechanical properties. This process is called curing (Figure 2).

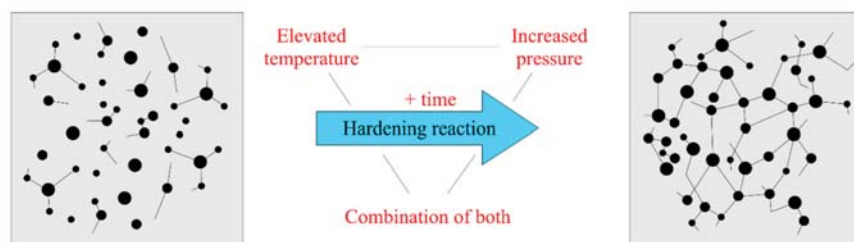


Figure 2. Diagram of a resin hardening process.

The standard hardening process includes elevated pressure and temperature, or a combination thereof, for a prescribed time. The specific method depends on the selected product. For some types of resins e.g., [15], better mechanical properties or higher temperature resistance are achieved through a slower and longer hardening process. These properties also depend on the molecular weight, the distribution of the macromolecules in the resin, and the phase state, among others [10]. It is necessary to consider the method of the hardening process. For example, in the production of TRC, it is not possible to use resins with higher temperature resistance, because the process of hardening would be overly complicated and financially demanding [16].

Another example of epoxy resin use is found in carbon lamellas, in the form of the additional external tensile reinforcement of existing structures. Without additional fire protection, the lamellas would achieve practically zero fire resistance, and the affected structure would be significantly weakened. In this case, it is relatively easy to design additional protection against elevated temperature, e.g., from board materials (Figure 3) [17].

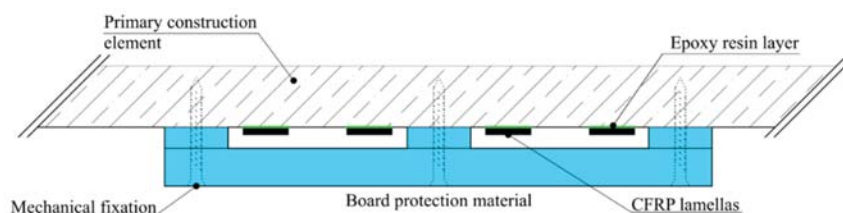


Figure 3. Protection of CFRP (Carbon-fiber-reinforced polymer) lamellas against elevated temperature in epoxy resin layers by board material.

An additional possible application of epoxy resins in concrete structures could be in the repair of damaged concrete structures [18], the modification of concrete surfaces, and the elimination of cracks on concrete surfaces [19]. The other possibility of using synthetic resins is in the improvement of mortar-based building materials [20].

A problem occurs when TRC is considered as a material for potential use in load-bearing constructions. From the perspective of fire protection, textile reinforcement is a combination of materials in which the loss of interaction between the materials is probable. Synthetic resins play a crucial role in TRC by redistributing tension to the entire strand of textile reinforcement. When the temperature rises to the synthetic resin glazing temperature, a massive increase in deformation, decrease in modulus of elasticity, and loss of interaction occurs. Several studies at elevated temperatures have dealt with the subject of textile-reinforced concrete [21]. In general, it can be considered that synthetic resins are advantageous for the tensile reinforcement matrix because their homogeneous structure allows for the full saturation of the textile reinforcement. At the same time, resins provide additional protection against mechanical damage during production and from atmospheric corrosion [22]. However, the wider use of these structures can be affected by their instability at elevated temperatures. The use of synthetic resins in the production of TRC is currently satisfactory at room temperatures, where an excellent interaction between the materials is achieved. The protection of TRC against loss of interaction is possible either by additional fire protection, as in the case of carbon lamellas, or by the design of a matrix material with sufficient temperature resistance higher than 700 °C. However, the advantage of not using additional fire protection is maintaining the subtle character of the TRC structure and its high visual quality.

Considering all these problematic areas of TRC with an epoxy resin matrix at elevated temperatures, an alternative material solution was sought to potentially substitute flammable epoxy resin, as it has been shown that this component contributes to the development of fire [8,23].

In reaction to the temperature instability of an organic matrix, several studies are examining how to replace the flammable organic matrix of textile reinforcement. One possible variant is to use textile fibers as a reinforcement layer in the mortar, which improves the mechanical properties of masonry [24]. Other studies investigated the influence of the inorganic matrix materials on the mechanical properties if textile reinforcement while using materials such as SiO₂, nano-silica, or micro-silica [25–28]. Simultaneously, cement suspensions and cement mixtures are also used. In the case of cement mixture for the impregnation of textile reinforcement, the combination of cement, micro silica, plasticizer, and water has been discussed [29]. In a study describing mechanical properties with impregnation of glass textile reinforcement, cement suspension with cement CEM 42,5 was used [30]. All these studies describe improvements to the mechanical properties of textile

reinforcements, and explain the influence of particle size on the depth of impregnation, but these studies dealt mainly with glass reinforcement. However, it is necessary to consider which types of textile reinforcement are more beneficial. Therefore, it is advisable to investigate the matrix alternative with carbon fiber because, in contrast with the individual glass fiber filaments, the carbon filaments are half the size [31].

Based on the mechanical properties and mechanical parameters (especially the size of the individual carbon filaments), it is appropriate to determine how these materials could be used with cement suspension impregnation. For this reason, a series of experiments have been proposed to verify the behavior of commonly available types of cement, as an obtainable and common material, in impregnating carbon reinforcement with the most straightforward possible application.

This solution would eliminate the low resistance of TRC structures to elevated temperatures [29]. On the other hand, a problem in the curing process could emerge. The size of the cement particles in the cement suspension is larger than the size of filaments in the carbon roving. The distribution of the cement particle size in cement generally ranges from 8 to 40 μm [32,33]. These particles might not penetrate the deeper layers of textile reinforcement, and the required interaction between the textile reinforcement and HPC may not occur (Figure 4).

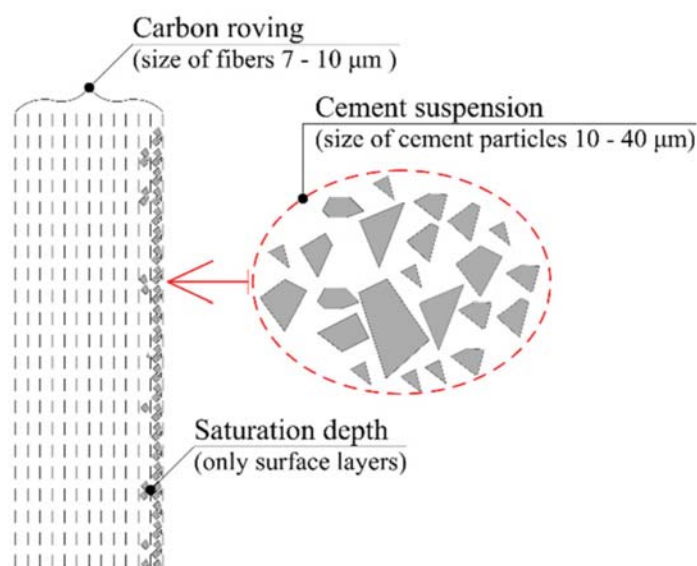


Figure 4. Scheme of carbon roving with cement suspension.

The TRC presented in this paper was developed at the Faculty of Civil Engineering, Czech Technical University (CTU), in Prague, and at the University Centre for Energy Efficient Buildings (UCEEB), CTU, in Prague. Following the development of this material, an alternative matrix of textile reinforcement was projected to verify this solution and evaluate the possibility of future use of cement suspension as an alternative material for textile reinforcement.

This work focuses on an alternative textile reinforcement matrix material because, from the viewpoint of fire protection, an epoxy resin matrix could theoretically lead to the collapse of an entire TRC construction [12,34,35]. Therefore, a cement suspension matrix was proposed which eliminates all flammable components of this composite material. Various methods of cement suspension application and depth of textile reinforcement saturation were investigated, based on the cement type. Mechanical properties were determined by four-point bending test and compared with traditional TRC samples with

an epoxy-resin matrix, which served as a positive control of the full-roving saturation. These tests were conducted at standard temperatures. Different cement types were also investigated from the viewpoint of cement particle distribution.

2. Materials and Methods

2.1. High-Performance Concrete Mixture

The HPC mixture used for the preparation of experimental samples was prepared according to Table 1. This HPC mixture was developed at the Czech Technical University in Prague, Czech Republic. By following the prescribed procedure, this material can reach a compressive strength of about 140.5 MPa according to [36], a tensile strength of 15.4 MPa according to [37], and a modulus of elasticity value of about 49.5 GPa [4].

Table 1. HPC component mixture of [4].

Mixture Components	Quantity
	kg·m ⁻³
CEM I 42.5 R	680
Silica sand	960
Silica flour (ground quartz)	325
Silica fume (microsilica)	175
Superplasticizer	29
Water	171
Total	2420

2.2. Textile Tensile Reinforcement

The carbon roving used for tensile reinforcement was developed by the Tenax company (Viganò (LC), Italy) as a commercially available product named Tenax STS40 F13 24K 1600tex. The material properties of the carbon roving are described in Table 2. Two types of cement were used for the subsequent saturation of the textile reinforcement: specifically, CEM 42.5 R and CEM 52.5 R.

Table 2. Material data of carbon roving [31].

Material Properties	Value	Units
Sizing properties	F13	-
Number of filaments	24 000	-
Nominal linear density	1600	tex
Filament diameter	7.0	µm
Density	1.77	g · cm ⁻³
Tensile properties		
Tensile strength	4000.0	MPa
Modulus of elasticity	240.0	GPa

2.3. Geometry of Experimental Samples

For the mechanical experiment, the experimental sample parameters were chosen according to [37,38], with modified specimen height. The distance between the centers of support was standard for a four-point bending test: 300 mm and 100 mm between loading support centers. The experimental plate samples were designed with dimensions of 100 mm × 360 mm × 18 mm and provided with two layers of textile reinforcement. The upper layer of reinforcement mesh was used only for construction reasons. Thus, only the reinforcement on the bottom bend side was considered as the primary tensile reinforcement. In a real construction, specimens are logically able to transmit a bend loading in both directions. The dimensions of the experimental sample and positions of its reinforcement mesh are depicted in Figure 5. These experimental sample shapes and sizes was also chosen based on their suitability for the subsequent verification of mechanical

properties in four-point bending tests. The thickness of the sample was adjusted to the approximate thickness of the TRC in real applications, and was also based on previous experiments [39,40]. Then, it was possible to compare the results. The bending moment in between the loading supports was constant. This was the monitored area where the cracks development and the collapse of the sample occurred. The mechanical-resistance experiments were conducted at standard (room) temperature.

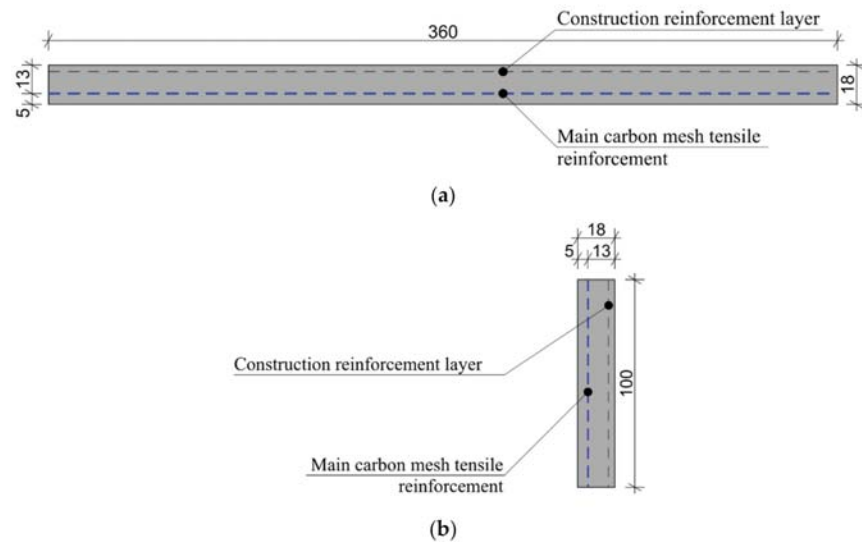


Figure 5. Description of the experimental sample and position of reinforcement mesh (unit: mm): (a) Plan view of the experimental sample; (b) Cross-section of the experimental sample.

In the first part of sample manufacturing, the rovings were saturated using the methods described in Table 3. After curing, they were fixed in silicon form and placed into a concrete beam with a length of 100 mm and cross-section area of 8 mm × 8 mm. This process minimized the risk of damaging the saturated fibers during cutting. These beam samples could be then cut without fiber breakage or defibration, and subjected to microscopy analysis. The geometry of experimental sample is displayed in Figure 6.

Table 3. Variants of experimental samples.

Description of Samples	Type of Saturation
A	Experimental samples saturated with CEM 42.5 R–pressure saturation.
B	Experimental samples saturated with CEM 52.5 R–pressure saturation.
C	Experimental samples saturated with CEM 42.5 R–surface saturation by a roller.
D	Experimental samples saturated with CEM 52.5 R–surface saturation by a roller.
E	Experimental samples without any saturation.
-	Reference samples with epoxy resin matrix–surface saturation by a roller.

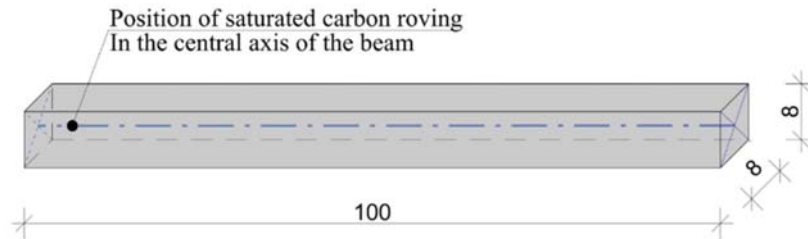


Figure 6. Description of the beam sample with the position of the saturated roving (unit: mm).

2.4. Microscopy

CEM 42.5 R and CEM 52.5 R samples were weighed on analytical scales and supplemented with water so that both suspensions contained the same quantity of particles in the specified volume. From both samples, 50 μL of suspension were taken and analyzed on a Zeiss LSM 780 (Carl Zeiss AG, Oberkochen, Germany) confocal microscope using the basic optical microscope settings and 100 \times magnification. The microscope photographs were analyzed using Cell Profiler 4.0.4. All analyzed samples were taken from three independent replicates for each type of cement suspension.

Images of beam samples were taken with a Canon EOS 5D Mark II camera (Canon Inc, Ōta, Japan) and the saturation depth was further analyzed using ImageJ, version 1.8.0.

2.5. Preparations of Experimental Samples

The development of the experimental samples comprised of textile reinforcement saturation in tension frames, preparation of production forms with the required size, and conditioning. Altogether, six experimental sample variants were developed in triplicate. Each sample was labelled with a serial letter (A-E) and a sample number (1-3) (Table 3).

The experimental samples of series A and B were saturated under pressure to achieve a deeper saturation of the carbon filaments. The process of saturation under increased pressure was further enhanced by the application of a significantly excessive amount of cement suspension, which was mechanically pressed into the roving. During this process, the impregnated fibers were at the same time tensioned on a tension frame and left to harden to form a solid reinforcing mesh.

In the samples of series C and D, the carbon fibers were tensioned on a tension frame. The layer of cement suspension was subsequently applied by using a roller. The fibers were tensioned on a tension frame in two layers. In the first layer, all the rovings were positioned in a longitudinal direction; and in a transverse direction in the second layer. In this case, the joints of the fibers occurred only at the fiber overlaps. However, according to [41], these joints do not affect the resulting tensile strength. The final form of the reinforcement mesh was completed with a 25 mm distance between the fibers. The final reinforcement mesh with hardened cement layers and the method of forming are described in Figure 7.

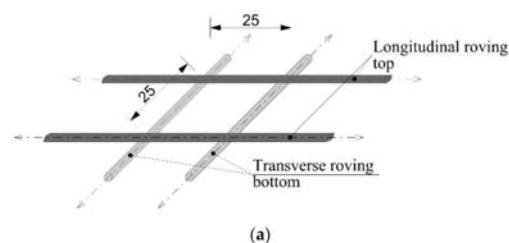


Figure 7. Cont.



Figure 7. Preparation of reinforcement mesh: (a) Method of carbon mesh preparation (unit: mm); (b) Mesh from carbon roving saturated with cement suspension—surface application by roller (from left): CEM 42.5 R, CEM 52.5 R.

Each experimental sample was conditioned for 28 days in a lime–water bath [37]. The beam samples were cut at one third of length and visually analyzed as described in Section 2.4, for the evaluation of the overall depth and percentage of saturation (Figure 8).

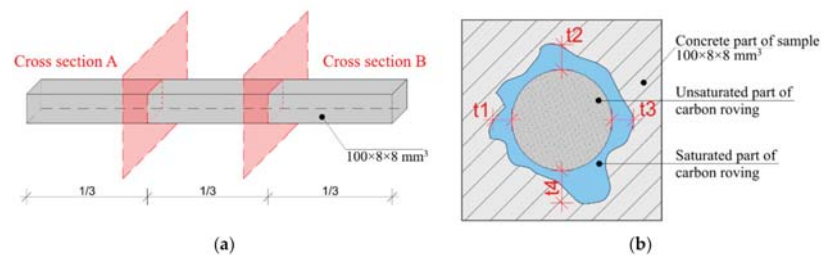


Figure 8. Experimental beam samples: (a) Scheme of experimental samples with cross-section position; (b) Method of the saturation depth evaluation.

2.6. Statistical Data Analysis

For the statistical evaluation of the saturation depth data (Figure 12), the so-called expanded uncertainty coefficient $k_{u1} = 2.0$ (interval 95% of the contained values) was used. In other statistical assessments, outliers were not considered. Values outside the 90% quantile range (10% of outlying values from top and bottom) were considered as outliers. For the statistical evaluation of cement particles distribution, a Student's t-test was used. All statistical analyses were performed in GraphPad Prism, version 8.0, and MS Excel, 2019. The four-point bending tests were performed in a Galbadini Quasar at 10 kN. According to device technical sheet, the measurement accuracy was $\pm 1\%$ (accuracy class 1) from the maximal load-cell value, in accordance with EN ISO 7500/1.

3. Results

3.1. Particle Size Distribution in Cement Suspension

In the first part of the assessment, cement particles were imaged using confocal microscopy. The distribution and size of the CEM 42.5 R and CEM 52.5 R particles were compared. Overall, 30 microscope photographs from three independent samples for each cement type were analyzed and mutually adjusted based on the numbers of analyzed particles, so that both examined samples contained the same number of particles (in total more than 20,000). From the microscope photographs (Figure 9), it is clear that CEM 52.5 R had overall better distribution in cement suspension, while CEM 42.5 R contained more particles bound together in the so-called floccules, which may cause a problem of

insufficient carbon filament saturation (3.2). Moreover, the size distribution of cement particles differed for the two types of cement. CEM 52.5 R had a median of a particle size $301.5 \mu\text{m}^2$ (corresponding to the mean value of one-side length of $9.8 \mu\text{m}$), while the median of the particle size in CEM 42.5 R was $397.8 \mu\text{m}^2$ (which was $11.3 \mu\text{m}$ in length). These measurements also correspond to the findings mentioned in [42]. When also considering the formation of floccules in CEM 42.5 R, the results indicate an overall poorer probability of deep carbon fibers saturation. From the frequency distribution chart in Figure 10, it follows that not only the median size of particles, but also the number of larger particles overall was less in CEM 52.5 R than in CEM 42.5 R ($p < 0.0001$).

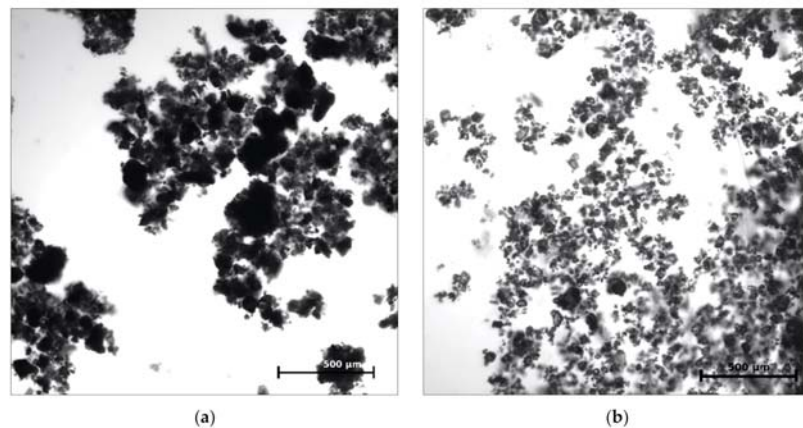


Figure 9. Microscope pictures of cement suspension: (a) CEM 42.5 R; (b) CEM 52.5 R.

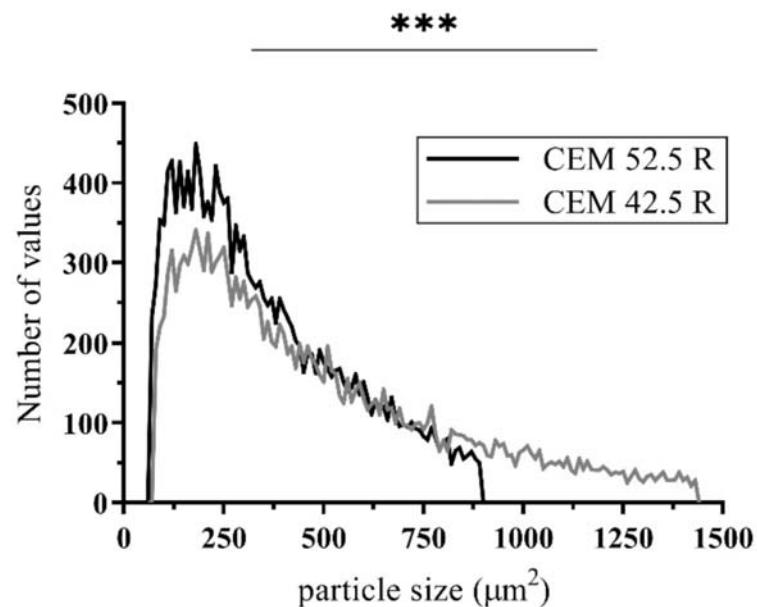


Figure 10. Comparison of size and distribution of cement particles in cement suspensions. A Student's *t* test was used for statistical testing; *** $p < 0.001$.

3.2. Saturation Depth of Beam Samples

Next, the hypothesis that the penetration of carbon roving strongly depends on cement type and saturation method was tested. An identical series of samples (A–E) was produced as described in Table 3, but in the shape of beam samples (Figure 6). The beams were cut in three parts. On each cross-section cut, the depth of saturation was measured (Figure 8).

The reason for using two different types of cement was to determine the effect of particle size on roving saturation depth. In the case of the epoxy resin matrix, the fibers were fully saturated by penetration from the surface (application by a roller). This was caused by the homogeneous structure of the resin. Two cement types with an overall higher quantity of small particles were chosen: CEM 52.5 R and CEM 42.5 R. As anticipated, the smaller cement particles could penetrate deeper and achieve a better interaction between the HPC and the tensile reinforcement. The white variant of CEM 52.5 R was chosen because of the easier subsequent identification of the saturation depth.

It is apparent from the photographs, when comparing the different methods of saturation and different types of cement, that the best results were obtained in the series A and B samples (pressure saturation method). Greater saturation depth was reached in series B samples, supporting the hypothesis that smaller particles penetrate the roving better. Detailed images of all beam samples are provided in Figure 11.

Unfortunately, after the hardening of the concrete mixture in sample E (natural penetration of cement suspension from the wet concrete mixture), it turned out that the number of cement particles penetrating the beam core was not sufficient (Figure 11). Most of the concrete mixture particles were only on the surface of the carbon roving, and the saturation was inadequate. The reason for the poor saturation of the carbon fibers with concrete mixture was the size of the particles in the mixture. Generally, the particle size median was approximately 9 μm (CEM 52.5 R) and 12 μm (CEM 42.5 R) (Figure 10). Due to the size of each carbon roving filament (7–10 μm), the cement mixture particles could not reach the core of the carbon roving. Therefore, there was not enough of the cement material in the core of the carbon roving, and the filaments were not fully activated.

A detailed chart of the average percent and saturation depth values is provided in Figure 12. It is obvious that the most effective method of saturation of textile reinforcement was pressure impregnation with cement suspension in CEM 52.5 R. A microscopy investigation determined that both the size of cement particles and the method of pressure saturation increased the saturation by 22% over that of cement CEM 42.5 R. In contrast, the increase in saturation between experimental samples C and D was only 9%. The type of cement used has an influence on the saturation depth (μm) in both methods of saturation. CEM 52.5 R was about 2.3 times better than CEM 42.5 R regarding saturation depth.

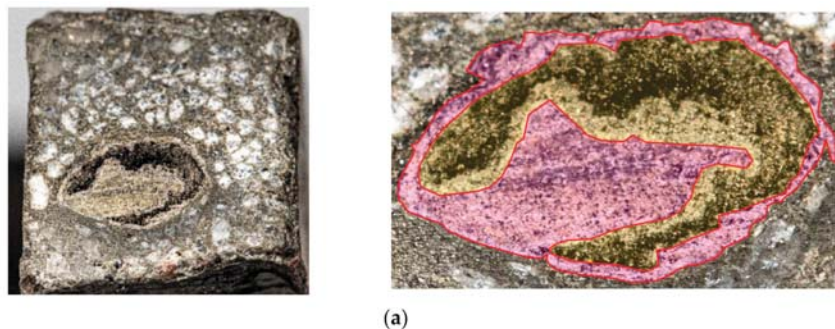


Figure 11. Cont.

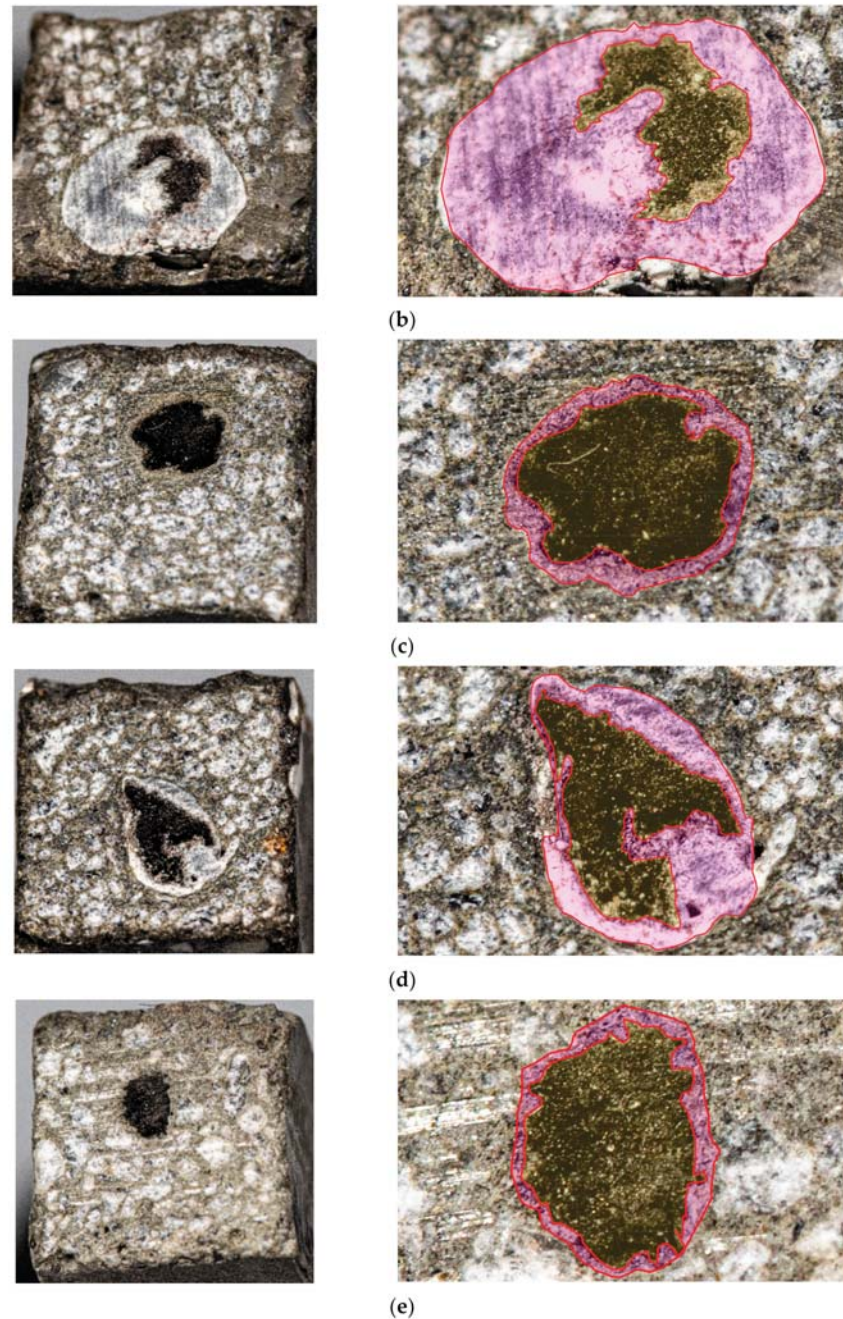


Figure 11. Cross-sections of beam samples. Left panels: whole cross-section area of beam sample. Right panels: detailed view of the cross-section area with the saturated part of the carbon roving in red and the non-saturated carbon roving in yellow: (a) Experimental series A—pressure saturation CEM 42.5 R; (b) Experimental series B—pressure saturation CEM 52.5 R; (c) Experimental series C—surface saturation by a roller CEM 42.5 R; (d) Experimental series D—surface saturation by a roller CEM 52.5 R; (e) Experimental series E—without saturation.

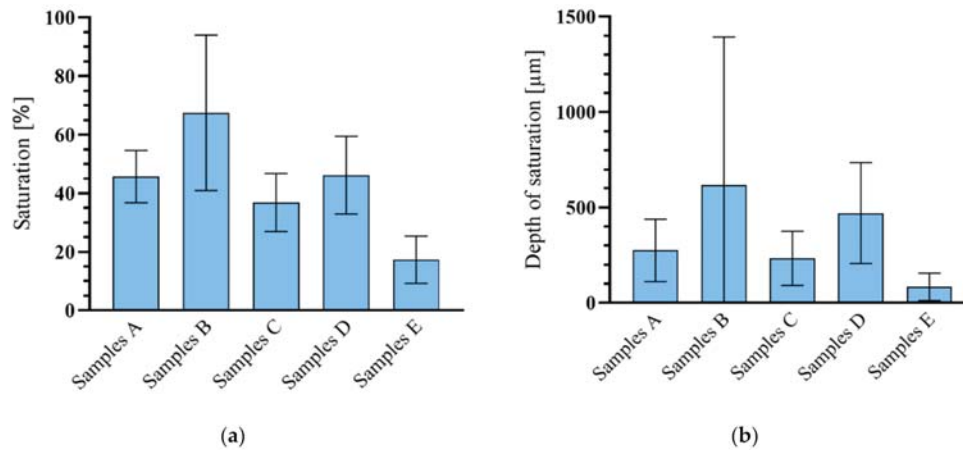


Figure 12. Evaluation of microscopic research of textile reinforcement saturation: (a) Fiber saturation expressed as a percentage; (b) Average depth of textile reinforcement saturation. Legend: Samples A—Experimental samples saturated with CEM 42.5 R using pressure saturation; Samples B—Experimental samples saturated with CEM 52.5 R using pressure saturation; Samples C—Experimental samples saturated with CEM 42.5 R using surface saturation by a roller; Samples D—Experimental samples saturated with CEM 52.5 R using surface saturation by a roller; Samples E—Experimental samples without saturation.

3.3. Four-Point Bending Tests

The mechanical test evaluation focused on verifying the influence of the cement suspension on performance by means of bending tests under four-point bending at normal temperature, according to [37]. As a reference, plate samples with an epoxy resin textile reinforcement matrix were used. The mechanical tests were terminated when the experimental sample was broken or when the trend of increasing values measured was stabilized. The four-point bending test was performed with a controlled constant load speed of 2.0 mm per minute.

From the following charts (Figure 13) it is evident that the first crack occurred in the interval from 1.1 to 1.6 kN. This value represents the tensile strength of the concrete part of the experimental sample. The course of behavior after the development of the first crack is essential, because it was found that the experimental sample (Figure 13b) is capable of further transmitting the tensile force. In the reference samples, there was evidence that after the first crack arose the force was still being transmitted to the tensile reinforcement before its tensile strength was exceeded. Subsequent progressive breakage of the sample was observed after exceeding approximately 4.7 kN.

In contrast, the other tested samples did not exceed the tensile strength and did not break. Samples of the A and B series showed a demonstrable reinforcement–concrete interaction, and the specimen retained the ability to at least partially transmit the bending force. The maximum achieved force of the A and B samples was only 28% of the capacity of the reference samples. The decreasing course of the force measured in samples of the A and B series began in the interval between 4–5 mm displacement, with the average force reaching 1.62 kN for series A and 1.63 kN for series B. However, only sample A3 from series A reached considerably higher values than the other samples from this series. After excluding sample A3, an average value of 1.35 kN was obtained. Nevertheless, series B was considered to be significant, as there was no considerable variance of the measured values, as was the case in series A.

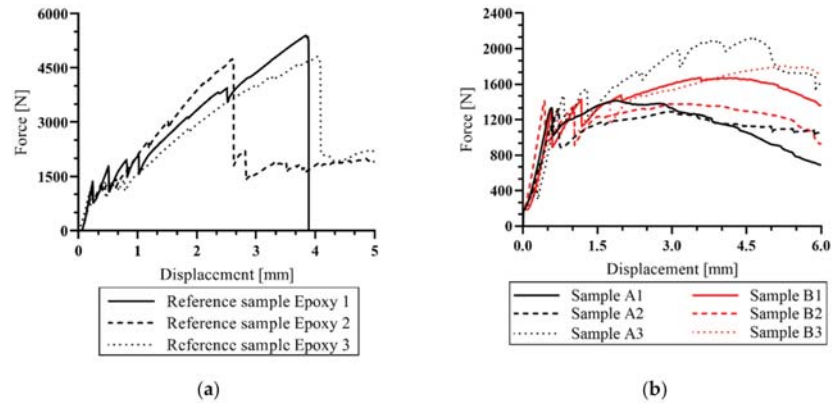


Figure 13. Measured data from four-point bending test: (a) Reference samples; (b) Comparison of sample series A and B.

During the mechanical tests, only one crack developed under the load support (samples C–E). In the reference samples, it was possible to observe a break of the sample, but in the rest of experimental samples (A–E series) the break did not occur because the tensile strength of the textile reinforcement was not exceeded. The formation of further cracks in the experimental samples was not observed, presumably because of the size and speed of crack development. Due to the increased deformation, the fibers of the textile reinforcement began to be pulled out from the sample (Figure 14).

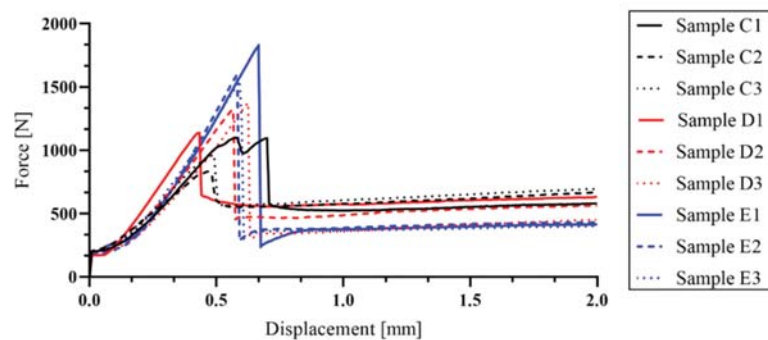


Figure 14. Course of values measured on samples from the C, D (surface saturation by a roller), and E (without any saturation) series.

4. Discussion

In a previous study, the main problematic properties of textile-reinforced concrete were described [8]. Although epoxy resin is an excellent material in the function of textile reinforcement matrix, its low resistance to elevated temperatures is problematic from the perspective of fire safety. Therefore, an alternative non-combustible matrix material that would naturally overcome the problem of low resistance at elevated temperatures was examined. A cement suspension matrix was used to verify its effect on the mechanical properties of the experimental samples at normal room temperature (20 °C). The mechanical properties measured in these samples were compared to values obtained from previous experiments and reference samples (Figure 13). Experimental samples in this work were made from high-performance concrete (HPC) with tensile reinforcement from carbon fibers.

In this study, the influence of the type of cement in the cement suspension as well as the type of textile reinforcement saturation procedure on the mechanical properties was examined. The saturation was performed in two different ways. The first method

was mechanical pressure saturation (series A and B). The second was surface saturation using a roller (series C and D). The same procedure was performed with the epoxy resin matrix (reference series Epoxy 1, 2 and 3). Series E was developed as the negative control without any matrix, where additional saturation of the concrete mixture was not applied. Some minor penetration of the cement suspension from the wet concrete mixture was, however, present. Based on the literature and material review, it was suggested that the problem of insufficient saturation could have occurred because of the size of cement particles [43]. The standard type of cement consists mainly of particles whose size is generally larger than each carbon filament of the textile roving ($>7 \mu\text{m}$). Therefore, a microscopy examination describing the distribution of the size of the cement particles in the suspension was carried out. This showed that the CEM 52.5 R had the dominant share of cement particles smaller than those of CEM 42.5 R (Figure 10). Also, the number of larger particles (whose area was larger than $1000 \mu\text{m}^2$) was greater in CEM 42.5 R. All these findings led to the conclusion that CEM 52.5 R should have had better performance in the subsequent mechanical experiments, because of the higher probability of achieving a deeper saturation of the textile reinforcement. However, it is necessary to consider the real quantity of saturated filaments in the carbon roving. There is a possibility that, although the depth of saturation may be sufficient, the risk (mainly in CEM 52.5 R) of carbon filament swelling endures. The increase of filament diameter can be interpreted wrongly as deep saturation when only a small quantity of filaments have actually been activated for interaction. The dependence of the mechanical performance on the extent of saturation was confirmed in the mechanical tests, where the B samples demonstrated the best load capacity.

Four types of reinforcement mesh were prepared by using a different cement type in the cement suspension and a different method of saturation. Two types of experimental samples were developed, plate ($100 \text{ mm} \times 360 \text{ mm} \times 18 \text{ mm}$) and beam ($8 \text{ mm} \times 8 \text{ mm} \times 100 \text{ mm}$). The plate samples were used for the four-point bending tests while the beam samples were used for the evaluation of the saturation depth. As expected, a deeper saturation of the textile reinforcement was achieved using CEM 52.5 R. For experimental samples of the B series, the average saturation reached 67%. In contrast, series A reached an average saturation of only 45%. The other experimental samples exhibited significantly lower depth of saturation, e.g., in series C it was 36%, series D 46%, and in series E (lowest percent saturation caused by migration from the concrete mixture), only 17%. It should be pointed out that the method of application of the cement suspension was found to have a significant impact on saturation. The difference in saturation between series A and B was 21%; between C and D, it was 9%. This means that the influence of cement particle size is important in a case when the small particles are mechanically pressurized into the textile reinforcement. Using this method, the best overall results were achieved. With surface application using a roller, there was no significant difference in the depth of saturation between CEM 42.5 R and CEM 52.5 R.

After this evaluation, experimental samples were prepared for the comparison of the influence of saturation on bending capacity. The assessment of each experimental sample was divided into two parts. The first part of the assessment was before the first crack formation (where the tensile strength of the concrete was exceeded) and the second one was after the crack had occurred. However, the second part was essential for the evaluation, because it was possible to observe whether there was an interaction between the materials. In the E series samples (without additional cement impregnation) there was the lowest saturation of textile reinforcement (due to the larger particle size in the concrete mixture) and after the development of the first crack, there was no interaction between the materials. Insufficient interaction led to the lack of tensile load transmission to the carbon-fiber reinforcement. By contrast, for the C and D series, the cement suspension formed a layer on the surface of the textile fibers after penetration. After that, this hardened layer prevented the penetration of the concrete mixture into the textile reinforcement. Therefore, in series C and D, it was not possible to achieve good adhesion between the textile reinforcement

and concrete, as only the surface application method was used. During the mechanical test, the thickness of the hardened suspension layer could not transfer the tensile stress to the tensile reinforcement.

Therefore, even in samples C and D, the interaction between the materials was not sufficient. Only in the series A and B samples was there sufficient saturation of the textile reinforcement. It was found that in a pressure saturation, the concrete mixture did not penetrate all the layers of textile reinforcement to a full extent. Nevertheless, the depth of impregnation was enough to cause sufficient interaction (load transfer) between the materials. As shown in Figure 11, it was possible to observe an increasing trend of the load curve in the A and B series after the formation of the first crack. This confirmed the similar trend of the particle size in the impregnation mixture, which was described on glass fibers in [24–29].

For the reasons described above, textile reinforcement saturation with CEM 52.5 R proves to be a possible variant usable for replacing the combustible synthetic matrix of textile concrete. When the reference samples and series B samples were compared, it was clear that the series B samples achieved approximately 30% efficiency of loading capacity (Figure 15). However, there could be a theoretical possibility to reach a loading capacity near to 100% by using more tensile reinforcement. It is evident from the mechanical test results (Figure 14) that the B series samples showed a similar trend of bending capacity increase, mainly in the initial phases of crack development, as has been shown in reference samples Epoxy 1. However, due to an alternative material used in this study, the results of this solution deviate from that of conventional TRC with an epoxy resin matrix [44–46] and a comparison of results is therefore problematic. The best-performing combinations (sample series A and B) will be further investigated by mechanical tests focusing on a detailed description of cement matrix behavior, for example the so-called pullout test based on simple co-interaction of one cement-saturated carbon roving with concrete. Furthermore, once sufficient performance has been determined at normal temperature, tests at elevated temperatures will be carried out.

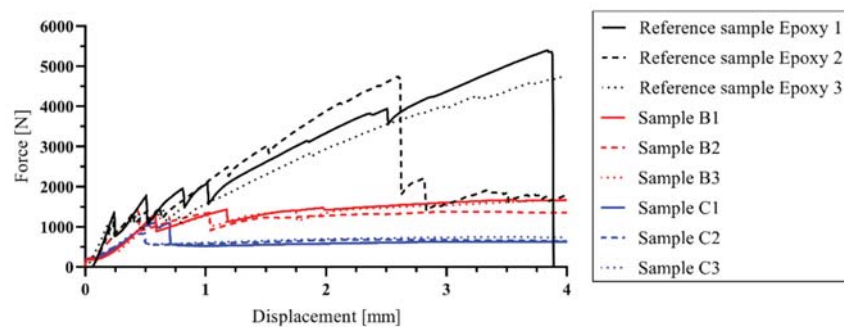


Figure 15. Evaluation of four-point bending tests of experimental samples from series A, B and C.

The next steps in future work are to try using different methods of saturation to achieve full saturation of textile reinforcement. This includes a verification of the data measured from the mechanical tests on experimental samples exposed to elevated temperature according to ISO 834.

Author Contributions: Conceptualization, R.F., E.F., M.P., T.V. and V.M.; methodology, R.F., E.F., J.Ř. and T.V.; software, R.F., E.F.; supervision, M.P., V.M.; resources, R.F. and T.V.; writing—original draft, R.F., E.F. and V.M. All authors have read and agreed to the published version of the manuscript.

Funding: This work was supported by the Grant Agency of the Czech Technical University in Prague, grant No. SGS21/094/OHK1/2T/11 project—Application of alternative materials in textile concrete and their evaluation at room temperature and at elevated temperature.

Institutional Review Board Statement: Not applicable.

Informed Consent Statement: Not applicable.

Data Availability Statement: The data presented in this study are available on request from the corresponding author.

Conflicts of Interest: The authors declare no conflict of interest. The funders had no role in the design of the study; in the collection, analyses, or interpretation of data; in the writing of the manuscript; or in the decision to publish the results.

References

1. Tailor Made Concrete Structures: New Solutions for Our Society. In Proceedings of the International FIB Symposium, Amsterdam, The Netherlands, 19–21 May 2008.
2. Hegger, J.; Schneider, H.; Sherif, A.; Molter, M.; Voss, N. Exterior Cladding Panels as An Application of Textile Reinforced Concrete. *ACI Symp. Publ.* **2004**, *224*, 55–70. [CrossRef]
3. Chira, A.; Kumar, A.; Vlach, T.; Laiblová, L.; Hájek, P. Textile-reinforced concrete facade panels with rigid foam core prisms. *J. Sandw. Struct. Mater.* **2016**, *18*, 200–214. [CrossRef]
4. Laiblová, L.; Pešta, P.; Kumar, A.; Hájek, P.; Fiala, C.; Vlach, T.; Kočí, V. Environmental Impact of Textile Reinforced Concrete Facades Compared to Conventional Solutions—LCA Case Study. *Materials* **2019**, *12*, 3194. [CrossRef]
5. Řepka, J.; Vlach, T.; Laiblová, L.; Hájek, P.; Ženišek, M.; Kokeš, P. Thin Lightweight Panels Made of Textile Reinforced Concrete. *Solid State Phenom.* **2017**, *259*, 238–243. [CrossRef]
6. Peled, A.; Bentur, A.; Mobasher, B. *Textile Reinforced Concrete*; CRC Press: Boca Raton, FL, USA, 2019; ISBN 978-1-351-64546-1.
7. Hegger, J.; Will, N.; Bruckermann, O.; Voss, S. Load-bearing behaviour and simulation of textile reinforced concrete. *Mater. Struct.* **2006**, *39*, 765–776. [CrossRef]
8. Fürst, R.; Pokorný, M.; Vlach, T.; Mózser, V. Study of behavior of textile-reinforced concrete with epoxy resin matrix in fire. *Fire Technol.* in press.
9. Kapsalis, P.; El Kadi, M.; Vervloet, J.; De Munck, M.; Wastiels, J.; Triantafillou, T.; Tysmans, T. Thermomechanical Behavior of Textile Reinforced Cementitious Composites Subjected to Fire. *Appl. Sci.* **2019**, *9*, 747. [CrossRef]
10. Ducháček, V. *Polymery: Výroba, Vlastnosti, Zpracování, Použití*, 2nd ed.; VŠCHT: Praha, Czech Republic, 2006; ISBN 80-7080-617-6.
11. Fidelus, J.D.; Wiesel, E.; Gojny, F.H.; Schulte, K.; Wagner, H.D. Thermo-mechanical properties of randomly oriented carbon/epoxy nanocomposites. *Compos. Part A Appl. Sci. Manuf.* **2005**, *36*, 1555–1561. [CrossRef]
12. de Andrade Silva, F.; Butler, M.; Hempel, S.; Toledo Filho, R.D.; Mechtcherine, V. Effects of elevated temperatures on the interface properties of carbon textile-reinforced concrete. *Cem. Concr. Compos.* **2014**, *48*, 26–34. [CrossRef]
13. Foreman, J.P.; Porter, D.; Behzadi, S.; Curtis, P.T.; Jones, F.R. Predicting the thermomechanical properties of an epoxy resin blend as a function of temperature and strain rate. *Compos. Part A Appl. Sci. Manuf.* **2010**, *41*, 1072–1076. [CrossRef]
14. Brameshuber, W. Textile reinforced concrete-state-of-the-art report of RILEM TC 201-TRC. In *Reunion Internationale des Laboratoires et Experts des Matériaux, Systemes de Construction et Ouvrages (RILEM)*; RILEM Publications SARL: Paris, France, 2006; ISBN 2-912143-99-3.
15. Moravec, R. Technical Sheet: Epoxy Resin Resistant up to 160 °C LH 300. Havel Composites CZ s.r.o. Available online: <https://www.havel-composites.com/uploads/files/products/659/8526af61ad9b157d63f68fcf16cebd65058e3b88.pdf> (accessed on 22 November 2020).
16. Nguyen, J.; Migonney, V.; Ruse, N.D.; Sadoun, M. Resin composite blocks via high-pressure high-temperature polymerization. *Dent. Mater.* **2012**, *28*, 529–534. [CrossRef]
17. GRENA, A.S. Technical Sheet: Požární Ochrana Uhlíkovo-Vláknitých CFRP Lamel Deskami Grenamat® AL. Available online: <https://www.grena.cz/res/dwe-files/1404056575.pdf> (accessed on 26 October 2020).
18. Soupionis, G.; Georgiou, P.; Zoumpoulakis, L. Polymer Composite Materials Fiber-Reinforced for the Reinforcement/Repair of Concrete Structures. *Polymers* **2020**, *12*, 2058. [CrossRef]
19. Huseien, G.F.; Sam, A.R.M.; Faridmehr, I.; Baghban, M.H. Performance of Epoxy Resin Polymer as Self-Healing Cementitious Materials Agent in Mortar. *Materials* **2021**, *14*, 1255. [CrossRef]
20. Anagnostopoulos, C.A.; Dimitriadi, M. Study on High Performance Polymer-Modified Cement Grouts. *Civil. Eng.* **2021**, *2*, 134–157. [CrossRef]
21. Kapsalis, P.; Tysmans, T.; Verbruggen, S.; Triantafillou, T. Preliminary High-Temperature Tests of Textile Reinforced Concrete (TRC). *Proceedings* **2018**, *2*, 522. [CrossRef]
22. Micelli, F.; Aiello, M.A. Residual tensile strength of dry and impregnated reinforcement fibres after exposure to alkaline environments. *Compos. Part B Eng.* **2019**. [CrossRef]
23. Mouritz, A.P.; Mathys, Z.; Gibson, A.G. Heat release of polymer composites in fire. *Compos. Part A Appl. Sci. Manuf.* **2006**, *37*, 1040–1054. [CrossRef]
24. Signorini, C.; Nobili, A.; Cedillo González, E.I.; Siligardi, C. Silica coating for interphase bond enhancement of carbon and AR-glass Textile Reinforced Mortar (TRM). *Compos. Part B Eng.* **2018**, *141*, 191–202. [CrossRef]
25. Bompadre, F.; Donnini, J. Surface Modification of Glass Textile for the Reinforcement of a Cement-Based Composite: A Review. *Appl. Sci.* **2021**, *11*, 2028. [CrossRef]

26. Lu, M.; Xiao, H.; Liu, M.; Li, X.; Li, H.; Sun, L. Improved interfacial strength of SiO₂ coated carbon fiber in cement matrix. *Cem. Concr. Compos.* **2018**, *91*, 21–28. [CrossRef]
27. Nadiv, R.; Peled, A.; Mechtcherine, V.; Hempel, S.; Schroefl, C. Micro- and nanoparticle mineral coating for enhanced properties of carbon multifilament yarn cement-based composites. *Compos. Part B Eng.* **2017**, *111*, 179–189. [CrossRef]
28. Di Maida, P.; Radi, E.; Sciancalepore, C.; Bondioli, F. Pullout behavior of polypropylene macro-synthetic fibers treated with nano-silica. *Constr. Build. Mater.* **2015**, *82*, 39–44. [CrossRef]
29. Schneider, K.; Michel, A.; Liebscher, M.; Terreri, L.; Hempel, S.; Mechtcherine, V. Mineral-impregnated carbon fibre reinforcement for high temperature resistance of thin-walled concrete structures. *Cem. Concr. Compos.* **2019**, *97*, 68–77. [CrossRef]
30. Cohen, Z.; Peled, A. Effect of nanofillers and production methods to control the interfacial characteristics of glass bundles in textile fabric cement-based composites. *Compos. Part A Appl. Sci. Manuf.* **2012**, *43*, 962–972. [CrossRef]
31. Teijin®. Technical Sheet: Carbon Roving Tenax STS40 F13 24K 1600tex. Available online: <https://shop1.r-g.de/en/art/205105STS> (accessed on 8 November 2020).
32. Lu, Z.C.; Haist, M.; Ivanov, D.; Jakob, C.; Jansen, D.; Leinitz, S.; Link, J.; Mechtcherine, V.; Neubauer, J.; Plank, J. Characterization Data of Reference Cement CEM I 42.5 R Used for Priority Program DFG SPP 2005 “Opus Fluidum Futurum—Rheology of Reactive, Multiscale, Multiphase Construction Materials”. *Data Brief* **2019**, *27*, 104699. [CrossRef]
33. Bentz, D.P.; Garboczi, E.J.; Haecker, C.J.; Jensen, O.M. Effects of cement particle size distribution on performance properties of Portland cement-based materials. *Cem. Concr. Res.* **1999**, *29*, 1663–1671. [CrossRef]
34. Rambo, D.A.S.; Silva, F.A.; Filho, R.D.T.; Gomes, O.F.M. Effect of Elevated Temperatures on the Mechanical Behavior of Basalt Textile Reinforced Refractory Concrete. *Mater. Des.* **2015**, *65*, 24–33. [CrossRef]
35. Nguyen, T.H.; Vu, X.H.; Si Larbi, A.; Ferrier, E. Experimental Study of the Effect of Simultaneous Mechanical and High-Temperature Loadings on the Behaviour of Textile-Reinforced Concrete (TRC). *Constr. Build. Mater.* **2016**, *125*, 253–270. [CrossRef]
36. ČSN EN 12390-3, *Testing Hardened Concrete-Part 3: Compressive Strength of Test Specimens*; Czech Office for Standards, Metrology and Testing: Prague, Czech Republic, 2020.
37. ČSN EN 12390-5, *Testing Hardened Concrete-Part 5: Flexural Strength of Test Specimens*; Czech Office for Standards, Metrology and Testing: Prague, Czech Republic, 2020.
38. ČSN EN 12390-1, *Testing Hardened Concrete-Part 1: Shape, Dimensions and Other Requirements for Specimens and Moulds*; Czech Office for Standards, Metrology and Testing: Prague, Czech Republic, 2013.
39. Vlach, T.; Laiblová, L.; Ženíšek, M.; Chira, A.; Kumar, A.; Hájek, P. The effect of surface treatments of textile reinforcement on mechanical parameters of HPC facade elements. *Key Engineering Materials* **2016**, *677*, 203–206. [CrossRef]
40. Vlach, T.; Laiblová, L.; Ženíšek, M.; Řepka, J.; Hájek, P. Soft insert for support modeling of slightly textile reinforced concrete. *Key Eng. Mater.* **2018**, *760*, 158–163. [CrossRef]
41. Soranakom, C.; Mobasher, B. Geometrical and Mechanical Aspects of Fabric Bonding and Pullout in Cement Composites. *Mater. Struct.* **2006**, *42*, 765–777. [CrossRef]
42. Lura, P. *Autogenous Deformation and Internal Curing of Concrete*; Delft University Press: Delft, The Netherlands, 2003; ISBN 978-90-407-2404-6.
43. Kuzielová, E.; Pach, L.; Palou, M. Evolution of lightweight foam concretes by water procedure. *Ceram. Silikáty* **2015**, *59*, 10–16.
44. Vlach, T.; Řepka, J.; Hájek, J.; Fürst, R.; Jirkalová, Z.; Hajek, P. Cohesion test of a single impregnated ar-glass roving in high-performance concrete. *Stavební Obz. Civ. Eng. J.* **2020**, *29*, 358–369. [CrossRef]
45. Saidi, M.; Gabor, A. Experimental analysis and analytical modelling of the textile/matrix interface shear stress in textile reinforced cementitious matrix composites. *Compos. Part A Appl. Sci. Manuf.* **2020**, *135*, 105961. [CrossRef]
46. Hegger, J.; Voss, S. Investigations on the bearing behaviour and application potential of textile reinforced concrete. *Eng. Struct.* **2008**, *30*, 2050–2056. [CrossRef]

PAPER IV

Experimental Evaluation of Carbon Reinforced TRC with Cement Suspension Matrix at Elevated Temperature

Authors: Richard Fürst, Petr Hejtmánek, Tomáš Vlach, Jakub Řepka,
Vladimír Mózer, Petr Hájek

Journal: Polymers

Publisher: MDPI

Volume and number: 14/11

Year of publication: 2022

Number of pages: 16

DOI: [10.3390/polym14112174](https://doi.org/10.3390/polym14112174)

Article

Experimental Evaluation of Carbon Reinforced TRC with Cement Suspension Matrix at Elevated Temperature

Richard Fürst ^{1,2,*} , Petr Hejtmánek ^{1,3}, Tomáš Vlach ^{1,4} , Jakub Řepka ^{1,4}, Vladimír Mózer ¹ and Petr Hájek ¹

- ¹ Czech Technical University in Prague, Faculty of Civil Engineering, Department of Architectural Engineering, 16629 Prague, Czech Republic; petr.hejtmánek@cvut.cz (P.H.); tomas.vlach@cvut.cz (T.V.); jakub.repka@cvut.cz (J.Ř.); vladimir.mozer@cvut.cz (V.M.); petr.hajek@cvut.cz (P.H.)
- ² Federal Institute for Materials Research and Testing (BAM), Division 7.3-Fire Engineering, Unter den Eichen 87, 12205 Berlin, Germany
- ³ Czech Technical University in Prague, University Centre for Energy Efficient Building, Fire Laboratory, 27343 Bustehrad, Czech Republic
- ⁴ Czech Technical University in Prague, University Centre for Energy Efficient Building, Laboratory of Composite Structures, 27343 Bustehrad, Czech Republic
- * Correspondence: richard.furst@cvut.cz; Tel.: +420-224-357-151

Abstract: Textile-reinforced concrete (TRC) is a new composite material comprising high-performance concrete and textile reinforcement from textile yarns with a matrix, usually consisting of epoxy resins (ER). The most significant advantage of ER is the homogenization of all filaments in the yarn and full utilization of its tensile potential. Nevertheless, ER matrix is a critical part of TRC design from the perspective of the fire resistance due to its relatively low resistance at temperatures of approximately 120 °C. This work expands the previously performed mechanical tests at normal temperatures with cement suspension (CS) as a non-combustible material for the yarn matrix. Here, the mechanical properties of CS matrix at elevated temperatures were verified. It was found that the addition of polypropylene fibers into HPC negatively affected the mechanical results of CS matrix specimens. Simultaneously, thermal insulation effect of the covering layers with different thicknesses did not significantly influence the residual bending strength of specimens with CS matrix and achieved similar results as reference specimens. Furthermore, all specimens with ER matrix progressively collapsed. Finally, CS as a textile reinforcement of yarn matrix appears to be a suitable solution for increasing the temperature resistance of TRC structures and for substituting synthetic resins.

Keywords: cement matrix; cement suspension; carbon fibers; textile reinforced concrete; high-performance concrete; elevated temperature; fire safety; fire resistance



Citation: Fürst, R.; Hejtmánek, P.; Vlach, T.; Řepka, J.; Mózer, V.; Hájek, P. Experimental Evaluation of Carbon Reinforced TRC with Cement Suspension Matrix at Elevated Temperature. *Polymers* **2022**, *14*, 2174. <https://doi.org/10.3390/polym14112174>

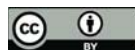
Academic Editors: Damian Palin, Neven Ukrainczyk and Bhaman Ghiassi

Received: 2 May 2022

Accepted: 25 May 2022

Published: 27 May 2022

Publisher's Note: MDPI stays neutral with regard to jurisdictional claims in published maps and institutional affiliations.



Copyright: © 2022 by the authors. Licensee MDPI, Basel, Switzerland. This article is an open access article distributed under the terms and conditions of the Creative Commons Attribution (CC BY) license (<https://creativecommons.org/licenses/by/4.0/>).

1. Introduction

Textile-reinforced concrete (TRC) is currently used mainly for non-load bearing structures, design elements, and for repairing or improving existing constructions [1–5]. However, the requirements for sustainability and resilience of structures are significantly higher than in previous years, especially regarding structure design efficiency, better material properties or usage of materials with lower carbon footprint [6,7]. The combination of high-performance concrete (HPC), textile reinforcement, and its synthetic matrix allows to implement subtler structures with mechanical properties comparable to traditional reinforced concrete structures. Moreover, when higher quality materials with better mechanical properties are used, it is possible to reduce the total quantity of used materials and decrease the final construction's carbon footprint [8–10]. In addition, TRC achieves excellent mechanical properties at ambient temperature (20 °C) and has a favorable impact on the environment [8–10].

Commonly used textile-reinforced concrete consists of HPC, tensile reinforcement consisting of carbon-fiber-reinforced polymer (CFRP) bars, and textile reinforcement as

shear reinforcement. Based on the combination of these materials with better mechanical properties than materials used for traditional reinforced structures, it is possible to reduce significant quantity of used materials and thus create structures with equal load-bearing capacities. TRC has not commonly been used for load-bearing structures so far, however, due to its excellent mechanical properties, the use of this composite material is expected also for load-bearing structures in the future. For this reason, a detailed assessment of TRC from a fire-resistance point of view is required. Several studies have already investigated the behavior of TRC at elevated temperatures. However, the exposure method was primarily based on isothermal temperature exposure [11–13]. Therefore, for the subsequent investigation, it is necessary to focus on temperature exposure conditions representing real fire situations. The exposure method fulfilling this condition reflects the standard temperature curve, according to EN 1363-1.

The main component of TRC is HPC exhibiting excellent mechanical properties like compressive strength at ambient and elevated temperatures. Nevertheless, using HPC is often associated with a lower water content due to the use of plasticizers. Moreover, it implies low porosity of the hardened concrete, contributing to the higher probability of spalling from a fire-resistance point of view.

Textile reinforcement constitutes the second part of TRC and the most commonly used materials are carbon, glass or aramid [14,15]. Due to the excellent resistance to atmospheric corrosion of textile reinforcement, it is possible to design the covering layers considering only mechanical interaction between materials. Consequently, the final covering layer thickness is around 5 to 10 mm [16] (Figure 1), making the final size of elements smaller, thus reducing the consumption of silicate material for matrix (with associated environmental savings).

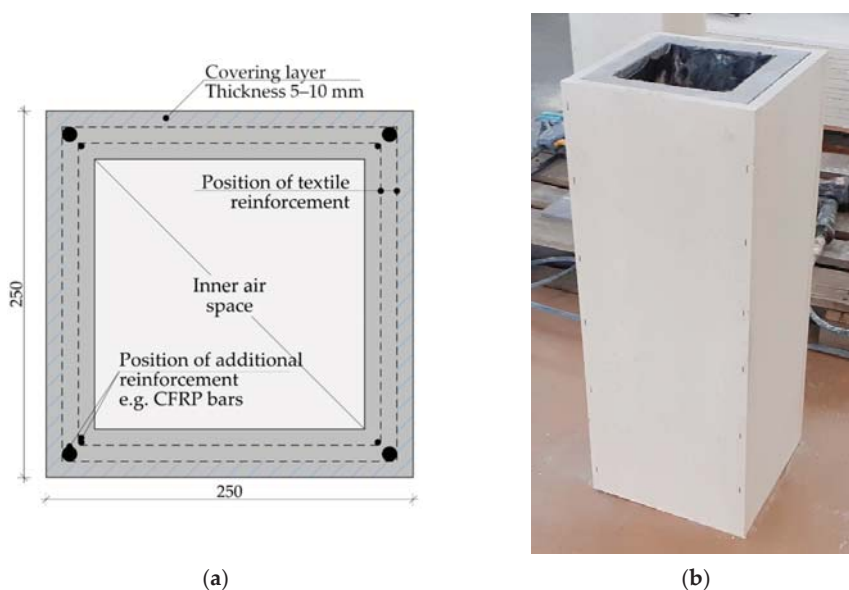


Figure 1. Scheme of the TRC beam structure (column) with hollow section 250 mm × 250 mm: (a) theoretical scheme of the column with additional CFRP bars reinforcement; (b) developed pattern of the TRC column with two layers of textile reinforcement and CFRP tension bars covered by fire protection board system.

The usage of thinner covering layers usually attaining approximately 10 mm, makes the spalling of concrete layers more important. The spalling of the surface covering layers may fundamentally affect the load-bearing capacity of the affected structural element. To avoid the spalling risk, surface reinforcing mesh or the addition of appropriate fibers with

a low melting temperature may be added into the concrete mixture, as per EN 1992-1-2. However, it is often not possible to use surface reinforcement due to the thinner cover layer. Therefore, polypropylene (PP) fibers are most commonly used in the HPC mixture to reduce the risk of concrete layer spalling [17,18]. Additionally, the subtle character of TRC structures and corresponding thinner cover layers do not provide sufficient thermal insulation. Therefore, the temperature rises significantly faster in contrast to the traditional reinforced concrete structures, where the covering layers are designed according to EN 1992-1-2, i.e., from 20 to 50 mm. Consequently, the reinforcing carbon fibers mesh degrades faster due to the higher temperature gradient and lower thermal mass of the TRC structure.

In general, carbon fibers have the best mechanical properties among other materials used as textile reinforcement. They also have the highest melting point compared to other materials, usually exceeding the temperatures attained during a fire (Table 1). The real fire conditions are simulated based on EN 1363-1 according to the ISO 834 standard temperature curve. The reached temperatures correspond to the duration of the fire and typically exceed 1000 °C. For this reason, the use of carbon reinforcement seems to be the most suitable solution at ambient and elevated temperatures because the risk of reinforcement deterioration is minor. Moreover, carbon-based materials are characterized as materials with the lowest energy requirements for its production. In contrast to carbon materials, basalt fibers generally have the lowest carbon footprint while maintaining a higher melting temperature than glass materials [8], as compared in Table 1. For this reason, basalt appears to be a possible alternative for substituting carbon fibers.

Table 1. Comparison of mechanical properties and melting points of selected textile reinforcement materials.

Mechanical Attribute	Type of Textile Reinforcement			Units
	Carbon Fibers [19]	Glass Fibers [20]	Basalt Fibers [21]	
Density	~2.0	~2.5	~2.75	kg·m ⁻³
Tensile strength (average)	4.3	3.5	~2.48	GPa
Modulus of elasticity (average)	240	57	76	GPa
Diameter of yarn's filament	7–10	10–16	~12.8	µm
Melting temperature	3650	800	1100	°C

The mechanical properties of textile reinforcement can be improved by a matrix, most commonly from synthetic resins. The matrix ensures redistribution of tensile stress into the whole textile yarn and allows full utilization of the textile reinforcement, resulting in better mechanical properties. Best results were observed with simple epoxy resin curing process and homogenous consistency, enabling full penetration of the tensile reinforcement [22,23]. On the other hand, increased brittleness was observed for textile reinforcement penetrated with epoxy resins. This implies brittle behavior when the tensile strength of reinforcement is exceeded. Therefore, structures reinforced by textile reinforcement with synthetic matrix attain lower ductility than traditional construction elements reinforced by steel reinforcement. An organic textile matrix can be substituted by inorganic materials like cement, cement suspensions, and mortars [24–27]. However, these materials do not achieve as excellent results as synthetic resins, primarily due to the non-homogeneity of penetration fluid. The resulting utilization of reinforcement is hence reduced (Figure 2).

The temperature resistance of synthetic resins is represented by a temperature interval called “glass transition temperature interval”. When this temperature interval is exceeded, the modulus of elasticity rapidly decreases, and deformations occur [28]. For commonly used resins, the glass transition temperature equals approximately to 80–120 °C. Due to the low temperature resistance, the synthetic resin matrix proves to be the weakest point of the TRC design from the perspective of fire resistance. Another possibility is to substitute it by synthetic resins with significantly higher temperature resistance exceeding, approximately, 240 °C [29]. However, the curing process of these resins is often significantly complicated

and usually requires elevated pressure and temperatures. For this reason, the use of these products with higher temperature resistance is often inappropriate due to technological processes in the construction of structures in civil engineering. Furthermore, these organic synthetic resins can also theoretically contribute to pressure increase within the structure due to the resin thermal decomposition products and subsequently negatively affect the spalling risk. Simultaneously, these decomposition products may also contribute to the development of fire [30,31].

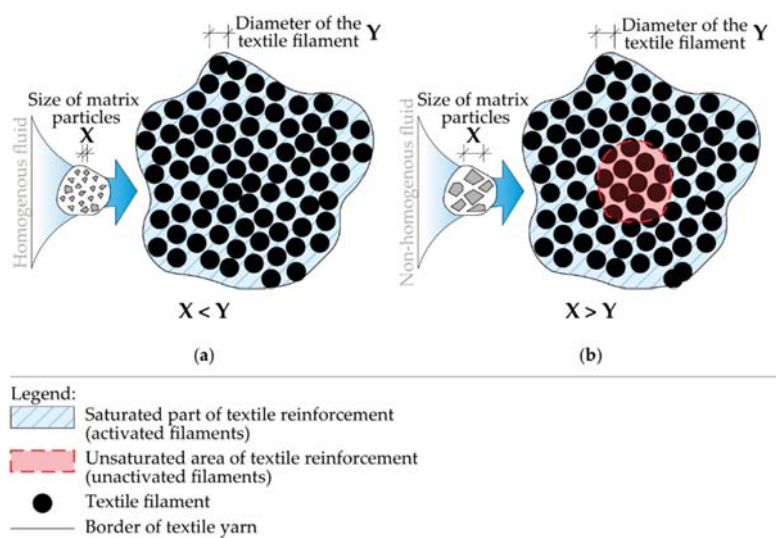


Figure 2. Scheme of tensile reinforcement saturation: (a) textile reinforcement penetrated by material with a homogenous structure such as epoxy resin—full activation of yarns is achieved; (b) textile reinforcement penetrated by suspension with particles larger than the filaments of the yarn—central part of yarn is not activated.

In general, the solution for preventing negative impact of synthetic resins during fire is to apply additional fire protection layers, i.e., boards or plasters. These protection systems can avoid the undesirable increase of temperature in the construction and thus prevent a weakening or collapse of the whole structure. The subtle character and environmental advantage will be infringed when an additional fire protection layer is applied. A suitable solution can be when materials with better temperature resistance are used instead of the additional fire protection systems, thus maintaining better carbon footprint, economic efficiency, and subtle character of the TRC structures.

A suitable solution can also be the use of non-flammable inorganic materials instead of synthetic resins. Previous research verified that cement suspension with CEM 52.5 R achieved an approximately 30% improvement in comparison with reference specimens with epoxy resin [32]. Although cement suspensions do not achieve such results at ambient temperature as synthetic resins, they significantly exceed their temperature resistance at elevated temperatures. For this reason, this work aims to demonstrate a comparison of the behavior of organic (epoxy resin) and inorganic (cement suspension) textile reinforcement matrices at elevated temperatures, according to the ISO temperature curve. The test specimens in this work were designed with carbon reinforcement, which achieved satisfactory temperature resistance and allowed to separate the influence of the textile reinforcement matrix at elevated temperatures for both matrix variants. Test specimens were also designed with and without PP fibers in the HPC mixture. A four-point bending test verified the resulting change in mechanical properties, including comparison with reference specimens that have not been exposed to fire.

Given the above, the main objective of this work is the determination of the interaction effect between the textile reinforcement and HPC in comparison to samples achieving high temperatures during the fire tests. The proposed hypothesis that cement-based suspension has sufficient performance to be a possible replacement for epoxy resin, will be tested through the proposed experimental evaluation and result analysis. This will provide the basis for a more effective design of load-bearing structures made from TRC without additional fire protection and describe the behavior of TRC with inorganic textile reinforcement matrix at elevated temperatures.

2. Materials and Methods

2.1. Test Specimens

The geometry of test specimens was chosen to reflect the application in subtle-walled structures, such as load-bearing wall panels, columns with a hollow cross-section or facade elements. Therefore, the dimension selected are 100 mm × 360 mm with a thickness of 30 mm. The test specimen series were designed with a different covering layer thicknesses, textile reinforcement matrix material, and the addition of PP fibers in the HPC mixture. Each series contained five identical samples that were exposed to elevated temperatures. At the same time, reference specimens were created for each test series. For the description and labelling of the test series, see Table 2.

Table 2. Description of the test series.

Labeling of Series ¹	Covering Layer [mm]	Tensile Reinforcement Variant [-]
C-0/ CPP-0	0	Textile reinforcement saturated with CEM 52.5 R suspension
S-0/ SPP-0	0	Prefabricated textile reinforcement saturated by epoxy resin
C-5/ CPP-5	5	Textile reinforcement saturated with CEM 52.5 R suspension
S-5/ SPP-5	5	Prefabricated textile reinforcement saturated by epoxy resin
C-10/ CPP-10	10	Textile reinforcement saturated with CEM 52.5 R suspension
S-10/ SPP-10	10	Prefabricated textile reinforcement saturated by epoxy resin

Legend: C—cement suspension; S—Solidian prefabricated grid; ¹ The test series marked as xPP-y indicate the addition of the PP fibers to the HPC mixture.

During the development of specimens, the tensile reinforcement layer was placed in different positions, depending on the specific specimen series (Figure 3). The thickness of the covering layer varied from 0 mm to 10 mm (Table 2). The corresponding covering layer position was defined by fixing the saturated reinforcing yarns in the mould walls. At the same time, accompanying beam and cube specimens for the determination of mechanical properties of HPC according to EN 12395-3 and EN 12390-5 were created. The dimensions of specimens were 40 mm × 40 mm × 160 mm and 100 mm × 100 mm × 100 mm.

Two different variants of textile reinforcement were used. The first variant contained a prefabricated carbon grid saturated by an epoxy resin matrix. This commercial product is available as Q85/85-CCE-21 from the Solidian company. The second variant of specimens used carbon rovings Tenax[®] E HTS 40. The second variant of reinforcement was subsequently impregnated with a cement suspension. The suspension was prepared from cement CEM 52.5 R according to [32] with water with a ratio of 1:2. Several rollers mechanically pressed and pulped the carbon yarn, which enabled deeper penetration of the cement suspension. Related mechanical properties of the textile reinforcement were drawn from the technical sheets of products and described in Table 3.

After the tensile reinforcement was placed in the correct height position, wire thermocouples were attached to the surface of the reinforcement layer. To prevent the shifting of the thermocouple's measuring end, all thermocouples were mounted on a support construction independent of the test specimen's mould. After 24 h, specimens were removed from the mould and subsequently conditioned for 28 days according to EN 12390-2 in the lime-water bath.

2.2. Fire Tests Instrumentation

All fire tests were carried out in a mobile fire furnace called miniFUR developed at CTU in Prague. The supporting structure of the test furnace is made of steel profiles covered by cement-fiber panels. The dimensions of the furnace combustion space are 800 mm × 800 mm × 1200 mm. Natural furnace ventilation is ensured through two inlet openings at the furnace bottom and two exhaust openings. The size of all vents is 100 mm × 300 mm. Temperature distribution within the fire furnace is accomplished by a sand burner positioned in the center. The fuel used is propane 2.5 and it is possible to apply temperature curves in the heated space corresponding to ISO 834 according to EN 1363-1.

There were 8 specimens tested at once: In both short ends of the furnace, aerated concrete block walls were mounted. In the wall, in the height of 530 mm above the furnace floor, steel frames were placed to accommodate and hold 4 specimens in position. An expansion space between the test specimen and the holding steel construction was left to prevent mechanical stress due to the thermal expansion of specimens. The surroundings around the steel structure with test specimens were protected by thermal insulation from mineral wool and aerated concrete blocks (Figure 4).

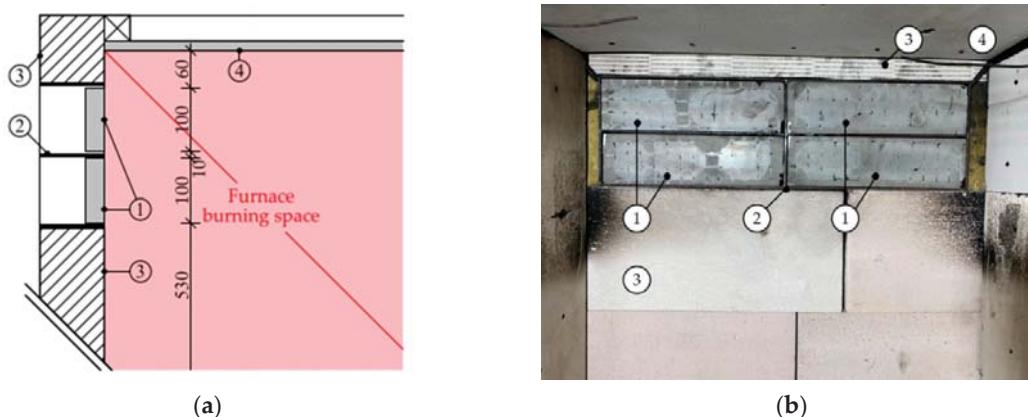


Figure 4. Scheme of the position of the test specimens: (a) side view on the specimen placements; (b) view from inside the furnace of the placed test specimens Legend: 1—exposed side of the test specimen; 2—steel construction holding test specimens; 3—furnace front wall from aerated concrete blocks thickness 100 mm; 4—ceiling of the furnace.

During the fire tests, the gas temperature was measured using eight sheathed thermocouples Ø 3.0 mm, type K. The thermocouples were placed at 300 mm and 600 mm from the furnace floor. Based on the measured data, the temperature course in the burning space was compared and controlled according to the temperature curve limits specified in EN 1363-1 for ISO 834. The temperature of the test specimens was monitored by wire thermocouples in the textile reinforcement layer. Data acquisition for all measured temperatures was provided through a measuring control panel, module EDAM-5019.

2.3. Mechanical Testing

The mechanical properties of the hardened concrete HPC mixture were determined according to EN 12395-3 and EN 12395-5. Tensile strength of the HPC was determined by the three-point bending test. Resulting tensile strength was calculated according to Equation (1).

$$f_{cf} = (3 \cdot F_t \cdot l) / (2 \cdot d_1 \cdot d_2^2) \quad (1)$$

where: f_{cf} —bending tensile strength (MPa); F_t —measured force value during the mechanical test; l —distance between supports (100 mm); d_1 and d_2 width of samples (mm). The resulting value was rounded to the nearest 0.1 MPa.

The compressive strength was determined as an average of the results from tested HPC cubes $100 \text{ mm} \times 100 \text{ mm} \times 100 \text{ mm}$ and fractions of the beam samples from three-point bending tests according to equation 2.

$$f_c = F_t / A_c = F_t / (d_1 \cdot d_2) \quad (2)$$

where: f_c —compression strength (MPa), F_t —maximum load value during the compression test (MPa); d_1 and d_2 —the sample cross-sectional area (mm). The resulted value was rounded to the nearest 0.5 MPa.

The bending strength of the reference plate specimens and residual bending strength of specimens exposed to elevated temperature was determined by a four-point bending test (Figure 5). The maximal applied force was measured during the mechanical test before the rupture, or when massive deformation of samples has occurred. The force applied during the mechanical test was transferred through a steel element with three degrees of freedom to eliminate geometric imperfections in the test body and to ensure uniform loading. The distance between the steel cylinders of mechanical press was 100 mm. The velocity of applied force was set at $2 \text{ mm} \cdot \text{min}^{-1}$. The entire mechanical test was carried out according to EN 12390-5.



Figure 5. Test specimen place in the mechanical press for four-point bending test.

The four-point bending mechanical tests were performed in the appropriate mechanical press Galbadini Quasar 10 kN. For test specimens with an epoxy resin matrix, Galbadini Quasar 100 kN was used. Based on the technical data sheets of measurement devices, the accuracy of measurements for both presses was determined as class 1 accuracy with a deviation $\pm 1\%$ from the maximal load-cell value (according to EN ISO 7500/1).

2.4. Statistical Evaluation Data Analysis

For measured gas temperature and temperature of the specimens exposed to fire, the expanded measurement uncertainty was determined with uncertainty coefficient $k_u = 2.0$ for the interval containing 95% of values. All statistical evaluation was performed in MS Excel 365 and GraphPad Prism 8.0.

3. Results and Discussion

3.1. Testing at Ambient Temperature

PP fibers have been added to the HPC mixture to reduce the risk of spalling of concrete layers according to EN 1992-1-2. Due to the PP fibers added in the HPC mixture, the final compressive strength was reduced by 9% and tensile strength by 2%. The resulting compressive strength of used HPC with/without PP fibers measured was 109.6/119.4 MPa, while for tensile strength of HPC with/without PP fibers it was 12.5/13.0 MPa.

The bending strength of all reference specimens was determined in four-point bending tests. Based on these mechanical tests, the negative influence of PP fibers in the concrete mixture on specimens, especially with cement suspension matrix (CPP series), was observed (Figure 6a–c). The maximum measured strength peak of specimens with cement matrix was shifted approximately 1 mm closer to the initial concrete crack at the tensile surface of the specimens. Concurrently, the maximum measured value of bending strength was approximately 24% less than for specimens without PP fibers (C series). In contrast, in test specimens with an epoxy resin matrix (SPP series), a significant effect of PP on the attained bending strength was not observed, as was the case for samples with cement suspension matrix (Figure 6d–f). Simultaneously, a different pattern of specimen failure can be observed. In specimens with a cement suspension matrix, the reinforcing carbon yarns were pulled out, and progressive collapse did not occur. On the contrary, the specimens with epoxy resin matrix were broken after reaching the tensile strength of carbon reinforcement.

3.2. Testing at Elevated Temperatures

In the second phase of experimental work, fire tests were performed. Each series of test specimens, excluding reference specimens, was exposed to the ISO 834 standard temperature curve according to EN 1363-1 (Figure 7a). A higher difference between the actual measured gas temperature and the ISO temperature curve was observed from the 5th to 8th minute. Nevertheless, the temperatures did not exceed the ISO temperature curve limits. For this reason, the temperature distribution in the test furnace was satisfactory for each fire test.

Temperatures measured on the unexposed side of the tensile reinforcement layer differed according to the thickness of the covering concrete layer (Figure 7b). For specimens with an epoxy resin matrix (SPP series), higher temperature was measured in the specimens of variants SPP0 and SPP5. This was caused by the complete or partial burning out of the epoxy resin material, as determined by visual analysis after the mechanical tests. In both cases (SPP-0 and SPP-5), the temperatures exceeded approximately 280 °C, implying an advanced epoxy resin decomposition phase. On the contrary, for specimens with a 10 mm cover layer (SPP-10), the temperature did not exceed 200 °C, and the epoxy resin did not burn out. The temperature difference of both samples' series with cement and epoxy resin matrix (with covering layer of 5 and 10 mm) was approximately 20 °C.

After fire exposure, the specimens with PP fibers (CPP/SPP series) added into the HPC mixture retained their integrity. However, for specimens without PP fibers, the destruction of all specimens occurred due to the increase of inner water vapor pressure and closed pore structure of HPC. The increased internal pressure, combined with the subtle character of specimens, has led to the loss of integrity of the entire test specimens without PP fibers before the end of the fire test. Therefore, it was impossible to determine the residual bending strength of these specimens.

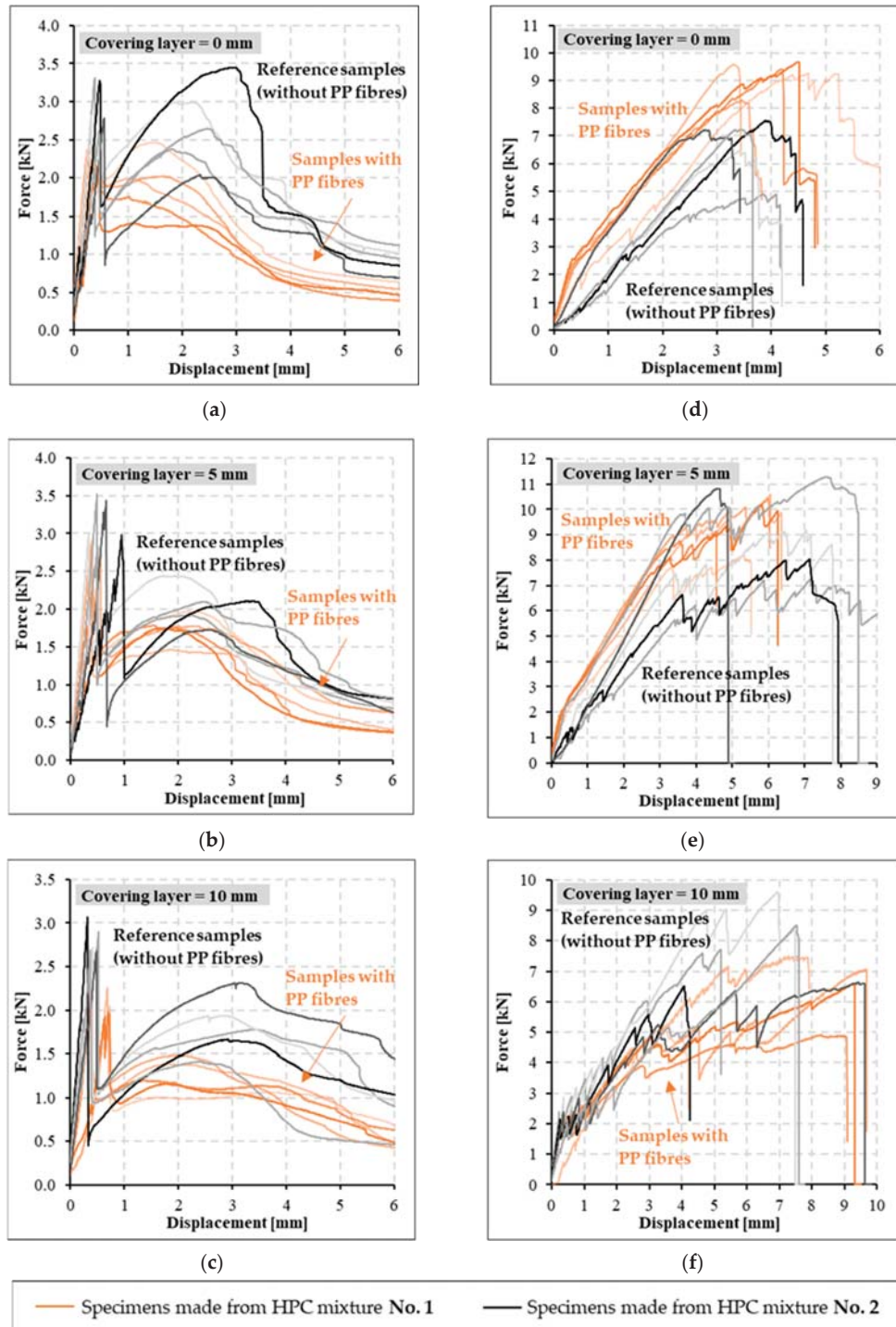


Figure 6. Bending strength of reference specimens with cement suspension matrix (a–c) and epoxy resin matrix (d–f) for different thickness of the covering layer.

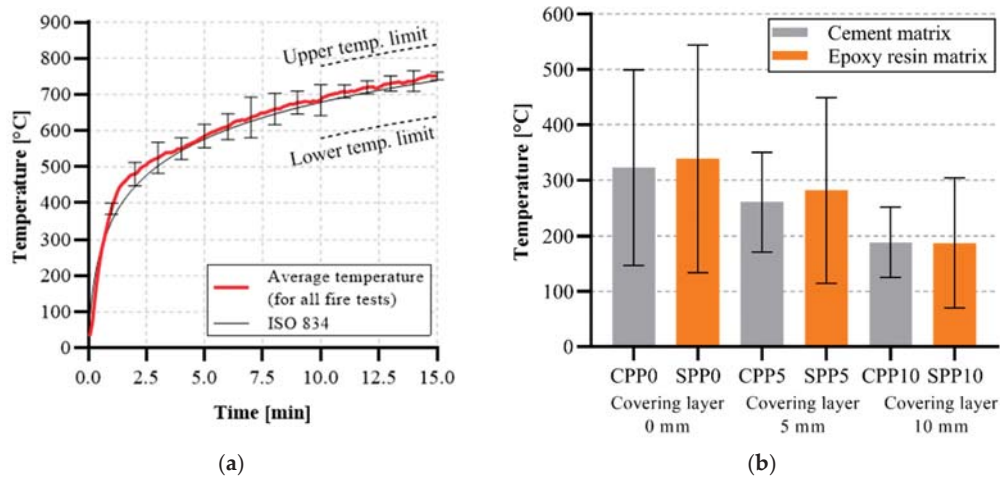


Figure 7. Measured temperature from the test furnace and tested specimens: (a) average temperature curve in the test furnace; (b) measured average temperatures of the specimens on the inner surface of the textile reinforcement for different covering layers and concrete mixture variants.

Different behavior was observed for test specimens with the addition of PP fibers using various materials of the textile reinforcement matrix. For cement suspensions specimens, spalling of concrete layers did not occur in any test. Only transverse cracks were observed because of the fire exposure, (Figure 8).



Figure 8. Test specimen with 10 mm covering layer and an addition of PP fibers in concrete mixture (HPC mixture No. 1)—the development of a transverse crack during a fire test.

Similar behaviour was observed for specimens with epoxy resin matrix and no covering layer (SPP-0). The absence of spalling may be due to the reinforcing layer being placed near the fire exposed surface. This layer allowed additional reinforcement against spalling. On the other hand, no additional pressure accumulation could occur due to the thermal degradation of the epoxy resin. In contrast, for the test specimens with a covering layer of 5 and 10 mm (series SPP-5 and SPP-10), a separation of the entire area of the covering layer at the exposed surface of the textile reinforcement was observed. It occurred probably due to the influence of the epoxy resin thermal decomposition products in combination with the epoxy resin's loss of mechanical strength and due to the phase transition. As a result, the covering layer was weakened at this point and subsequently, the covering layer spalled off. Especially specimens with a cover layer of 5 mm showed only local spalling due to the possibility of water vapor and epoxy resin thermal decomposition products migration to the outside of the test specimen. On the contrary, for specimens with a covering layer equal to 10 mm (SPP-10), a cavity was formed between the covering layer and the rest of the test specimen. In most cases, the covering layers fell off, leaving the textile reinforcement directly exposed to fire. Therefore, it was not possible to determine residual bending

strength. The smooth surface character of the textile reinforcement saturated by epoxy resin is also a significant contribution to the covering layer spalling at the zone of the reinforcing mesh. Moreover, due to the phase transition of epoxy resin, the epoxy resin is losing its mechanical properties. Therefore, the adhesion between materials weakened. Only in one case of the SPP-10 test series the specimen's integrity was maintained and it was possible to determine the residual bending strength (Figure 9).

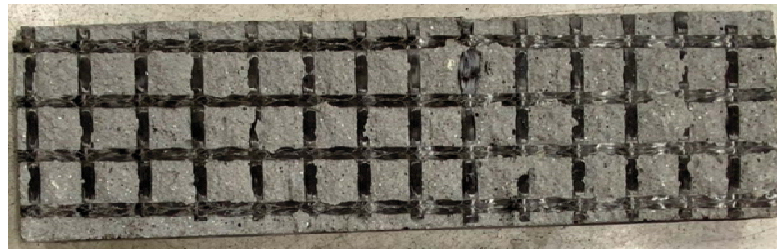


Figure 9. Test specimen of SPP10 series after the covering layer spalled off after the fire experiment (no direct exposure of the reinforcing layer during fire test occurred).

Based on the four-point bending test data, the residual bending strength of specimens exposed to elevated temperatures was determined. It was observed that the textile reinforcement from epoxy resin completely burned out due to the direct fire exposure of textile reinforcement or due to exceeding the ignition temperature of epoxy resin (Figure 7b) when the covering layer did not spall. On the contrary, cement matrix was damaged on the surface only partially and the interaction between materials remain undisturbed to a certain extent (Figure 10).

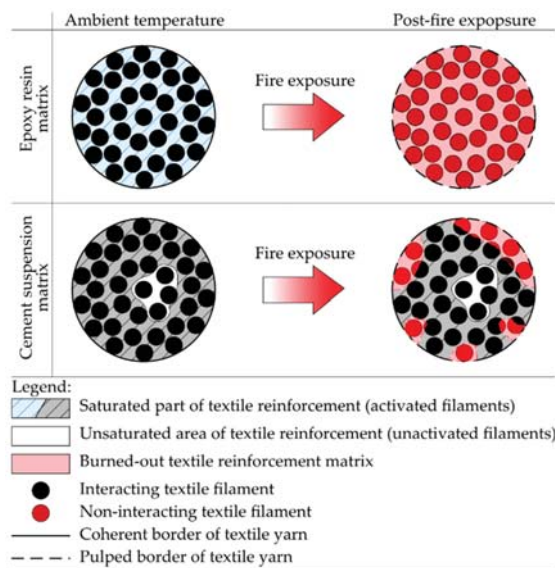


Figure 10. Schematic description of the fire exposure influence to a different type of textile reinforcement matrix.

Tested specimens with cement suspension matrix at elevated temperatures showed a similar trend of bending strength capacity as the reference specimens (Figure 11a–c). The results show that these specimens did not incur a significant decrease of mechanical bending strength as in the case of samples with the epoxy resin matrix. This was caused by

better temperature resistance of the cement suspension matrix material. Due to temperature effects, the bending strength decreased by approximately 40%. Simultaneously, the cement suspension samples showed a significant increase in ductility. Higher ductility was caused by gradual pull out of individual filaments of the carbon yarn during the whole mechanical test. In contrast to the specimens with an epoxy resin matrix, textile reinforcement did not drop out during mechanical tests, and the progressive break did not occur.

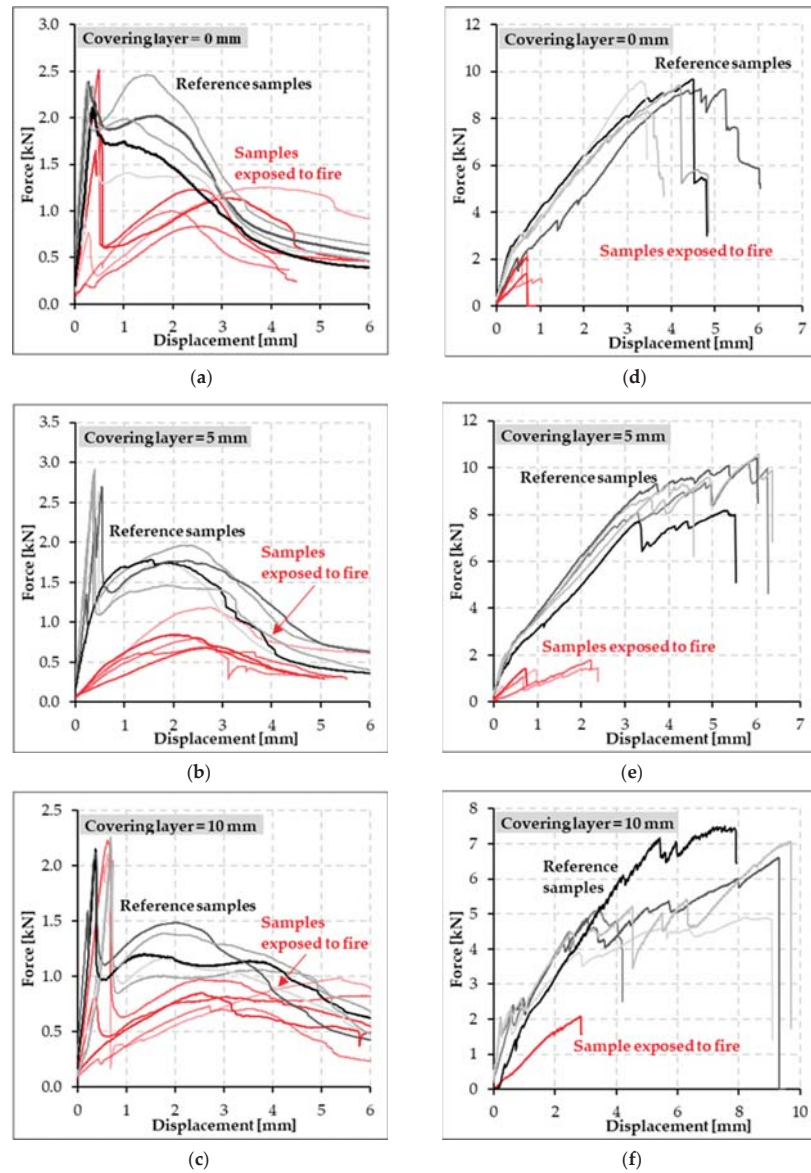


Figure 11. Comparison of the resulting residual strength of the test plate specimens after the fire test with reference specimens: (a–c) test plate specimens with cement suspension matrix; (d–f) test plate specimens with epoxy resin textile reinforcement matrix. Note: All specimens mentioned in Figure 11 were made according to Table 4 from the HPC mixture No. 1.

In tested specimens with an epoxy resin matrix (SPP series), we observed a significant degradation of the epoxy resin due to the attained temperatures during the fire test (Figure 7). Therefore, a significant loss of mechanical properties of these specimens occurred (Figure 11d–f). During the fire tests, this matrix was partially burned out. Subsequently, the ability to homogenize the individual filaments in the textile yarn was infringed. In contrast to the reference specimens with epoxy resin matrix, a progressive break did not occur when the tensile strength of textile reinforcement was reached. Specimens with epoxy resin tensile reinforcement matrix exposed to elevated temperature were broken due to the pulling of textile reinforcement or breakage due to absent interaction between the textile reinforcement and HPC—the textile reinforcement disengaged from HPC.

4. Conclusions

Based on previous experimental work [32], where the behavior of the cement suspension matrix was analyzed at ambient temperature, the experimental investigation described in this study focused on assessing residual bending strength at elevated temperature. As part of the experimental work, plate test specimens with dimensions 100 mm × 360 mm × 30 mm with different textile reinforcement matrix materials were tested. Also, the influence of the presence of polypropylene (PP) fibers in the high-performance concrete (HPC) mixture was assessed. Based on tests at ambient and elevated temperatures, the conclusions of the study are summarized as follows:

- Bending strength of specimens with cement suspension matrix (CPP series) decreased by approximately 24% due to the addition of the PP fibers into the HPC mixture. Simultaneously, the measured peak of the bending strength and the corresponding deformation were reduced by approximately 1 mm. However, based on the fire tests, the absence of PP fibers in the HPC mixture negatively affected the mechanical properties of these specimens at elevated temperatures. All test specimens without PP fibers failed due to the massive spalling of the concrete layers, and it was not possible to determine their residual bending strength.
- Performed fire tests clearly demonstrated the positive effect of improved temperature resistance while using a non-combustible matrix of cement-based textile reinforcement. Although the test specimens did not achieve as high bending strengths as those with an epoxy resin matrix, no progressive failure occurred due to the loss of engagement among the materials after exposure to fire. Concurrently, specimens with cement suspension show significantly better performance than the samples without any matrix of textile reinforcement as described in [32]. Moreover, a similar trend of attained bending strength was observed for the reference specimens, although the residual bending strength decreased by approximately 40%.
- Tested specimens with cement suspension showed different failure modes. There was no progressive break but a gradual pulling out of the textile reinforcement. That is why these samples showed significantly higher ductility than samples with epoxy resin matrix.
- For test specimens with cement suspension matrix, spalling of the concrete layers did not occur, in contrast to the test specimens with synthetic resin matrix. Generally, epoxy resins can facilitate the spalling of the concrete layer. This is due to the originating epoxy resin thermal decomposition products during the fire test. These products can contribute to the pressure from the evaporated water and accelerate the spalling of the concrete layers. Simultaneously, upon contact with flames, these products can ignite and thus directly contribute to the development of a fire.

The study shows that using silica-based materials as a textile reinforcement matrix positively affects mechanical properties of specimens after exposure to elevated temperature. However, it is mainly a matter of finding a compromise between maximum bending potential, ductile behavior, or preservation of mechanical properties after exposure to fire. Due to the better temperature stability of silicate (non-flammable) suspension, there was no rapid decrease in residual bending strength.

A similar trend of decreasing bending strength was described in the study [13], where the specimens with glass textile reinforcement were tested. However, in other studies evaluating TRC at elevated temperatures, it was impossible to compare the measured results effectively due to different testing methodologies [11,12]. Nevertheless, since the measured strengths were lower than reference samples at ambient temperature, it is necessary to research this topic further and verify the use of other matrix materials, such as geopolymers, or search for a different method of impregnating textile fibers. In addition, more fire tests shall be performed, in order to get results of TRC behavior that correspond to fire exposure according to realistic fire, which is in agreement with Kapsalis et al. [33].

Given the results of the experimental study presented, it may be stated that the hypothesis of suitability of cement suspension as a replacement for epoxy resin matrix has been confirmed at elevated temperatures. Nonetheless, the performance of cement-based matrix at normal temperatures is not sufficient, hence further research will be focused on noncombustible matrix materials, geopolymers in particular.

Author Contributions: Conceptualization, R.F., T.V., P.H. (Petr Hejtmánek), V.M. and P.H. (Petr Hájek); methodology, R.F., J.Ř., T.V. and P.H. (Petr Hejtmánek); software, R.F. and J.Ř.; supervision V.M. and P.H. (Petr Hájek); resources, R.F., J.Ř. and T.V.; writing—original draft, R.F., P.H. (Petr Hejtmánek), T.V., V.M., J.Ř. and P.H. (Petr Hájek). All authors have read and agreed to the published version of the manuscript.

Funding: This work was supported by the Grant Agency of the Czech Technical University in Prague, grant No. SGS21/094/OHK1/2T/11 project—Application of alternative materials in textile concrete and their evaluation at room temperature and at elevated temperature.

Institutional Review Board Statement: Not applicable.

Informed Consent Statement: Not applicable.

Data Availability Statement: The data presented in this study are available on request from the corresponding author.

Conflicts of Interest: The authors declare no conflict of interest.

References

1. Giese, A.C.H.; Giese, D.N.; Dutra, V.F.P.; Filho, L.C.P.D.S. Flexural Behavior of Reinforced Concrete Beams Strengthened with Textile Reinforced Mortar. *J. Build. Eng.* **2021**, *33*, 101873. [[CrossRef](#)]
2. Larbi, A.S.; Agbossou, A.; Hamelin, P. Experimental and Numerical Investigations about Textile-Reinforced Concrete and Hybrid Solutions for Repairing and/or Strengthening Reinforced Concrete Beams. *Compos. Struct.* **2013**, *99*, 152–162. [[CrossRef](#)]
3. Hegger, J.; Schneider, H.; Sherif, A.; Molter, M.; Voss, S. Exterior Cladding Panels As An Application Of Textile Reinforced Concrete. *ACI Symp. Publ.* **2004**, *224*, 55–70. [[CrossRef](#)]
4. Hegger, J.; Voss, S. Investigations on the Bearing Behaviour and Application Potential of Textile Reinforced Concrete. *Eng. Struct.* **2008**, *30*, 2050–2056. [[CrossRef](#)]
5. Holčapek, O.; Vogel, F. Bond Properties of Concrete Beams Strengthened by AR-Glass Textile and Basalt Textile Reinforced Concrete. *Appl. Mech. Mater.* **2016**, *825*, 7–10. [[CrossRef](#)]
6. Makul, N. Modern Sustainable Cement and Concrete Composites: Review of Current Status, Challenges and Guidelines. *Sustain. Mater. Technol.* **2020**, *25*, e00155. [[CrossRef](#)]
7. Müller, H.S.; Haist, M.; Vogel, M. Assessment of the Sustainability Potential of Concrete and Concrete Structures Considering Their Environmental Impact, Performance and Lifetime. *Constr. Build. Mater.* **2014**, *67*, 321–337. [[CrossRef](#)]
8. Portal, N.W.; Lundgren, K.; Wallbaum, H.; Malaga, K. Sustainable Potential of Textile-Reinforced Concrete. *J. Mater. Civ. Eng.* **2015**, *27*, 04014207. [[CrossRef](#)]
9. Laiblová, L.; Pešta, J.; Kumar, A.; Hájek, P.; Fiala, C.; Vlach, T.; Kočí, V. Environmental Impact of Textile Reinforced Concrete Facades Compared to Conventional Solutions—LCA Case Study. *Materials* **2019**, *12*, 3194. [[CrossRef](#)]
10. Maxineasa, S.G.; Taranu, N.; Bejan, L.; Isopescu, D.; Banu, O.M. Environmental Impact of Carbon Fibre-Reinforced Polymer Flexural Strengthening Solutions of Reinforced Concrete Beams. *Int. J. Life Cycle Assess.* **2015**, *20*, 1343–1358. [[CrossRef](#)]
11. Donnini, J.; De Caso y Basalo, F.; Corinaldesi, V.; Lancioni, G.; Nanni, A. Fabric-Reinforced Cementitious Matrix Behavior at High-Temperature: Experimental and Numerical Results. *Compos. Part B Eng.* **2017**, *108*, 108–121. [[CrossRef](#)]
12. De Andrade Silva, F.; Butler, M.; Hempel, S.; Toledo Filho, R.D.; Mechtcherine, V. Effects of Elevated Temperatures on the Interface Properties of Carbon Textile-Reinforced Concrete. *Cem. Concr. Compos.* **2014**, *48*, 26–34. [[CrossRef](#)]
13. Kapsalis, P.; Tysmans, T.; Verbruggen, S.; Triantafyllou, T. Preliminary High-Temperature Tests of Textile Reinforced Concrete (TRC). *Proceedings* **2018**, *2*, 522. [[CrossRef](#)]

14. Colombo, I.G.; Magri, A.; Zani, G.; Colombo, M.; di Prisco, M. Erratum to: Textile Reinforced Concrete: Experimental Investigation on Design Parameters. *Mater. Struct.* **2013**, *46*, 1953–1971. [[CrossRef](#)]
15. Peled, A.; Bentur, A.; Mobasher, B. *Textile Reinforced Concrete*; CRC Press: Boca Raton, FL, USA, 2019; ISBN 978-1-351-64546-1.
16. Vlach, T.; Laiblová, L.; Řepka, J.; Jirkalová, Z.; Hájek, P. EXPERIMENTAL VERIFICATION OF IMPREGNATED TEXTILE REINFORCEMENT SPLICING BY OVERLAPPING. *Acta Polytech. CTU Proc.* **2019**, *22*, 128–132. [[CrossRef](#)]
17. Kalifa, P.; Menneteau, F.-D.; Quenard, D. Spalling and Pore Pressure in HPC at High Temperatures. *Cem. Concr. Res.* **2000**, *30*, 1915–1927. [[CrossRef](#)]
18. Kalifa, P.; Chéné, G.; Gallé, C. High-Temperature Behaviour of HPC with Polypropylene Fibres. *Cem. Concr. Res.* **2001**, *31*, 1487–1499. [[CrossRef](#)]
19. Teijin®. Technical Sheet: Carbon Roving Tenax STS40 F13 24K 1600tex. Available online: <https://shop1.r-g.de/en/art/205105STS> (accessed on 20 March 2022).
20. Deák, T.; Czigány, T. Chemical Composition and Mechanical Properties of Basalt and Glass Fibers: A Comparison. *Text. Res. J.* **2009**, *79*, 645–651. [[CrossRef](#)]
21. Černý, M.; Glogar, P.; Sucharda, Z.; Chlup, Z.; Kotek, J. Partially pyrolyzed composites with basalt fibres—Mechanical properties at laboratory and elevated temperatures. *Compos. Part A Appl. Sci. Manuf.* **2009**, *40*, 1650–1659. [[CrossRef](#)]
22. Feng, J.; Guo, Z. Temperature-Frequency-Dependent Mechanical Properties Model of Epoxy Resin and Its Composites. *Compos. Part B Eng.* **2016**, *85*, 161–169. [[CrossRef](#)]
23. Mohan, P. A Critical Review: The Modification, Properties, and Applications of Epoxy Resins. *Polym. Plast. Technol. Eng.* **2013**, *52*, 107–125. [[CrossRef](#)]
24. Bompadre, F.; Donnini, J. Surface Modification of Glass Textile for the Reinforcement of a Cement-Based Composite: A Review. *Appl. Sci.* **2021**, *11*, 2028. [[CrossRef](#)]
25. Di Maida, P.; Radi, E.; Sciancalepore, C.; Bondioli, F. Pullout Behavior of Polypropylene Macro-Synthetic Fibers Treated with Nano-Silica. *Constr. Build. Mater.* **2015**, *82*, 39–44. [[CrossRef](#)]
26. Zhao, J.; Liebscher, M.; Michel, A.; Junger, D.; Trindade, A.C.C.; Silva, F.D.A.; Mechtcherine, V. Development and testing of fast curing, mineral-impregnated carbon fiber (MCF) reinforcements based on metakaolin-made geopolymers. *Cem. Concr. Compos.* **2021**, *116*, 103898. [[CrossRef](#)]
27. Mechtcherine, V.; Michel, A.; Liebscher, M.; Schneider, K.; Großmann, C. Mineral-impregnated carbon fiber composites as novel reinforcement for concrete construction: Material and automation perspectives. *Autom. Constr.* **2020**, *110*, 103002. [[CrossRef](#)]
28. Isayev, A.I. *Encyclopedia of Polymer Blends*, 1st ed.; Wiley-VCH: Weinheim, Germany, 2016; Volume 3, ISBN 978-3-527-31931-2.
29. Marianne, G. *Brydson's Plastics Materials*, 8th ed.; Elsevier: Boston, MA, USA, 2017; ISBN 978-0-323-35824-8.
30. Fürst, R.; Pokorný, M.; Vlach, T.; Mózer, V. Study of Behavior of Textile-Reinforced Concrete with Epoxy Resin Matrix in Fire. *Fire Technol.* **2022**, *58*, 53–74. [[CrossRef](#)]
31. Salasinska, K.; Barczewski, M.; Borucka, M.; Górný, R.L.; Kozikowski, P.; Celiński, M.; Gajek, A. Thermal Stability, Fire and Smoke Behaviour of Epoxy Composites Modified with Plant Waste Fillers. *Polymers* **2019**, *11*, 1234. [[CrossRef](#)]
32. Fürst, R.; Fürst, E.; Vlach, T.; Řepka, J.; Pokorný, M.; Mózer, V. Use of Cement Suspension as an Alternative Matrix Material for Textile-Reinforced Concrete. *Materials* **2021**, *14*, 2127. [[CrossRef](#)]
33. Kapsalis, P.; Tysmans, T.; Hemelrijck, D.V.; Triantafyllou, T. State-of-the-Art Review on Experimental Investigations of Textile-Reinforced Concrete Exposed to High Temperatures. *J. Compos. Sci.* **2021**, *5*, 290. [[CrossRef](#)]